Emission Factors for Crop Residue and Prescribed Fires in the Eastern US During FIREX-AQ

Katherine R Travis, James H Crawford, Amber J Soja, Emily M Gargulinski, Richard H Moore, Elizabeth B Wiggins, Glenn S Diskin, Joshua P Digangi, John B Nowak, Hannah Halliday, et al.

HAL Id: hal-04360944
https://hal.inrae.fr/hal-04360944

Submitted on 22 Dec 2023

AGU
ADVANCING EARTH AND SPACE SCIENCES

JGR Atmospheres

RESEARCH ARTICLE

Key Points:
- Corn residue burned at higher modified combustion efficiency than rice or soybean residue
- Impacts of fire emissions >6 hr downwind on OH reactivity will be more influenced by species that are less important at the source
- Emission factors from crop residue fires agreed better with previous results from the same region than with global compilations

Supporting Information:

Supporting Information may be found in the online version of this article.

Correspondence to:

K. R. Travis,
katherine.travis@nasa.gov

Author Contributions:

Conceptualization: Katherine R. Travis, James. H. Crawford, Robert J. Yokelson, Jessica L. McCarty

Emission Factors for Crop Residue and Prescribed Fires in the Eastern US During FIREX-AQ

Katherine R. Travis[1], James. H. Crawford[1], Amber J. Soja[1,2], Emily M. Gargulinski[1,2], Richard H. Moore[1], Elizabeth B. Wiggins[1], Glenn S. Diskin[1], Joshua P. DiGangi[1], John B. Nowak[1], Hannah Halliday[1,3], Robert J. Yokelson[4], Jessica L. McCarty[5,6], Isobel J. Simpson[7], Donald R. Blake[7], Simone Meinardi[7], Rebecca S. Hornbrook[8], Eric C. Apel[8], Alan J. Hills[8], Carsten Warneke[9], Matthew M. Coggon[9], Andrew W. Rollins[9], Jessica B. Gilman[9], Caroline C. Womack[9,10], Michael A. Robinson[9,10], Joseph M. Katich[9,10], Jeff Peischl[9,10], Georgios I. Gkatzelis[9,10,11], Ilann Bourgeois[9,10,12], Pamela S. Rickly[9,10,13], Aaron Lamplugh[9,10,14], Jack E. Dibb[15], Jose L. Jimenez[10,16], Pedro Campuzano-Jost[10,16], Douglas A. Day[10,16], Hongyu Guo[10,16], Demetrios Pagonis[10,16], Paul O. Wennberg[17,18], John D. Crounse[17,18], Lu Xu[9,17], Thomas F. Hanisco[19], Glenn M. Wolfe[19], Jin Liao[19,20], Jason M. St. Clair[19,21], Benjamin A. Nault[22], Alan Fried[23], and Anne E. Perring[24]

[1]NASA Langley Research Center, Hampton, VA, USA, [2]National Institute of Aerospace, Hampton, VA, USA, [3]Air Methods and Characterization Division, U.S. Environmental Protection Agency, Office of Research and Development, Center for Environmental Measurement and Modeling, Research Triangle Park, NC, USA, [4]Department of Chemistry, University of Montana, Missoula, MT, USA, [5]Department of Geography, Miami University, Oxford, OH, USA, [6]NASA Ames Research Center, Moffett Field, CA, USA, [7]University of California, Irvine, CA, USA, [8]Atmospheric Chemistry Observations & Modeling Laboratory, NCAR, Boulder, CO, USA, [9]NOAA Chemical Sciences Laboratory (CSL), Boulder, CO, USA, [10]Cooperative Institute for Research in Environmental Sciences (CIRES), University of Colorado, Boulder, CO, USA, [11]Now at IEK-8: Troposphere, Forschungszentrum Jülich GmbH, Jülich, Germany, [12]Now at University Savoie Mont Blanc, INRAE, CARRTEL, Thonon-Les-Bains, France, [13]Now at Air Pollution Control Division, Colorado Department of Public Health and Environment, Denver, CO, USA, [14]Now at Institute of Behavioral Science, University of Colorado Boulder, Boulder, CO, USA, [15]Earth Systems Research Center, University of New Hampshire, Durham, NH, USA, [16]Department of Chemistry, University of Colorado, Boulder, CO, USA, [17]Division of Geological and Planetary Sciences, California Institute of Technology, Pasadena, CA, USA, [18]Division of Engineering and Applied Science, California Institute of Technology, Pasadena, CA, USA, [19]NASA Goddard Space Flight Center, Greenbelt, MD, USA, [20]Universities Space Research Association, Columbia, MD, USA, [21]Joint Center for Earth Systems Technology, University of Maryland, Baltimore, MD, USA, [22]CACC, Aerodyne Research, Inc., Billerica, MA, USA, [23]Institute for Arctic and Alpine Research, University of Colorado, Boulder, CO, USA, [24]Department of Chemistry, Colgate University, Hamilton, NY, USA

Abstract Agricultural and prescribed burning activities emit large amounts of trace gases and aerosols on regional to global scales. We present a compilation of emission factors (EFs) and emission ratios from the eastern portion of the Fire Influence on Regional to Global Environments and Air Quality (FIREX-AQ) campaign in 2019 in the United States, which sampled burning of crop residues and other prescribed fire fuels. FIREX-AQ provided comprehensive chemical characterization of 53 crop residue and 22 prescribed fires. Crop residues burned at different modified combustion efficiencies (MCE), with corn residue burning at higher MCE than other fuel types. Prescribed fires burned at lower MCE (<0.90) which is typical, while grasslands burned at lower MCE (0.90) than normally observed due to moist, green, growing season fuels. Most non-methane volatile organic compounds (NMVOCs) were significantly anticorrelated with MCE except for ethanol and NMVOCs that were measured with less certainty. We identified 23 species where crop residue fires differed by more than 50% from prescribed fires at the same MCE. Crop residue EFs were greater for species related to agricultural chemical use and fuel composition as well as oxygenated NMVOCs possibly due to the presence of metals such as potassium. Prescribed EFs were greater for monoterpenes (5×). FIREX-AQ crop residue average EFs generally agreed with the previous agricultural fire study in the US but had large disagreements with global compilations. FIREX-AQ observations show the importance of regionally-specific and fuel-specific EFs as first steps to reduce uncertainty in modeling the air quality impacts of fire emissions.

Plain Language Summary Crop residue and prescribed fires emit pollution that impacts air quality. FIREX-AQ provided observations of these emissions to better characterize their variability with a detailed set of chemical observations. These observations showed significant differences in the emissions from burning different crops (corn, rice, soybean, wheat) compared to other prescribed fires or grasslands that may be due to

Data curation: Amber J. Soja, Emily M. Gargulinski, Richard H. Moore, Elizabeth B. Wiggins

Formal analysis: Katherine R. Travis, Amber J. Soja, Emily M. Gargulinski, Elizabeth B. Wiggins, Jessica L. McCarty, Rebecca S. Hornbrook

Investigation: Katherine R. Travis, Richard H. Moore, Elizabeth B. Wiggins, Glenn S. Diskin, Joshua P. DiGangi, John B. Nowak, Hannah Halliday, Isobel J. Simpson, Donald R. Blake, Simone Meinardi, Rebecca S. Hornbrook, Eric C. Apel, Alan J. Hills, Carsten Warneke, Matthew M. Coggon, Andrew W. Rollins, Jessica B. Gilman, Caroline C. Womack, Michael A. Robinson, Joseph M. Katich, Jeff Peischl, Georgios I. Gkatzelis, Ilann Bourgeois, Pamela S. Rickly, Aaron Lamplugh, Jack E. Dibb, Jose L. Jimenez, Pedro Campuzano-Jost, Douglas A. Day, Hongyu Guo, Demetrios Pagonis, Paul O. Wennberg, John D. Crounse, Lu Xu, Thomas F. Hanisco, Glenn M. Wolfe, Jin Liao, Jason M. St. Clair, Benjamin A. Nault, Alan Fried, Anne E. Perring

Methodology: Katherine R. Travis, James. H. Crawford, Isobel J. Simpson, Rebecca S. Hornbrook, Jessica B. Gilman, Caroline C. Womack, Georgios I. Gkatzelis, Jose L. Jimenez, Pedro Campuzano-Jost, Douglas A. Day, Hongyu Guo, Demetrios Pagonis, Paul O. Wennberg, Glenn M. Wolfe, Benjamin A. Nault

Visualization: Katherine R. Travis, Emily M. Gargulinski

Writing – original draft: Katherine R. Travis

Writing – review & editing: Katherine R. Travis, James. H. Crawford, Amber J. Soja, Emily M. Gargulinski, Richard H. Moore, Elizabeth B. Wiggins, Glenn S. Diskin, Joshua P. DiGangi, John B. Nowak, Hannah Halliday, Robert J. Yokelson, Jessica L. McCarty, Isobel J. Simpson, Donald R. Blake, Rebecca S. Hornbrook, Eric C. Apel, Alan J. Hills, Carsten Warneke, Matthew M. Coggon, Andrew W. Rollins, Jessica B. Gilman, Caroline C. Womack, Michael A. Robinson, Joseph M. Katich, Jeff Peischl, Georgios I. Gkatzelis, Ilann Bourgeois, Pamela S. Rickly, Aaron Lamplugh, Jack E. Dibb, Jose L. Jimenez, Pedro Campuzano-Jost, Douglas A. Day, Hongyu Guo, Demetrios Pagonis, Paul O. Wennberg, Lu Xu, Glenn M. Wolfe, Jin Liao, Jason M. St. Clair, Benjamin A. Nault, Alan Fried, Anne E. Perring

differences in the fuel composition, the use of agricultural chemicals, and moisture levels. Overall, FIREX-AQ observations for crop residue fires compared better with previous results in the region than with globally averaged information. The campaign observed even greater variability across EFs than previous studies, suggesting that new methods must be developed to take this into account to improve predictions of the air quality impacts of burning these fuels.

1. Introduction

Land management activities frequently use prescribed fires to decrease vegetative fuel loads (biomass), cycle nutrients, select for native species, decrease invasive species, and maintain landscape diversity. Burning of crop residue is a related type of planned fire. Globally, crop waste may be plowed back into the soil, used as fuel or livestock fodder, or burned in the field. Burning may happen in piles or spread across the field after mechanized harvesting (Yevich & Logan, 2003). Agricultural burning estimates in the United States (US) average 1 million ha/yr (McCarty et al., 2009) and appear to be increasing in the southern US (Lin et al., 2014). Non-agricultural prescribed fires (hereafter referred to as prescribed fires) in the US are estimated to burn 4–5 million ha/yr (Jaffe et al., 2020; Melvin, 2018). For comparison, over the past 40 years wildfires in the US burned on average 2 million ha/year (NIFC, 2022) albeit with a generally increasing trend (Jaffe et al., 2020). Prescribed and agricultural fires tend to be small and/or short-lived and consume less fuel per area than wildfires (Akagi et al., 2011). Both may escape detection by satellites and are underrepresented in emissions inventories (Koplitz et al., 2018; Larkin et al., 2020; Nowell et al., 2018; Randerson et al., 2012; Soja et al., 2009; Warneke et al., 2023; Yokelson et al., 2011).

Fire emissions can be hazardous to human health (Adetona et al., 2016; Bell et al., 2009; Doubleday et al., 2020; Naeher et al., 2007; Reid et al., 2016; Zanobetti et al., 2009), generating fine particulate matter <2.5 µm (PM$_{2.5}$, Hays et al., 2005; Hodshire et al., 2019; Janhall et al., 2010; Kaulfus et al., 2017; Ortega et al., 2013), non-methane volatile organic compounds (NMVOCs) including hazardous air pollutants (e.g., formaldehyde, benzene, polycyclic aromatic hydrocarbons (PAHs), Dickinson et al., 2022; O'Dell et al., 2020; Samburova et al., 2016; Wentworth et al., 2018), and producing ozone (Baker et al., 2016; Bourgeois et al., 2021; Jaffe et al., 2020; Koplitz et al., 2018; O'Dell et al., 2020). Fires may also resuspend deposited pollution (Eckhardt et al., 2007). Agricultural and prescribed burning in the US tends to maximize in spring, with smaller peaks in summer and fall (Korontzi et al., 2008; Tulbure et al., 2011). Different crop residue is burned in each season (McCarty, 2011). These fires are a large source of PM$_{2.5}$ in the Southeast US and can result in exceedances of the National Ambient Air Quality Standard (Afrin & Garcia-Menendez, 2020; Kaulfus et al., 2017; Tian et al., 2009; Zeng et al., 2008). Increases in both PM$_{2.5}$ and ozone that are attributable to burning in the Southeast US have been observed in urban areas (Akagi et al., 2013; Y. Hu et al., 2008; S. Lee et al., 2008).

Models are used to retrospectively determine or forecast air quality and health impacts from agricultural and prescribed burning (Kelly et al., 2019; Zhou et al., 2018). These simulations require knowledge of fuel-specific emission factors (EFs) of air pollutant species. These measurements are limited for a number of EFs including for furans, phenols, butadienes, and monoterpenes that have been recognized as important sources of OH reactivity not generally considered in chemical transport models (Carter et al., 2022; Permar et al., 2023). Many commonly-used inventories do not include agricultural and prescribed fires as a separate land cover type, or if they do, a global average EF is used for each species. Commonly used global compilations of EFs (Akagi et al., 2011; Andreae, 2019) aggregate studies including a wide variety of both crop residue fuels and prescribed burning activities from regions across the world that represent a range of agricultural techniques and burning practices. Some species have no available direct EF measurements for even these aggregated fuel types (e.g., ethanol) and have been estimated from field or lab measurements of other fuel types.

Only a few studies have provided crop-specific EFs, and then only across a limited range of species. McCarty (2011) provided a compilation of seven EFs (CO$_2$, methane, CO, NO$_2$, SO$_2$, PM$_{2.5}$, and PM$_{10}$) for eight crop types. During the MILAGRO campaign in 2006 (Yokelson et al., 2011) and the SEAC⁴RS campaign in 2013 (Liu et al., 2016), EFs including some NMVOCs were reported for crop residue burning loose in the field for 14 fires in Mexico and 15 fires in the Southeast US. These emissions were statistically different from the Akagi et al. (2011) global average for "crop residue," which included observations from burning loose residue in fields in Mexico and rice straw burning in piles at low combustion efficiency, as

is common in Asia. This difference indicates that the variability in crop-specific EFs is large and not well understood. Crop residue burning has been shown to emit more NMVOCs than other fuel types including prescribed fire fuels (Stockwell et al., 2014, 2015) possibly due to differences in fuel composition (Hatch et al., 2015; Santiago-De La Rosa et al., 2018; Stockwell et al., 2014). The availability of NMVOC EFs is larger for prescribed fire fuels than crop residue, but many EFs were measured in a laboratory setting that may not be representative of ambient conditions (Koss et al., 2018; Selimovic et al., 2018; Stockwell et al., 2014, 2015; Yokelson et al., 2013). Airborne measurements of EFs for prescribed fires in the US (Akagi et al., 2013; Burling et al., 2011; May et al., 2014, 2015; Müller et al., 2016; Yokelson et al., 1999) have generally been included in global average compilations (Akagi et al., 2011; Andreae, 2019) but under the broad category of "temperate forest fires."

In this work we report results from the NOAA/NASA Fire Influence on Regional to Global Environments and Air Quality (FIREX-AQ) campaign, which was an interagency intensive study of North American fires that took place from July to September 2019 (https://asdc.larc.nasa.gov/project/FIREX-AQ). FIREX-AQ included dedicated sampling of crop residue burned loose in the field and prescribed fires in the Eastern US with a comprehensive suite of instruments measuring gas- and aerosol-phase species (Warneke et al., 2023). FIREX-AQ included a western phase sampling wildfires and EFs for these fires are described in Gkatzelis et al. (2023). We determine EFs for all available gas-phase and aerosol species emitted from crop residue and prescribed fires during this eastern phase of the campaign. We assess differences in EFs across fuel types, discuss any observed dependence on burning characteristics such as modified combustion efficiency (MCE), and evaluate the applicability of global agricultural and prescribed EFs to regionally-specific fires. As some models move towards increasing complexity in their treatment of fire emissions (Rabin et al., 2018), this work will support the inclusion of fuel-specific EFs.

2. Description of Crop Residue and Prescribed Fire Plumes Sampled During FIREX-AQ

The FIREX-AQ campaign sampled crop residue burning and prescribed fires across a range of fuels on seven flights from 21 August to 3 September 2019. A full description of the campaign is provided in Warneke et al. (2023). Fires encompassing four crop residues (corn, rice, soybean, winter wheat) and five prescribed burning activities (slash, piles, grassland, shrubland, pine savanna understory) were identified by the FIREX-AQ Fuel2Fire team (Schwarz & Fuel2Fire Team, 2023; Warneke et al., 2023) using a combination of classifications that include the International Geosphere Biosphere Programme (IGBP, Loveland et al., 1999) scheme for landscape-scale classifications, the Fuel Characteristic Classification System (FCCS, Ottmar et al., 2007; Prichard et al., 2013) for forest constituents, and the 2019 Cropland Data Layer (CDL, Boryan et al., 2011; D. M. Johnson & Mueller, 2010) for crop types. Fuels for individual fires are given by Warneke et al. (2023). We separately present EFs for the Blackwater River State Forest (BRSF) understory prescribed fire in Florida which was coordinated to coincide with FIREX-AQ sampling on 30 August 2019. The freshest pass is compared against wildfire fresh smoke from the western component of FIREX-AQ in Gkatzelis et al. (2023). The major FIREX-AQ eastern fuel types and their definitions are given below, and these can be found in detail in Warneke et al. (2023) and Schwarz and Fuel2Fire Team (2023).

2.1. Crop Residue Fires

- Planned burning on lands used for raising crops (specifically corn, rice, soybean, winter wheat).

2.2. Prescribed Fires—Any Fire Intentionally Ignited as Part of Land Management Strategies

- Slash: Managed extensive burning of logging residue and land clearing slash, primarily not in piles. Fuels can include shrubs, grasses, duff, and coniferous and deciduous residue.
- Piles: Piles from yard waste or slash piled from land clearing or logging residue.
- Grassland: Dominated by grasses and other non-woody herbaceous cover (<2 m in height), with tree and shrub cover <10%.
- Shrubland: Dominated by woody/shrub perennials, <2 m in height (cover 10%–60%). The foliage can be either coniferous or deciduous.
- BRSF: Understory burn of primarily shrubs, grasses, and litter from pine, oak, and magnolia forest.
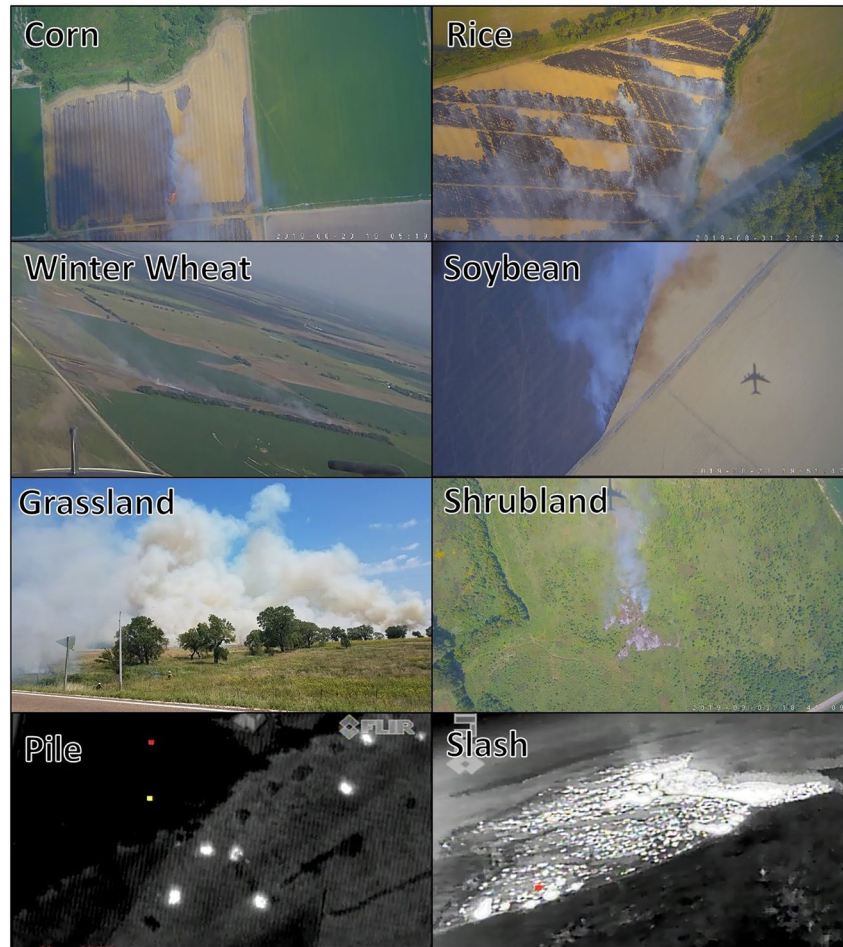
Figure 1. Example photographs for fuel types sampled during the Eastern US component of FIREX-AQ, from the DC-8 visible camera (corn, rice, soybean, winter wheat, shrubland), DC-8 infrared camera (piles, slash), and a ground-based camera (grassland).

Figure 1 provides representative photographs taken during FIREX-AQ of the fire types described above. Fire plumes were generally sampled directly over or near the burning field and were visible from the aircraft. Infrared photos are provided for slash and pile fires to highlight the difference in burning method.

Figure 2 shows the location and fuel types of the crop residue and prescribed fire plumes sampled during FIREX-AQ and analyzed here. Most sampled crop residue fires were in the Mississippi River Valley region from
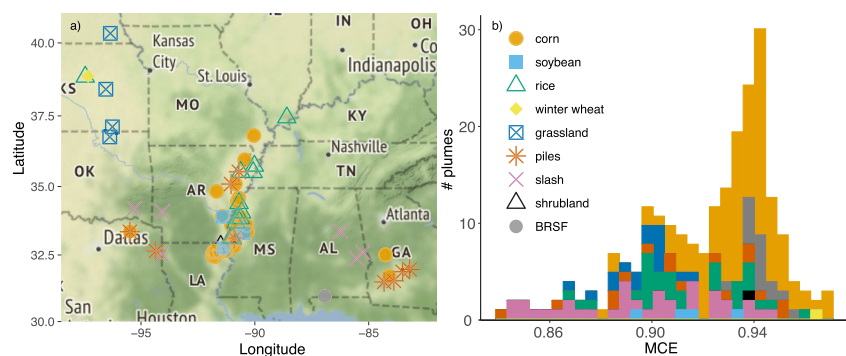
Figure 2. Crop residue and prescribed fire plumes sampled during FIREX-AQ, colored by fuel type. (a) Map of fire locations. (b) Stacked histogram of modified combustion efficiency (MCE) for sampled plumes.

Table 1
Details for Crop Residue and Prescribed Fires Sampled During FIREX-AQ[a]

Fuel	Crop residue fires					Prescribed fires					
	Corn	Rice	Soybean	Winter wheat	Avg	Slash	Piles	Shrubland	Avg	Grassland	BRSF
# Fires	37	12	3	1	53	7	9	1	17	4	1
# Plumes analyzed[b]	108	29	4	1	142	34	16	1	51	15	20
MCE (sd)	0.935 (0.017)	0.914 (0.023)	0.914 (0.017)	0.965 (N/A)	0.930 (0.020)	0.896 (0.031)	0.911 (0.032)	0.940 (N/A)	0.902 (0.032)	0.897 (0.012)	0.942 (0.006)
Date(s) sampled	21, 23, 26, 30, 31 August, 03 September	23, 29, 31 August, 03 September	23, 31 August	29 August	N/A	21, 26, 30, 31 August	21, 23, 26, 30 August, 03 September	03 September	N/A	29 August	30 August

Note. N/A, Not applicable.
[a]Fire locations are shown in Figure 2a. [b]Plume analysis described in Section 3.

southern Illinois to northern Louisiana, with several additional crop residue fires in Texas, Kansas, and Georgia. Grassland fires were sampled in Nebraska, Kansas, and Oklahoma, and slash and pile fires were sampled in Oklahoma, Texas, Arkansas, Mississippi, Alabama, and Georgia. The BRSF understory prescribed fire was in Florida. There were insufficient samples of any one given fuel type to determine if there was any regional dependence in emission factors. Table 1 lists the number of plumes and fires used in the analysis described in Section 3 for each fuel type and the dates on which each fuel type was sampled. In 2019, corn was the largest crop in terms of cultivated area in the US (Capehart & Proper, 2019). Approximately half of all sampled fires during the FIREX-AQ campaign eastern component in August–September 2019 were burning post-harvest corn residues. This is in contrast to Pouliot et al. (2017) who classified many fire detections in corn (and soybean) fields as non-agricultural burning for much of the midwestern US based on official correspondence from the Iowa State University Extension and Outreach stating "burning corn and soybean fields is just not a practice that is used in Iowa and many other Midwest states…." In more recent inventories, fires detected in corn fields have been classified or reclassified as generic agricultural burning in the National Fire Emissions Inventory to account for the possibility that grassy areas next to the corn fields were burning. During FIREX-AQ, corn residue was directly observed to be burning in Georgia, Mississippi, Louisiana, Arkansas, Texas, and Missouri.

3. Determination of FIREX-AQ Emission Factors From Aircraft Observations

Table 2 describes the aircraft observations used in this work and provides references describing the instrument analytical techniques. FIREX-AQ included both continuous and discrete measurements. From the continuous measurements, aircraft data were available at 5 Hz or faster for select instruments, and at 1 Hz for the remaining instruments. From instruments that require longer integration times (iWAS, TOGA-TOF, WAS), data were available at sampling resolutions between 10 and ~45 s. Data were checked for alignment in time from all the instruments using the CO observations from the DACOM instrument. For the discrete samples, iWAS-, TOGA-, and WAS-merges of the 1 Hz data were generated for more accurate comparisons between co-measured species and CO mixing ratios. The TOGA-merge used here weighted concentrations to account for variable instrument fill times and is provided in the Data Availability section. Fire plumes were identified visually and confirmed by enhancements above background for CO and black carbon (BC) as described by Warneke et al. (2023).

In approximately 30% of transects, there appeared to be overlapping plumes based on differences in the ratio of CO to CO_2. For these cases we deconvoluted these transects into individual plumes (distinct peaks in the data) based on the observed change in this ratio. We excluded from our analysis poorly-defined plumes where the coefficient of determination (r^2) for CO and CO_2 was <0.90 or the maximum CO (5 Hz) was too low for a thorough analysis (<400 ppb). The average plume sampling time was 8 s, with a minimum of 3 s and a maximum of 41 s.

EFs from biomass burning activities were calculated according to Equation 1 (Yokelson et al., 1999),

$$EF_i\left(\frac{g}{kg}\right) = F_c \times 1000\left(\frac{g}{kg}\right) \times \frac{MW_i(g)}{12(g)} \times \frac{C_i}{C_T}, \tag{1}$$

where EF_i is the mass (g) of species i emitted per mass (kg) of dry fuel burned, F_c is the fuel carbon fraction, MW_i is the molecular weight of species i, C_i is the number of moles of species i, and C_T is the total number of moles of emitted carbon. We assumed that F_c was 41% for crop residue fuels, 46% for grasslands and shrublands, and 51% for piles and slash, assuming coniferous slash as a likely fuel (A. S. Johnson & Hale, 2002) according to Stockwell et al. (2014).

Table 2
Description of the Aircraft Observations Used in This Work[a]

Instrument	PI	Species	Sampling frequency	References
Diode laser spectrometer (Differential Absorption Carbon monOxide Measurement, DACOM)	Glenn Diskin	CO, CH_4	5 Hz	Sachse et al. (1987, 1991)
Non-dispersive Infrared Spectrometer (NDIR; LI-COR 7000)	Glenn Diskin	CO_2	5 Hz	Anderson et al. (1996)
NOAA PTR-ToF-MS	Carsten Warneke	VOCs, nitrogen-containing species	5 Hz	Yuan et al. (2017)
NCAR Trace Organic Gas Analyzer with Time-of-Flight Mass Spectrometer (TOGA-TOF)	Eric Apel	VOCs, nitrogen-containing species, halocarbons	Typically every 1.75 min	Apel et al. (2015)
UCI Whole Air Sampler (WAS)	Don Blake	VOCs, alkyl nitrates, halocarbons, sulfur compounds	Up to 168 samples/flight	Simpson et al. (2020)
NOAA Integrated Whole Air Sampler (iWAS)	Jessica Gilman	VOCs	Up to 72 samples/flight	Lerner et al. (2017)
NASA In Situ Airborne Formaldehyde (ISAF)	Tom Hanisco	Formaldehyde	10 Hz	Cazorla et al. (2015)
Compact Atmospheric Multispecies Spectrometer (CAMS)	Alan Fried	Formaldehyde, ethane	1 Hz	Richter et al. (2015)
NOAA Airborne Cavity Enhanced Spectrometer (ACES)	Caroline Womack	Glyoxal, methylglyoxal, HONO, NO_2	1 Hz	Min et al. (2016)
Caltech CIMS (CIT-CIMS)	Paul Wennberg	H_2O_2, HCN, organic acids, etc.	1 Hz	St. Clair et al. (2010) and Crounse et al. (2006)
NOAA Iodide ToF-CIMS (NOAA CIMS)	Patrick Veres	HONO, HCN, HNCO, HCOOH, halogenated species	1 Hz	Veres et al. (2020)
NOAA NO_yO_3 four-channel chemiluminescence (NOAA CL) instrument	Tom Ryerson	NO, NO_2	1 Hz	Bourgeois et al. (2022)
NOAA Laser Induced Fluorescence (NOAA LIF)	Drew Rollins	NO, SO_2	5 Hz	Rollins et al. (2020)
CU High-Resolution Time-of-Flight Aerosol Mass Spectrometer (CU HR-ToF-AMS)	Jose Jimenez	Non-refractive PM_1, aerosol composition (OC, SO_4, NO_3, NH_4, NR-Chl, K)	Mostly 5 Hz in plumes, 1 Hz otherwise	Nault et al. (2018, 2021), Guo (2020), and Guo et al. (2021)
CU Extractive Electrospray Ionization Mass Spectrometer (EESI-MS)	Jose Jimenez	Particulate levoglucosan and 4-nitrocatechol	1 Hz	Pagonis et al. (2021) and Lopez-Hilfiker et al. (2019)
NOAA SP2	Joshua Schwarz	BC	1 Hz	Schwarz et al. (2008)
NASA Langley Aerosol Research Group (LARGE) BMI Mixing Condensation Particle Counter (CPC) and Laser Aerosol Spectrometer (LAS)	Rich Moore	CN, size distribution	10 Hz, 1 Hz	Moore et al. (2021)
NCAR Charge-coupled device (CCD) Actinic Flux Spectroradiometers (CAFS)	Sam Hall	Photolysis frequencies	1 Hz	Hall et al. (2018)

[a]For a listing of all available observations during FIREX-AQ, see (Warneke et al., 2023).

The value of C_i/C_T here is calculated according to Equation 2, where $\Delta C_i/\Delta CO$ is the emission ratio (ER). The ER is the slope of the species i with CO or the plume excess of species i over background divided by the excess CO over background. The emitted carbon (C_T) was assumed to be encompassed by $s = CO_2 + CO + CH_4$ ($N = 3$) which were available for all analyzed plumes and $\Delta C_s/\Delta CO$ is the ER for each species, s. NC_s is the number of carbon atoms in species s. Including carbon contained in organic aerosol (OA) and NMVOCs in C_T would decrease calculated EFs by approximately 5% (Yokelson et al., 2013).

$$\frac{C_i}{C_T} = \frac{\frac{\Delta C_i}{\Delta CO}}{\sum_{s=1}^{N}\left(NC_s \times \frac{\Delta C_s}{\Delta CO}\right)} \tag{2}$$

All plumes were sampled directly overhead and likely underwent minimal photochemical aging, except for BRSF. In all cases, any aged plumes were removed using the ratio of maleic anhydride to furan (MA/F) <0.2 from the PTR-ToF-MS as a filter (Gkatzelis et al., 2023). While this photochemical clock cannot be directly related to OH exposure due to uncertainties in the chemical mechanism, Gkatzelis et al. (2023) showed that it was well correlated with physical smoke age and a ratio of 0.2 roughly corresponded to 30 min of aging. Applying this MA/F filter removed 40% of the BRSF plumes, 1 slash residue plume, and 4 corn residue plumes from the analysis. The average MA/F for agriculture residue (0.06 ± 0.03) was not statistically different than the MA/F for prescribed fires (0.05 ± 0.03) suggesting similar aging across fuel types.

Several instrument teams measured large suites of species, many of which may not be emitted from fires, such as human-made compounds like chlorofluorocarbons (CFCs). To determine whether species were emitted from the studied fires, either as part of the fuel itself or other associated sources of pollution such as heated soils or re-suspended applied/deposited chemicals, we assessed their relationship to CO using ordinary least squares regression and the Pearson correlation coefficient (r). While species may be formed after emission by a variety of different chemical or physical processes (e.g., oxidation by various mechanisms, rapid condensation) we expect all species emitted from a fire to scale with CO. We only report EFs for species where r^2 with CO was greater than 0.70, calculated for each individual plume. For the lower time resolution (>1 Hz) instruments, as it was more difficult to obtain strong correlations for narrow plumes, we did not report species with either a negative or negligible correlation ($r^2 < 0.2$) with CO across all fire plume data. Species with EFs obtained in only a few plumes at low concentrations such as 2-methyl-3-buten-2-ol (MBO) were also not reported. All species measured but not reported are listed by instrument in Table 3. Many species were co-measured by multiple instruments. Species with known interferences or unresolved isomers that were better resolved by other instrumentation are also listed in Table 3 and not reported for that instrument. For example, oxygenated NMVOCs (OVOCs) are a less robust measurement than NMVOCs for the WAS instrument (Simpson et al., 2011) so OVOCs from WAS were excluded. The measurement of ammonia required special consideration as the slope method described below does not account for the tailing of measured concentrations that occurred during plume sampling. Ammonia (and NH_x) EFs are therefore treated separately and described by Tomsche et al. (2023). Data from all FIREX-AQ instrumentation are available at https://asdc.larc.nasa.gov/project/FIREX-AQ.

The ER ($\Delta C_i/\Delta CO$) is often calculated by subtracting background values and taking the ratio of the difference of the excess mixing ratios (difference method). The ER may also be calculated from the slope between the species and CO (slope method). We used the slope method for data measured at 1 Hz or 5 Hz within the plume only and the difference method for instruments that measured at <1 Hz (TOGA-TOF, WAS, and iWAS). We defined the background as the measurement immediately prior to the plume interception. The average background CO was 140 ppb. As background samples were not always available for each plume for TOGA-TOF, WAS, and iWAS, we took the following approach. Background CO has the largest influence on the calculation of ER using the difference method, and therefore we used the value obtained by the DACOM instrument. The background value for individual NMVOCs was obtained from the closest instrument measurement (TOGA-TOF, WAS, iWAS) with CO at background concentration below 200 ppb. For comparison, the average difference method methane EF across all plumes (4.5 g kg^{-1}) was within 7% of the slope method (4.2 g kg^{-1}).

After removing plumes that were poorly characterized by the observations as described above, we obtained EFs for 228 individual plumes across 75 different fires (Table 1). There were 53 crop residue fires and 22 prescribed fires. Table 4 provides the average EFs for individual crop residue (corn, rice, soybean), and prescribed (slash, piles), and grassland fuels. Grassland EFs are presented separately as they had noticeable differences in EFs from other fuels as described further in Section 4. Hereafter, "prescribed fires" includes piles, slash, and shrubland.

Table 3
Measurements During FIREX-AQ That Were Not Used for Emission Factor Calculations

Instrument	Species
CU HR-ToF-AMS	Iodine[a], ClO_4[a], Bromine[a], Sea salt[a], MSA[a]
NCAR TOGA-TOF	C_2Cl_4[b], $CHCl_3$[b], $CHBr_3$[b], CH_2Br_2[b], $CHBrCl_2$[b], CH_3CCl_3[c], CH_2Cl_2[c], $CHBr_2Cl$[d], CH_2ClI[d], 1,2-Dichloroethane[b], HFC-134a[b], HCFC-22[b], HCFC-141b[c], HCFC-142b[c], Limonene/d3-Carene[d], Propane[d], Propene[d], MBO[d], Isopropyl nitrate[b], Isobutyl nitrate + 2-Butyl nitrate[b], CH_3CN[e], C_2H_5OH[b], Acrolein[e], Benzene[e], Toluene[e], CH_2O[f], CH_3CHO[e], Styrene[e]
NOAA iWAS	C_2Cl_4[b], $CHCl_3$[b], Cyclohexane[d], 3-Methylpentane[d], 2,2,4-Trimethylpentane[b], 2,2-Dimethylbutane[b], CH_3CN[e], Benzene[e], Toluene[e]
UCI WAS	C_2Cl_4[b], $CHCl_3$[b], $CHBr_3$[c], $CHBrCl_2$[c], $CHBr_2Cl$[c], CH_3CCl_3[b], C_2HCl_3[b], CCl_4[b], Chlorobenzene[d], Halon 1211[c], Halon 1301[b], Halon 2402[b], CFC-11[b], CFC-12[b], CFC-113[c], CFC-114[b], HCFC-22[b], HFC-134a[b],HFC-152a[b], HCFC-142b[b], HCFC-141b[b], HFC-365mfc[b], 2,3,4-Trimethylpentane[b], 1,2-Dichloroethane[b], Limonene[d], 2-Methylpentane[b], 3-Methylpentane[b], 2,3-Dimethylbutane[b], 2-Butyl nitrate[b], 3-Pentyl nitrate[b], Isopropyl nitrate[b], 3-Methyl-2-butyl nitrate[b], CH_3CN[e], Acrolein[e], Benzene[e], Toluene[e], Styrene[e], MVK[g], MACR[g], MEK[g], Methyl acetate[g], i-Butanal[g], Butanal[g], Furan[g]
NOAA CIMS	Cl_2[b], HPMTF[d], BrO[b], BrCN[b], BrCl[b]
CIT-CIMS	ISOPN[b]
NOAA PTR-ToF-MS	CH_2O[d], Phenol[h], Furan[i], Isoprene[j]

[a]Not reported in plumes due to interferences from OA. [b]Insignificant ($p > 0.05$) or weak ($r^2 < 0.2$) relationship with CO. [c]Significant ($p < 0.05$) negative relationship with CO. [d]Few (<5) or no valid observations. [e]All measurements agree thus we report the data for the NOAA PTR-ToF-MS only. [f]Not used in favor of the higher rate In Situ Airborne Formaldehyde (ISAF) and Compact Atmospheric Multispecies Spectrometer (CAMS) observations. [g]Disagrees with TOGA-TOF, and OVOCs are a less robust measurement than VOCs for the WAS group (Simpson et al., 2011). [h]Disagrees with CIT-CIMS, likely due to interference from fragmentation or contribution from additional isomers. [i]Disagrees with TOGA-TOF due to interferences. [j]Disagrees with TOGA-TOF, WAS, and iWAS, due to interference from aldehyde fragmentation.

The shrubland, winter wheat, and intensively-studied understory fire (BRSF) EFs are given in Table S1 of Supporting Information S2 as they represent only one fire each. We also provide the average crop residue EFs (including winter wheat) and average prescribed EFs (including shrubland) in Table 4. ERs are listed in Table S2 of Supporting Information S2. Different numbers of calculated EFs were obtained for different instruments. To address this, we calculated the average crop residue and prescribed EFs by weighting the fuel-specific average EFs by the fraction of that fuel listed in Table 1. Where data for a species was completely missing for a given fuel type, we used the corn residue value for crop residue fires and the pile or slash value for prescribed fires.

The EFs (Table 4, Table S1 in Supporting Information S2) and ERs (Table S2 in Supporting Information S2) for NMVOCs are presented as having either primarily near-field (shorter-lived: <6 hr) or farther afield (longer-lived: >6 hr) impacts determined by their lifetimes against reaction with OH (5×10^6 molecule cm^{-3}) and daytime (10–17 LT) photolysis frequencies from the NCAR CAFS instrument. These lifetimes are provided in Table S1 of Supporting Information S2. One species, 2,3-butanedione, has a significantly shorter lifetime against photolysis (~hours) than OH oxidation (days). Many of the species reported react with other oxidants such as the nitrate radical at night (Decker et al., 2019) but here we focus on daytime chemistry. To avoid calculating total NMVOC EF and ER for individual plumes that were missing data for important NMVOCs, we required that measurements were available for the four most abundant shorter-lived and longer-lived NMVOCs described further in Section 4. Table S3 in Supporting Information S2 lists the species included in the total NMVOC EF and ER.

We report a particulate matter <1 μm (PM_1) EF and ER that is the sum of BC, OA, ammonium, sulfate, nitrate, chloride, and potassium. We also report a particulate organic carbon (OC) EF that is determined by dividing the OA observations by the co-measured ratio of OA to OC for each plume. The average OA/OC was 1.9 ± 0.09 and was not significantly different between crop residue and prescribed fires. The OA/OC from the wildfires sampled during FIREX-AQ was 1.9 ± 0.2 (Gkatzelis et al., 2023). Both are higher than the value of 1.6 used by Andreae (2019) based on fresh biomass smoke and may represent some aging from the point of emission even though fires were sampled generally directly overhead.

The NOAA PTR-ToF-MS instrument measurements can have contributions from multiple individual NMVOCs in a single reported mass (Koss et al., 2018). Where measurements were available from other instruments that

Table 4.
Average Emission Factors (EF, g kg⁻¹) for Crop Residue and Prescribed Fires[1]

Names	Formula	Instrument[2]	Crop residue								Prescribed fuels							
			Corn	n	Rice	n	Soybean	n	Average[3,4]	n	Slash	n	Piles	n	Average[5]	n	Grassland	n
Methane	CH_4	DACOM	3.01 (1.24)	108	3.66 (1.68)	108	3.89 (0.708)	4	3.17 (0.948)	142	8.41 (2.48)	34	7.26 (3.31)	16	7.48 (2.03)	51	4.52 (0.742)	15
Carbon monoxide	CO	DACOM	65 (17)	108	85 (23)	108	86 (18)	4	71 (13)	142	125 (36)	34	108 (37)	16	113 (25)	51	113 (13)	15
Carbon dioxide	CO_2	NIR spect.	1,412 (29)	108	1,378 (40)	108	1,376 (29)	4	1,403 (22)	142	1,655 (63)	34	1,684 (66)	16	1,666 (44)	51	1,506 (23)	15
Shorter-lived NMVOC																		
Formaldehyde[6]	CH_2O	CAMS, ISAF	1.57 (0.597)	107	2.34 (0.870)	28	1.68 (0.257)	4	1.75 (0.471)	139	1.79 (0.454)	34	1.96 (0.696)	16	1.90 (0.413)	51	3.46 (0.527)	15
Propadiene	C_3H_4	WAS	0.011 (0.005)	50	0.017 (0.007)	13	0.023	1	0.013 (0.004)	64	0.013 (0.004)	10	0.014 (0.006)	5	0.013 (0.004)	16	0.063 (0.017)	4
Propene	C_3H_6	iWAS, WAS	0.343 (0.182)	69	0.681 (0.405)	15	0.413 (0.310)	2	0.423 (0.160)	86	0.585 (0.224)	17	0.525 (0.310)	6	0.537 (0.188)	24	0.671 (0.288)	9
Acetaldehyde	C_2H_4O	PTRMS[7]	2.09 (0.749)	81	3.81 (1.44)	20	3.32	1	2.54 (0.616)	103	1.96 (0.465)	27	2.34 (0.734)	11	2.17 (0.433)	39	4.07 (0.532)	10
1-Buten-3-yne	C_4H_4	WAS	0.011 (0.005)	47	0.015 (0.007)	12	0.024	1	0.013 (0.004)	60	0.012 (0.003)	10	0.015 (0.008)	4	0.013 (0.004)	15	0.062 (0.022)	4
1,2-Butadiene	C_4H_6	WAS	0.004 (0.001)	35	0.005 (0.003)	8	0.007	1	0.004 (0.001)	44	0.004 (0.001)	9	0.002	1	0.003 (0.0005)	11	0.012 (0.004)	4
2-Butyne	C_4H_6	WAS	0.002 (0.0007)	26	0.003 (0.0009)	3	NA	NA	0.002 (0.0006)	29	0.003 (0.002)	7	NA	NA	0.003 (0.002)	7	0.005 (0.002)	2
1,3-Butadiene	C_4H_6	WAS	0.096 (0.042)	50	0.157 (0.087)	13	0.201	1	0.116 (0.036)	64	0.126 (0.058)	10	0.135 (0.063)	5	0.125 (0.041)	16	0.323 (0.089)	4
1,3-Butadiyne	C_4H_2	WAS	8.73e-4 (5.25e-4)	19	0.001 (0.0008)	3	NA	NA	9.81e-4 (4.42e-4)	22	0.001 (0.0004)	3	NA	NA	0.001 (0.0004)	3	0.005 (0.002)	3
Acrolein	C_3H_4O	PTRMS	0.815 (0.296)	82	1.25 (0.479)	20	1.27	1	0.933 (0.233)	104	0.751 (0.180)	27	0.984 (0.328)	11	0.874 (0.189)	39	1.39 (0.190)	9
cis-2-Butene	C_4H_8	iWAS, WAS	0.02 (0.01)	67	0.033 (0.024)	15	0.016 (0.002)	2	0.023 (0.009)	84	0.033 (0.016)	15	0.032 (0.022)	6	0.032 (0.013)	22	0.018 (0.005)	9
i-Butene	C_4H_8	iWAS, WAS	0.085 (0.085)	68	0.154 (0.097)	16	0.078 (0.011)	2	0.100 (0.065)	86	0.142 (0.061)	17	0.109 (0.084)	6	0.121 (0.051)	24	0.120 (0.027)	9
trans-2-Butene	C_4H_8	iWAS, WAS	0.027 (0.018)	70	0.043 (0.025)	16	0.020 (0.003)	2	0.030 (0.014)	88	0.042 (0.021)	17	0.042 (0.031)	6	0.040 (0.019)	24	0.020 (0.006)	9
1-Butene	C_4H_8	iWAS, WAS	0.072 (0.04)	69	0.141 (0.088)	15	0.086 (0.074)	2	0.088 (0.035)	86	0.108 (0.041)	17	0.103 (0.058)	6	0.103 (0.035)	24	0.128 (0.060)	9
Glyoxal	$C_2H_2O_2$	ACES	0.401 (0.161)	103	0.464 (0.174)	20	0.464 (0.146)	4	0.419 (0.122)	127	0.241 (0.068)	28	0.291 (0.164)	11	0.265 (0.091)	40	0.717 (0.095)	13
Propanal	C_3H_6O	PTRMS, TOGA spec.[8]	0.222 (0.085)	81	0.383 (0.169)	20	0.314	1	0.262 (0.070)	103	0.229 (0.056)	27	0.303 (0.083)	11	0.268 (0.049)	39	0.419 (0.053)	9
Furan	C_4H_4O	TOGA	0.301 (0.258)	41	0.345 (0.233)	11	NA	NA	0.311 (0.206)	52	1.01 (0.540)	9	0.405	1	0.632 (0.222)	10	0.340 (0.137)	4
Cyclopentene	C_5H_8	WAS	0.005 (0.003)	34	0.008 (0.004)	11	NA	NA	0.006 (0.003)	45	0.010 (0.004)	6	0.009	1	0.009 (0.002)	7	0.017	1
Isoprene	C_5H_8	TOGA, iWAS, WAS	0.204 (0.291)	56	0.489 (0.509)	16	0.477 (0.594)	2	0.284 (0.241)	74	0.257 (0.212)	17	0.992 (0.802)	5	0.631 (0.433)	22	0.207 (0.175)	9
trans-1,3-Pentadiene	C_5H_8	iWAS, WAS	0.023 (0.012)	66	0.038 (0.028)	14	0.023 (0.008)	2	0.027 (0.011)	82	0.035 (0.019)	15	0.031 (0.010)	6	0.032 (0.010)	22	0.043 (0.013)	8
Methyl vinyl ketone	C_4H_6O	PTRMS, TOGA spec.[8]	0.432 (0.152)	81	0.810 (0.340)	21	0.632	1	0.526 (0.131)	104	0.527 (0.133)	23	0.615 (0.215)	12	0.562 (0.126)	36	0.606 (0.085)	10
Methacrolein	C_4H_6O	PTRMS, TOGA spec.[8]	0.114 (0.04)	81	0.281 (0.118)	21	0.2	1	0.156 (0.039)	104	0.171 (0.043)	23	0.138 (0.048)	12	0.150 (0.031)	36	0.177 (0.025)	10
2-Butenals	C_4H_6O	PTRMS, TOGA spec.[8]	0.292 (0.103)	81	0.448 (0.188)	21	0.353	1	0.328 (0.084)	104	0.199 (0.050)	23	0.296 (0.103)	12	0.249 (0.058)	36	0.651 (0.091)	10
2-Methyl-1-butene	C_5H_{10}	iWAS, WAS	0.018 (0.02)	66	0.034 (0.021)	15	0.016 (0.003)	2	0.021 (0.015)	83	0.028 (0.013)	17	0.024 (0.020)	6	0.025 (0.012)	24	0.020 (0.005)	9
3-Methyl-1-butene	C_5H_{10}	iWAS, WAS	0.011 (0.006)	66	0.022 (0.014)	16	0.010 (0.0001)	2	0.014 (0.005)	84	0.018 (0.007)	17	0.016 (0.010)	5	0.016 (0.006)	23	0.023 (0.004)	9
2-Methyl-2-butene	C_5H_{10}	WAS	0.008 (0.005)	36	0.019 (0.011)	10	NA	NA	0.010 (0.005)	46	0.014 (0.007)	7	0.025 (0.013)	2	0.019 (0.007)	9	0.009 (0.002)	2
1-Pentene	C_5H_{10}	iWAS, WAS	0.02 (0.013)	68	0.044 (0.023)	15	0.023 (0.014)	2	0.026 (0.011)	85	0.025 (0.008)	17	0.022 (0.011)	6	0.023 (0.007)	24	0.036 (0.010)	9
cis-2-Pentene	C_5H_{10}	iWAS, WAS	0.006 (0.003)	62	0.010 (0.005)	15	0.006 (0.0005)	2	0.007 (0.003)	79	0.010 (0.005)	16	0.009 (0.007)	5	0.009 (0.004)	22	0.009 (0.002)	7

Table 4
Continued

Names	Formula	Instrument[2]	Crop residue								Prescribed fuels							
			Corn	n	Rice	n	Soybean	n	Average[3,4]	n	Slash	n	Piles	n	Average[5]	n	Grassland	n
trans-2-Pentene	C5H10	iWAS, WAS	0.013 (0.011)	68	0.020 (0.010)	16	0.011 (0.0006)	2	0.015 (0.008)	86	0.017 (0.009)	17	0.015 (0.012)	5	0.016 (0.008)	23	0.011 (0.003)	9
Methylglyoxal[9]	C3H4O2	ACES	1.23 (0.538)	95	1.74 (0.837)	17	1.62 (0.462)	4	1.37 (0.430)	116	0.927 (0.299)	24	0.941 (0.486)	10	0.915 (0.285)	35	2.11 (0.445)	13
Butanal	C4H8O	PTRMS, TOGA spec.[8]	0.031 (0.013)	82	0.069 (0.032)	18	0.043	1	0.040 (0.011)	102	0.038 (0.011)	24	0.041 (0.013)	10	0.040 (0.008)	35	0.030 (0.004)	9
Isobutanal	C4H8O	PTRMS, TOGA spec.[8]	0.041 (0.017)	82	0.092 (0.043)	18	0.059	1	0.053 (0.015)	102	0.048 (0.014)	24	0.042 (0.013)	10	0.045 (0.009)	35	0.050 (0.006)	9
Ethene hydroxyperoxide	C2H6O3	CIT-CIMS	0.016 (0.008)	103	0.022 (0.016)	27	0.028 (0.012)	4	0.018 (0.007)	135	0.016 (0.006)	32	0.014 (0.006)	12	0.016 (0.004)	45	0.035 (0.006)	15
2-Methylfuran	C5H6O	TOGA	0.086 (0.096)	41	0.080 (0.066)	11	NA	NA	0.085 (0.076)	52	0.262 (0.192)	9	0.131	1	0.177 (0.079)	10	0.041 (0.026)	4
3-Methylfuran	C5H6O	TOGA	0.021 (0.019)	39	0.025 (0.015)	11	NA	NA	0.022 (0.015)	50	0.037 (0.024)	9	0.043	1	0.038 (0.010)	10	0.012 (0.008)	4
2(3H)-Furanone	C4H4O2	PTRMS	0.692 (0.266)	84	1.03 (0.511)	22	0.844	1	0.774 (0.219)	108	0.523 (0.127)	23	0.605 (0.256)	11	0.576 (0.145)	35	1.04 (0.139)	10
3,4-Methyl-1-pentene	C6H12	WAS	0.003 (0.002)	18	0.007 (0.005)	6	NA	NA	0.004 (0.002)	24	0.004 (0.002)	4	NA	NA	0.004 (0.002)	4	NA	NA
1-Hexene	C6H12	WAS	0.028 (0.025)	48	0.053 (0.032)	13	0.054	1	0.035 (0.020)	62	0.023 (0.009)	10	0.028 (0.016)	4	0.025 (0.009)	15	0.081 (0.021)	4
2,3-Butanedione + 2-Oxobutanal + 1,4-Butanedial[10]	C4H6O2	PTRMS	1.09 (0.414)	81	1.69 (0.695)	21	1.44	1	1.24 (0.329)	104	0.768 (0.231)	27	0.961 (0.431)	12	0.873 (0.247)	40	1.12 (0.215)	10
Phenol	C6H6O	CIT-CIMS	0.146 (0.058)	103	0.200 (0.085)	26	0.242 (0.064)	4	0.162 (0.045)	134	0.121 (0.037)	33	0.134 (0.047)	14	0.127 (0.029)	48	0.186 (0.037)	15
Furfural	C5H4O2	TOGA	0.481 (1.03)	37	0.044 (0.047)	6	NA	NA	0.382 (0.795)	43	0.046 (0.063)	7	0.626	1	0.350 (0.026)	8	0.017 (0.011)	4
2,5-Dimethylfuran + 2-Ethylfuran + unknown[11]	C6H8O	PTRMS	0.426 (0.172)	81	0.785 (0.361)	22	0.550 (0.046)	2	0.510 (0.145)	106	0.534 (0.205)	24	0.511 (0.166)	12	0.503 (0.122)	37	0.398 (0.071)	8
Methylcyclohexane	C7H14	iWAS, WAS	0.002 (0.005)	38	0.002 (0.003)	7	6.91e-4	1	0.002 (0.004)	46	0.005 (0.003)	15	0.015 (0.021)	4	0.010 (0.011)	20	0.010 (0.005)	8
1-Heptene	C7H14	WAS	0.014 (0.008)	41	0.026 (0.019)	13	0.024	1	0.018 (0.007)	55	0.012 (0.006)	10	0.018 (0.018)	3	0.015 (0.010)	14	0.034 (0.006)	3
Styrene	C8H8	PTRMS	0.053 (0.026)	69	0.111 (0.034)	17	0.102	1	0.068 (0.020)	88	0.074 (0.023)	19	0.105 (0.063)	8	0.086 (0.035)	27	0.183 (0.034)	8
Benzaldehyde	C7H6O	PTRMS	0.09 (0.032)	80	0.155 (0.049)	21	0.135 (0.042)	2	0.107 (0.025)	104	0.124 (0.026)	22	0.126 (0.040)	11	0.118 (0.024)	33	0.193 (0.032)	7
Ethylbenzene	C8H10	PTRMS, TOGA + WAS + iWAS spec.[12]	0.025 (0.01)	76	0.055 (0.026)	19	0.047	1	0.033 (0.009)	97	0.043 (0.015)	24	0.051 (0.032)	10	0.046 (0.018)	35	0.063 (0.013)	8
o-Xylene	C8H10	PTRMS, TOGA + WAS + iWAS spec.[12]	0.021 (0.009)	76	0.039 (0.019)	19	0.04	1	0.026 (0.007)	97	0.043 (0.015)	24	0.035 (0.022)	10	0.037 (0.013)	35	0.028 (0.006)	8
m,p-Xylene	C8H10	PTRMS, TOGA + WAS + iWAS spec.[12]	0.034 (0.014)	76	0.114 (0.054)	19	0.045	1	0.052 (0.016)	97	0.103 (0.035)	22	0.071 (0.044)	10	0.081 (0.028)	35	0.051 (0.010)	8
2-Methylphenol (=o-cresol) + Anisol[13]	C7H8O	PTRMS	0.539 (0.209)	83	0.896 (0.385)	22	0.81	1	0.629 (0.170)	107	0.765 (0.251)	26	0.658 (0.235)	11	0.678 (0.162)	38	0.608 (0.131)	10
Cresol	C7H8O	CIT-CIMS	0.094 (0.046)	96	0.131 (0.071)	26	0.124 (0.035)	4	0.103 (0.036)	127	0.134 (0.056)	31	0.115 (0.051)	11	0.120 (0.035)	43	0.093 (0.024)	14
Creosols	C8H10O2	PTRMS	0.176 (0.075)	77	0.241 (0.103)	22	0.242 (0.025)	2	0.192 (0.057)	102	0.509 (0.225)	23	0.296 (0.141)	9	0.370 (0.119)	33	0.172 (0.035)	9
5-Methylfurfural + Benzene diols (Catechol/Resorcinol)[14]	C6H6O2	PTRMS	1.08 (0.466)	79	1.76 (0.811)	22	1.60 (0.098)	2	1.26 (0.374)	104	1.67 (0.592)	24	1.33 (0.453)	11	1.42 (0.342)	36	1.35 (0.263)	9

Table 4
Continued

Names	Formula	Instrument[2]	Crop residue								Prescribed fuels							
			Corn	n	Rice	n	Soybean	n	Average[3,4]	n	Slash	n	Piles	n	Average[5]	n	Grassland	n
1-Octene	C_8H_{16}	WAS	0.011 (0.006)	40	0.022 (0.013)	11	0.02	1	0.014 (0.005)	52	0.013 (0.007)	9	0.013 (0.0007)	2	0.012 (0.003)	12	0.023 (0.007)	4
Benzofuran	C_8H_6O	PTRMS	0.066 (0.025)	73	0.100 (0.036)	19	0.1	1	0.075 (0.019)	94	0.086 (0.026)	19	0.090 (0.024)	9	0.083 (0.017)	28	0.119 (0.029)	6
C9 aromatics[15]	C_9H_{12}	PTRMS	0.041 (0.031)	57	0.117 (0.053)	17	0.038 (0.012)	2	0.058 (0.025)	76	0.088 (0.036)	25	0.105 (0.062)	9	0.092 (0.036)	34	0.063 (0.017)	8
1,2,4-Trimethylbenzene	C_9H_{12}	WAS	0.007 (0.004)	33	0.014 (0.011)	8	NA	NA	0.008 (0.004)	41	0.012 (0.006)	10	0.016 (0.006)	2	0.014 (0.004)	13	0.008	1
1,3,5-Trimethylbenzene	C_9H_{12}	WAS	0.002 (0.002)	18	0.002 (0.0000)	2	NA	NA	0.002 (0.001)	20	0.005 (0.0009)	4	0.003	1	0.004 (0.0004)	6	NA	NA
2-Ethyltoluene	C_9H_{12}	WAS	0.004 (0.002)	25	0.007 (0.007)	4	NA	NA	0.004 (0.002)	29	0.005 (0.002)	7	0.004	1	0.005 (0.0009)	9	0.006	1
3-Ethyltoluene	C_9H_{12}	WAS	0.006 (0.003)	35	0.012 (0.010)	7	NA	NA	0.007 (0.004)	42	0.011 (0.006)	10	0.024 (0.020)	3	0.017 (0.011)	14	0.010 (0.0001)	2
4-Ethyltoluene	C_9H_{12}	WAS	0.006 (0.007)	29	0.009 (0.008)	5	NA	NA	0.006 (0.006)	34	0.006 (0.003)	8	0.006	1	0.006 (0.001)	10	0.006	1
i-Propylbenzene[16]	C_9H_{12}	WAS	0.002 (0.001)	14	0.001 (0.0002)	2	NA	NA	0.002 (0.0010)	16	0.004 (0.001)	6	0.003	1	0.003 (0.0005)	7	0.006	1
n-Propylbenzene[14]	C_9H_{12}	WAS	0.003 (0.002)	27	0.007 (0.005)	5	0.004 (0.001)	2	0.004 (0.002)	32	0.004 (0.001)	7	0.003	1	0.004 (0.0005)	9	0.006	1
Guaiacol	$C_7H_8O_2$	PTRMS	0.565 (0.226)	81	0.850 (0.343)	22	0.75	1	0.633 (0.176)	105	0.885 (0.347)	24	0.685 (0.286)	11	0.748 (0.208)	36	0.452 (0.162)	9
1-Nonene	C_9H_{18}	WAS	0.008 (0.006)	36	0.016 (0.013)	9	0.013	1	0.010 (0.005)	46	0.009 (0.003)	8	0.011 (0.009)	2	0.010 (0.005)	11	0.024 (0.010)	3
Naphthalene	$C_{10}H_8$	PTRMS	0.046 (0.033)	57	0.140 (0.109)	14	0.082	1	0.069 (0.034)	73	0.084 (0.030)	14	0.100 (0.029)	5	0.088 (0.020)	19	0.245 (0.045)	6
n-Nonane	C_9H_{20}	iWAS, WAS	0.008 (0.014)	58	0.014 (0.015)	13	0.007	1	0.009 (0.010)	72	0.010 (0.006)	16	0.016 (0.013)	4	0.013 (0.007)	21	0.008 (0.003)	8
Monoterpenes[17]	$C_{10}H_{16}$	PTRMS	0.022 (0.023)	30	0.283 (0.168)	17	0.072	1	0.084 (0.042)	48	0.581 (0.602)	21	1.00 (0.913)	3	0.771 (0.543)	24	0.182 (0.098)	7
α-pinene	$C_{10}H_{16}$	TOGA, iWAS, WAS	0.01 (0.022)	41	0.041 (0.058)	4	0.004 (0.001)	2	0.016 (0.020)	47	0.189 (0.160)	18	0.178 (0.337)	5	0.172 (0.190)	23	0.021 (0.017)	8
β-Pinene/Myrcene	$C_{10}H_{16}$	TOGA, WAS	0.008 (0.011)	31	0.023 (0.032)	3	0.011	1	0.012 (0.011)	35	0.026 (0.021)	12	0.102 (0.146)	4	0.065 (0.078)	16	0.015 (0.005)	2
β-Pinene	$C_{10}H_{16}$	WAS	0.006 (0.012)	19	0.030 (0.041)	2	0.011	1	0.012 (0.013)	22	0.035 (0.015)	7	0.093 (0.128)	3	0.064 (0.068)	10	0.012 (0.0002)	2
Myrcene	$C_{10}H_{16}$	WAS	0.003 (0.002)	14	0.005 (0.005)	2	NA	NA	0.003 (0.002)	16	0.007 (0.006)	5	0.038 (0.038)	3	0.023 (0.020)	8	0.007	1
Camphene	$C_{10}H_{16}$	TOGA, WAS	0.006 (0.007)	4	0.004	1	NA	NA	0.006 (0.006)	5	0.024 (0.039)	16	0.043 (0.034)	2	0.032 (0.024)	18	0.011 (0.003)	4
Tricyclene[14]	$C_{10}H_{16}$	TOGA, WAS	0.01 (0.032)	28	0.003 (0.002)	3	NA	NA	0.008 (0.024)	31	0.009 (0.014)	15	0.022 (0.028)	3	0.015 (0.016)	18	0.005 (0.002)	5
1-Decene	$C_{10}H_{20}$	WAS	0.008 (0.005)	36	0.024 (0.024)	8	0.011	1	0.012 (0.006)	45	0.008 (0.004)	8	0.014 (0.006)	3	0.011 (0.003)	12	0.019 (0.003)	4
n-Decane	$C_{10}H_{22}$	iWAS, WAS	0.008 (0.013)	52	0.010 (0.008)	10	0.009	1	0.009 (0.010)	63	0.010 (0.007)	15	0.010 (0.008)	4	0.010 (0.005)	20	0.013 (0.005)	7
Syringol	$C_8H_{10}O_3$	PTRMS	0.134 (0.073)	70	0.121 (0.045)	16	0.175 (0.104)	2	0.133 (0.054)	88	0.188 (0.096)	18	0.145 (0.095)	9	0.155 (0.064)	28	0.060 (0.028)	7
n-Undecane	$C_{11}H_{24}$	WAS	0.004 (0.002)	22	0.006 (0.006)	3	NA	NA	0.004 (0.002)	25	0.004 (0.002)	3	0.013 (0.007)	2	0.009 (0.004)	6	0.028 (0.029)	2
Longer-lived NMVOCs																		
Ethyne	C_2H_2	iWAS, WAS	0.171 (0.104)	68	0.318 (0.166)	15	0.272 (0.312)	2	0.210 (0.085)	85	0.162 (0.070)	17	0.211 (0.069)	6	0.189 (0.047)	24	0.971 (0.651)	9
Ethene	C_2H_4	iWAS, WAS	0.745 (0.38)	69	1.50 (0.669)	15	1.09 (1.05)	2	0.936 (0.317)	86	1.03 (0.295)	17	1.07 (0.363)	6	1.04 (0.227)	24	2.90 (1.22)	9
Ethane	C_2H_6	CAMS, WAS, iWAS	0.481 (0.318)	89	0.683 (0.356)	25	0.569 (0.203)	3	0.532 (0.242)	117	0.949 (0.303)	29	0.879 (0.433)	13	0.891 (0.261)	43	0.464 (0.195)	15
Methanol	CH_4O	PTRMS	1.34 (0.581)	81	1.71 (0.746)	20	4.69 (4.68)	2	1.60 (0.513)	104	2.27 (0.701)	26	2.10 (0.686)	12	2.14 (0.464)	39	1.11 (0.296)	10
Propyne	C_3H_4	WAS	0.04 (0.018)	51	0.057 (0.029)	13	0.065	1	0.045 (0.015)	65	0.049 (0.017)	10	0.052 (0.018)	5	0.050 (0.012)	16	0.186 (0.058)	4
Propane	C_3H_8	iWAS, WAS	0.147 (0.102)	67	0.212 (0.212)	15	0.192 (0.140)	2	0.164 (0.088)	84	0.295 (0.121)	17	0.248 (0.217)	6	0.263 (0.125)	24	0.086 (0.076)	7
Formic acid	CH_2O_2	NOAA CIMS, PTRMS	0.522 (0.288)	79	0.721 (0.427)	26	0.777 (0.421)	3	0.583 (0.225)	109	0.414 (0.114)	28	0.652 (0.325)	13	0.604 (0.178)	42	0.901 (0.264)	13

Table 4
Continued

Names	Formula	Instrument[2]	Crop residue								Prescribed fuels							
			Corn	n	Rice	n	Soybean	n	Average[3,4]	n	Slash	n	Piles	n	Average[5]	n	Grassland	n
Ethanol	C_2H_6O	PTRMS	0.203 (0.315)	15	0.292 (0.202)	2	0.626	1	0.257 (0.225)	19	0.161 (0.069)	11	0.690	1	0.431 (0.029)	12	0.309 (0.257)	2
1-Butyne	C_4H_6	WAS	0.005 (0.002)	39	0.007 (0.003)	9	0.012	1	0.006 (0.002)	49	0.005 (0.001)	9	0.006 (0.003)	3	0.006 (0.002)	13	0.016 (0.004)	4
Acetone	C_3H_6O	PTRMS, TOGA spec.[8]	0.65 (0.248)	81	1.19 (0.527)	20	0.856	1	0.779 (0.210)	103	0.856 (0.209)	27	0.776 (0.212)	11	0.798 (0.141)	39	0.713 (0.091)	9
n-Butane	C_4H_{10}	TOGA, iWAS, WAS	0.048 (0.057)	72	0.086 (0.082)	16	0.056 (0.047)	2	0.057 (0.045)	90	0.075 (0.038)	20	0.061 (0.034)	5	0.066 (0.024)	26	0.062 (0.042)	7
Isobutane	C_4H_{10}	TOGA, iWAS, WAS	0.012 (0.015)	65	0.017 (0.016)	17	0.022 (0.022)	2	0.013 (0.012)	84	0.028 (0.013)	20	0.023 (0.016)	5	0.024 (0.010)	26	0.012 (0.009)	9
Methyl formate	$C_2H_4O_2$	TOGA, iWAS	0.041 (0.058)	62	0.045 (0.026)	15	0.027	1	0.041 (0.042)	78	0.048 (0.025)	17	0.038 (0.030)	5	0.044 (0.019)	23	0.037 (0.016)	7
Acetic acid + Glycolaldehyde[18]	$C_2H_4O_2$	PTRMS	1.87 (0.81)	82	2.60 (1.23)	21	2.12	1	2.03 (0.631)	105	1.87 (0.871)	27	1.94 (0.598)	12	1.94 (0.478)	40	2.36 (0.405)	9
Isopropanol	C_3H_8O	TOGA, WAS	0.009 (0.011)	51	0.010 (0.008)	13	0.005	1	0.009 (0.008)	65	0.008 (0.005)	11	0.007 (0.004)	3	0.007 (0.003)	15	0.013 (0.007)	5
Cyclopentane	C_5H_{10}	WAS	0.002 (0.002)	26	0.003 (0.003)	6	NA	NA	0.002 (0.002)	32	0.002 (0.001)	6	0.002	1	0.002 (0.0005)	7	0.005 (0.003)	3
Methyl ethyl ketone	C_4H_8O	PTRMS, TOGA spec.[8]	0.198 (0.08)	82	0.323 (0.152)	18	0.22	1	0.225 (0.066)	102	0.216 (0.061)	24	0.217 (0.068)	10	0.214 (0.044)	35	0.149 (0.019)	9
Isopentane	C_5H_{12}	TOGA, iWAS, WAS	0.015 (0.027)	63	0.033 (0.048)	15	0.024 (0.028)	2	0.020 (0.022)	80	0.022 (0.019)	20	0.029 (0.008)	4	0.025 (0.009)	25	0.024 (0.015)	9
n-Pentane	C_5H_{12}	TOGA, iWAS, WAS	0.018 (0.019)	69	0.041 (0.047)	16	0.021 (0.018)	2	0.024 (0.017)	87	0.029 (0.018)	20	0.034 (0.002)	4	0.031 (0.008)	25	0.042 (0.027)	9
Hydroxyacetone + Methyl acetate + Ethyl formate[19]	$C_3H_6O_2$	PTRMS	1.92 (0.72)	82	3.03 (1.31)	21	2.56	1	2.19 (0.583)	105	1.39 (0.378)	26	1.74 (0.880)	12	1.61 (0.491)	39	2.22 (0.356)	9
Methyl acetate	$C_3H_6O_2$	TOGA	0.38 (0.369)	41	0.468 (0.364)	11	NA	NA	0.400 (0.297)	52	0.540 (0.274)	9	0.839	1	0.667 (0.113)	10	0.125 (0.042)	4
Benzene	C_6H_6	PTRMS	0.283 (0.123)	78	0.545 (0.171)	20	0.711	1	0.364 (0.094)	100	0.561 (0.154)	26	0.545 (0.159)	11	0.519 (0.105)	37	1.29 (0.194)	9
Methylcyclopentane	C_6H_{12}	iWAS, WAS	0.004 (0.007)	55	0.008 (0.010)	13	0.001 (0.0007)	2	0.005 (0.006)	70	0.004 (0.002)	15	0.010 (0.008)	3	0.007 (0.004)	19	0.007 (0.009)	8
Cyclohexane	C_6H_{12}	WAS	0.004 (0.005)	37	0.013 (0.010)	7	0.007	1	0.006 (0.004)	45	0.004 (0.002)	10	0.010 (0.005)	2	0.007 (0.003)	13	0.017 (0.006)	4
3-Methylpentane	C_6H_{14}	TOGA	0.003 (0.004)	37	0.004 (0.004)	6	NA	NA	0.004 (0.003)	43	0.004 (0.003)	8	0.007	1	0.005 (0.001)	9	0.008 (0.006)	4
2-Methylpentane	C_6H_{14}	TOGA, iWAS, WAS	0.011 (0.035)	61	0.007 (0.009)	12	0.002	1	0.009 (0.025)	74	0.008 (0.005)	19	0.011 (0.004)	5	0.009 (0.003)	25	0.016 (0.016)	8
n-Hexane	C_6H_{14}	TOGA, iWAS, WAS	0.016 (0.02)	70	0.021 (0.018)	17	0.006 (0.003)	2	0.016 (0.015)	89	0.018 (0.007)	20	0.020 (0.012)	6	0.019 (0.007)	27	0.028 (0.019)	10
Propene hydroxyperoxide	$C_3O_3H_8$	CIT-CIMS	0.022 (0.014)	99	0.022 (0.013)	26	0.032 (0.019)	4	0.022 (0.010)	130	0.008 (0.003)	25	0.016 (0.009)	6	0.013 (0.005)	32	0.012 (0.002)	15
Toluene	C_7H_8	PTRMS*	0.209 (0.083)	80	0.439 (0.190)	20	0.349	1	0.266 (0.072)	102	0.384 (0.131)	26	0.340 (0.181)	11	0.347 (0.110)	38	0.427 (0.071)	9
Maleic anhydride	$C_4H_2O_3$	PTRMS*	0.06 (0.038)	76	0.078 (0.052)	18	0.065 (0.008)	2	0.064 (0.029)	97	0.061 (0.030)	24	0.086 (0.042)	11	0.080 (0.026)	36	0.109 (0.050)	10
2,3-Dimethylpentane	C_7H_{16}	WAS	0.014 (0.033)	12	NA	NA	NA	NA	0.014 (0.033)	12	0.002 (0.0009)	5	0.002	1	0.002 (0.0004)	6	0.004 (0.003)	4
2,4-Dimethylpentane	C_7H_{16}	iWAS	0.011 (0.007)	40	0.014 (0.015)	7	0.012	1	0.012 (0.006)	48	0.028 (0.011)	11	0.022 (0.019)	4	0.024 (0.011)	16	0.006 (0.001)	6
2-Methylhexane	C_7H_{16}	WAS	0.008 (0.015)	20	0.013 (0.017)	2	NA	NA	0.009 (0.012)	22	0.003 (0.002)	9	0.013 (0.005)	2	0.008 (0.003)	11	0.007 (0.002)	4
3-Methylhexane	C_7H_{16}	WAS	0.006 (0.01)	16	0.005 (0.005)	4	NA	NA	0.005 (0.008)	20	0.004 (0.004)	10	0.017 (0.004)	2	0.011 (0.002)	12	0.013 (0.007)	4
n-Heptane	C_7H_{16}	TOGA, WAS	0.013 (0.013)	56	0.028 (0.034)	11	0.004	1	0.016 (0.012)	68	0.019 (0.011)	16	0.025 (0.009)	5	0.021 (0.007)	22	0.041 (0.023)	7
Ethynylbenzene	C_8H_6	TOGA, WAS	0.009 (0.008)	55	0.012 (0.010)	11	0.014	1	0.010 (0.006)	67	0.006 (0.003)	14	0.014 (0.012)	3	0.010 (0.006)	18	0.049 (0.019)	7

Table 4
Continued

Names	Formula	Instrument[2]	Crop residue								Prescribed fuels							
			Corn	n	Rice	n	Soybean	n	Average[3,4]	n	Slash	n	Piles	n	Average[5]	n	Grassland	n
2,2,4-Trimethylpentane	C$_8$H$_{18}$	TOGA, iWAS, WAS	0.005 (0.013)	46	0.004 (0.004)	11	0.002	1	0.005 (0.009)	58	0.002 (0.002)	17	0.008 (0.012)	5	0.005 (0.007)	23	0.004 (0.002)	7
n-Octane	C$_8$H$_{18}$	TOGA, iWAS, WAS	0.008 (0.007)	58	0.017 (0.016)	11	NA	NA	0.010 (0.007)	69	0.010 (0.006)	16	0.020 (0.011)	3	0.015 (0.006)	20	0.013 (0.005)	7
Hydroxybenzoquinone	C$_6$H$_4$O$_3$	PTRMS	0.125 (0.07)	79	0.183 (0.115)	22	0.124 (0.017)	2	0.137 (0.055)	104	0.147 (0.047)	21	0.146 (0.051)	11	0.146 (0.033)	33	0.159 (0.022)	9
ΣShorter-lived NMVOC[20]	N/A[21]	Table S3 in Supporting Information S2	13.65 (4.45)	68	23.16 (8.44)	12	18.71	1	16.09 (3.72)	81	14.39 (5.25)	20	13.68 (5.22)	7	13.77 (3.51)	28	19.52 (3.17)	9
ΣLonger-lived NMVOC	N/A	Table S3 in Supporting Information S2	8.79 (3.01)	77	13.72 (4.84)	19	12.75	1	10.05 (2.37)	98	10.04 (2.96)	26	10.16 (2.92)	11	10.16 (1.97)	38	12.86 (2.35)	9
Nitrogen-containing Species																		
Hydrogen cyanide	HCN	NOAA CIMS, CIT-CIMS, PTRMS, TOGA	0.257 (0.145)	105	0.477 (0.255)	29	0.295 (0.154)	4	0.310 (0.117)	139	0.229 (0.167)	34	0.399 (0.408)	15	0.313 (0.227)	50	0.786 (0.222)	15
Nitrogen oxide	NO	NOAA LIF, NOAA NOyO3	0.36 (0.271)	106	0.280 (0.289)	29	0.167 (0.042)	4	0.342 (0.200)	140	0.087 (0.065)	34	0.155 (0.066)	16	0.118 (0.044)	51	0.148 (0.093)	15
Nitrogen dioxide	NO$_2$	ACES, NOAA NOyO3	1.83 (0.586)	105	1.72 (0.569)	23	1.27 (0.123)	4	1.84 (0.429)	133	1.03 (0.468)	34	1.19 (0.466)	14	1.06 (0.313)	49	1.35 (0.306)	15
NOx (as NO)	NO	NOAA LIF, NOAA NO$_y$O$_3$	1.55 (0.531)	104	1.36 (0.490)	23	0.995 (0.103)	4	1.53 (0.387)	132	0.758 (0.347)	34	0.933 (0.341)	14	0.810 (0.230)	49	1.03 (0.242)	15
Acetonitrile	CH$_3$CN	PTRMS	0.228 (0.115)	81	0.529 (0.261)	21	0.647 (0.426)	2	0.319 (0.103)	105	0.170 (0.067)	25	0.199 (0.086)	11	0.184 (0.053)	37	0.383 (0.060)	9
Isocyanic acid	HNCO	NOAA CIMS, PTRMS	0.441 (0.201)	88	0.690 (0.424)	27	0.355 (0.332)	4	0.497 (0.171)	120	0.322 (0.264)	29	0.639 (0.329)	12	0.471 (0.206)	41	1.05 (0.388)	13
Nitrous acid	HONO	ACES, NOAA CIMS	0.387 (0.139)	96	0.379 (0.157)	25	0.421 (0.120)	3	0.388 (0.103)	125	0.311 (0.142)	30	0.403 (0.196)	12	0.341 (0.119)	42	0.638 (0.193)	13
Acrylonitrile	C$_3$H$_3$N	PTRMS, TOGA, WAS, iWAS	0.056 (0.04)	95	0.082 (0.031)	24	0.047 (0.050)	2	0.061 (0.029)	122	0.043 (0.036)	28	0.045 (0.024)	12	0.045 (0.019)	41	0.181 (0.119)	13
Propionitrile	C$_3$H$_4$N	TOGA, WAS	0.035 (0.032)	134	0.060 (0.051)	32	0.032	2	0.041 (0.026)	168	0.018 (0.006)	28	0.026 (0.013)	8	0.022 (0.007)	38	0.080 (0.035)	14
Nitromethane	CH$_3$NO$_2$	PTRMS	0.056 (0.016)	76	0.080 (0.026)	16	0.078	1	0.062 (0.013)	94	0.053 (0.014)	19	0.075 (0.044)	10	0.061 (0.024)	29	0.145 (0.015)	8
Pyrrole + Butenenitrile[22]	C$_4$H$_5$N	PTRMS	0.085 (0.042)	81	0.199 (0.097)	18	0.257 (0.170)	2	0.119 (0.038)	102	0.042 (0.015)	23	0.062 (0.032)	10	0.051 (0.018)	34	0.150 (0.027)	9
Pyrrole	C$_4$H$_5$N	TOGA	0.027 (0.028)	28	0.008	1	NA	NA	0.023 (0.022)	29	0.009 (0.007)	2	0.015	1	0.012 (0.003)	3	NA	NA
Methyl nitrate	CH$_3$NO$_3$	TOGA, WAS	0.003 (0.003)	64	0.003 (0.002)	15	0.003	1	0.003 (0.002)	80	0.001 (0.0007)	16	0.003 (0.002)	4	0.002 (0.001)	21	0.004 (0.002)	7
Ethyl nitrate	C$_2$H$_5$NO$_3$	TOGA, WAS	6.05e-4 (4.96e-4)	54	0.002 (0.003)	12	9.74e-5	1	8.37e-4 (7.23e-4)	67	4.88e-4 (4.85e-4)	13	7.29e-4 (2.14e-5)	3	6.45e-4 (2.00e-4)	17	8.78e-4 (9.46e-4)	5
Methacrylonitrile	C$_4$H$_5$N	TOGA	0.016 (0.01)	36	0.031 (0.017)	10	NA	NA	0.020 (0.009)	46	0.014 (0.007)	8	NA	NA	0.014 (0.007)	8	0.049 (0.025)	4
Benzonitrile	C$_7$H$_5$N	PTRMS	0.032 (0.016)	76	0.076 (0.033)	18	0.040 (0.003)	2	0.042 (0.013)	97	0.040 (0.013)	20	0.043 (0.012)	8	0.041 (0.008)	29	0.073 (0.011)	8
n-Propyl nitrate	C$_3$H$_7$NO$_3$	WAS	1.21e-4 (1.46e-4)	41	2.68e-4 (3.08e-4)	8	3.82e-5	1	1.50e-4 (1.26e-4)	50	2.40e-4 (2.39e-4)	6	3.88e-4 (3.74e-4)	3	3.18e-4 (1.00e-4)	10	3.99e-4 (3.36e-4)	3

Table 4
Continued

Names	Formula	Instrument[2]	Corn	n	Rice	n	Soybean	n	Average[3,4]	n	Slash	n	Piles	n	Average[5]	n	Grassland	n
			Crop residue								Prescribed fuels							
Ethene hydroxynitrate	$C_2O_4H_5N$	CIT-CIMS	0.001 (0.0009)	46	0.001 (0.0006)	10	0.001 (0.0002)	2	0.001 (0.0007)	58	0.001 (0.0008)	5	2.47e-4	1	6.07e-4 (3.39e-4)	6	0.002 (0.0009)	10
Dinitrogen pentoxide	N_2O_5	NOAA CIMS	1.23e-4 (9.63e-5)	32	2.36e-4 (1.41e-4)	6	NA	NA	1.49e-4 (8.10e-5)	38	2.73e-4 (1.29e-4)	4	8.15e-5	1	1.56e-4 (5.31e-5)	5	4.18e-4 (3.83e-4)	5
Propene hydroxynitrate	$C_3O_4H_7N$	CIT-CIMS	0.002 (0.001)	70	0.002 (0.002)	16	0.002 (0.0004)	3	0.002 (0.0010)	89	0.002 (0.001)	19	0.002 (0.001)	4	0.002 (0.0008)	23	0.002 (0.0006)	11
Butene hydroxynitrates	$C_4H_9NO_4$	CIT-CIMS	0.003 (0.002)	62	0.005 (0.005)	12	0.002 (0.0006)	3	0.003 (0.002)	77	0.004 (0.004)	17	0.006 (0.008)	6	0.005 (0.005)	23	0.003 (0.0007)	8
Nitrophenol	$C_6H_5NO_3$	CIT-CIMS	0.004 (0.002)	23	0.007 (0.003)	5	NA	NA	0.005 (0.002)	29	0.004 (0.001)	2	NA	NA	0.004 (0.001)	2	0.006 (0.001)	2
Nitrocresol	$C_7H_7NO_3$	CIT-CIMS	0.006 (0.003)	69	0.011 (0.008)	16	0.006 (0.001)	2	0.007 (0.003)	88	0.006 (0.003)	14	0.006 (0.002)	4	0.006 (0.002)	19	0.009 (0.002)	10
Nitrocatechol	$C_6H_5NO_4$	CIT-CIMS	0.013 (0.007)	83	0.019 (0.008)	20	0.017 (0.006)	3	0.015 (0.005)	107	0.009 (0.003)	20	0.012 (0.006)	6	0.011 (0.003)	27	0.012 (0.003)	11
Nitromethylcatechol	$C_7H_7NO_4$	CIT-CIMS	0.006 (0.003)	76	0.008 (0.004)	16	0.010 (0.006)	4	0.007 (0.002)	96	0.005 (0.004)	18	0.005 (0.002)	5	0.006 (0.002)	24	0.007 (0.001)	10
NOy	NO_y	NOAA NO,O_3	NA	NA	NA	NA	NA	NA	NA	NA	NA	NA	NA	NA	NA	NA	NA	NA
Halogenated Species																		
Methyl chloride	CH_3Cl	WAS	0.516 (0.41)	51	0.497 (0.402)	12	0.094	1	0.488 (0.308)	64	0.024 (0.017)	8	0.094 (0.099)	4	0.095 (0.053)	13	0.162 (0.120)	4
Chloroethane	C_2H_5Cl	WAS	0.002 (0.002)	47	0.002 (0.002)	12	NA	NA	0.002 (0.001)	59	6.2e-4 (7.36e-4)	5	0.001 (0.002)	4	0.001 (0.0009)	10	0.001 (0.0004)	3
Nitryl chloride	$ClNO_2$	NOAA CIMS	1.59e-4 (1.22e-4)	33	1.64e-4 (6.21e-5)	9	5.88e-5	1	1.55e-4 (8.87e-5)	43	3.58e-5 (1.90e-5)	6	2.75e-4 (3.22e-4)	2	1.61e-4 (1.71e-4)	8	1.03e-4 (2.55e-5)	7
Dichloromethane[23]	CH_2Cl_2	TOGA, WAS	0.004 (0.008)	32	0.009 (0.014)	10	NA	NA	0.005 (0.007)	42	NA	NA	NA	NA	NA	NA	NA	NA
Chloroacetic acid	$C_2H_3O_2Cl$	NOAA CIMS	8.98e-5 (4.75e-5)	16	1.82e-4 (1.67e-4)	2	5.58e-5	1	1.09e-4 (5.08e-5)	19	NA	NA	3.94e-4 (3.75e-4)	2	3.94e-4 (3.75e-4)	2	2.67e-4 (2.07e-4)	2
Methyl bromide	CH_3Br	TOGA, WAS	0.002 (0.002)	63	0.008 (0.005)	15	NA	NA	0.004 (0.002)	78	5.45e-4 (3.78e-4)	14	0.006 (0.004)	3	0.003 (0.002)	18	0.005 (0.003)	6
Chlorobenzene	C_6H_5Cl	TOGA	5.39e-4 (4.86e-4)	35	0.001 (0.0008)	8	NA	NA	6.56e-4 (4.20e-4)	43	2.46e-4 (2.44e-4)	7	9.79e-4	1	6.20e-4 (1.00e-4)	8	4.56e-4 (1.97e-4)	3
Methyl iodide	CH_3I	TOGA, WAS	7.62e-4 (8.51e-4)	61	0.002 (0.002)	15	3.26e-4	1	0.001 (0.0007)	77	0.001 (0.0007)	16	0.003 (0.004)	5	0.002 (0.002)	22	0.001 (0.0006)	7
Dibromomethane	CH_2Br_2	WAS	0.001 (0.0007)	48	0.002 (0.002)	12	0.002	1	0.001 (0.0006)	61	9.89e-4 (7.84e-4)	10	0.001 (0.0002)	5	0.001 (0.0003)	16	0.001 (0.0003)	3
Aerosols																		
Black carbon	BC	NOAA SP2	0.129 (0.065)	44	0.091 (0.102)	8	0.118 (0.068)	2	0.120 (0.052)	54	0.180 (0.144)	16	0.265 (0.222)	11	0.219 (0.132)	28	0.309 (0.154)	9
Organic carbon	OC	AMS	8.25 (4.02)	100	15.29 (8.08)	23	9.24 (2.12)	3	9.88 (3.35)	127	11.58 (4.88)	19	8.94 (4.12)	15	10.14 (2.97)	35	14.22 (2.02)	12
Organic aerosol	OA	AMS	16.02 (7.93)	100	28.11 (14.83)	23	17.83 (4.51)	3	18.85 (6.48)	127	22.47 (9.84)	19	17.69 (8.37)	15	19.96 (6.00)	35	27.34 (3.98)	12
Levoglucosan[24]	$C_6H_{10}O_5$	EESI	2.06 (0.989)	36	2.08 (1.24)	12	1.31	1	2.02 (0.763)	49	5.49 (3.02)	19	4.11 (2.35)	6	4.44 (1.76)	25	3.20 (0.575)	13
4-Nitrocatechol	$C_6H_5NO_4$	EESI	0.021 (0.015)	47	0.056 (0.057)	5	0.016 (0.001)	2	0.028 (0.017)	54	0.059 (0.079)	13	0.042 (0.025)	9	0.052 (0.035)	23	0.043 (0.022)	8
Ammonium[25]	NH_4	AMS	0.614 (0.441)	96	0.538 (0.533)	20	0.209 (0.120)	3	0.567 (0.331)	120	0.111 (0.066)	15	0.155 (0.170)	11	0.184 (0.094)	27	0.296 (0.102)	11
Chloride	Cl	AMS	1.34 (0.905)	97	1.08 (0.829)	23	0.599 (0.199)	3	1.22 (0.659)	124	0.039 (0.020)	12	0.208 (0.246)	12	0.169 (0.131)	25	0.425 (0.091)	12
Potassium	K	AMS	0.391 (0.217)	94	0.327 (0.259)	18	0.288 (0.061)	3	0.365 (0.162)	116	0.044 (0.010)	10	0.127 (0.103)	6	0.085 (0.055)	16	0.136 (0.036)	10
Nitrate[26]	NO_3	AMS	0.401 (0.323)	100	0.590 (0.517)	23	0.330 (0.049)	3	0.442 (0.254)	127	0.465 (0.211)	18	0.420 (0.259)	15	0.487 (0.162)	34	0.716 (0.176)	12
Sulfate	SO_4	AMS	0.105 (0.137)	55	0.259 (0.345)	12	0.067 (0.0000)	2	0.138 (0.126)	69	0.060 (0.006)	6	0.097 (0.106)	2	0.123 (0.056)	9	0.251 (0.038)	5

Table 4
Continued

Names	Formula[2]	Instrument[2]	Crop residue								Prescribed fuels							
			Corn	n	Rice	n	Soybean	n	Average[3,4]	n	Slash	n	Piles	n	Average[5]	n	Grassland	n
PM_1[27]	NA	AMS	18.8 (8.56)	100	30.66 (15.62)	23	19.38 (4.58)	3	21.47 (6.95)	127	23.14 (10.03)	19	18.65 (8.46)	15	20.97 (6.09)	35	29.19 (4.29)	12
CN > 3 nm[28] (1E15)	N/A	LARGE	5.34 (2.34)	79	6.41 (2.66)	19	5.90 (1.48)	3	5.61 (1.78)	101	4.57 (1.14)	28	5.52 (1.73)	15	5.04 (1.03)	44	5.84 (1.75)	10
Sulfur-containing Species																		
Methanethiol	CH_3SH	TOGA	0.021 (0.021)	41	0.055 (0.046)	11	NA	NA	0.028 (0.019)	52	0.009 (0.004)	9	0.033	1	0.021 (0.001)	10	0.038 (0.010)	4
Sulfur dioxide	SO_2	NOAA LIF	0.906 (0.28)	105	0.883 (0.230)	29	0.625 (0.226)	4	0.894 (0.203)	139	0.343 (0.223)	30	0.530 (0.333)	16	0.430 (0.198)	47	1.07 (0.194)	14
Carbonyl sulfide	OCS	WAS	0.033 (0.03)	42	0.050 (0.052)	12	NA	NA	0.037 (0.026)	54	0.017 (0.011)	8	0.065 (0.059)	3	0.043 (0.031)	12	0.057 (0.046)	3
Dimethyl sulfide	C_2H_6S	PTRMS, TOGA, WAS	0.015 (0.015)	79	0.016 (0.015)	21	0.034 (0.041)	2	0.016 (0.012)	102	0.003 (0.002)	16	0.021 (0.011)	8	0.013 (0.006)	25	0.005 (0.003)	6
Carbon disulfide	CS_2	TOGA	7.68e-4 (5.73e-4)	37	0.001 (0.0010)	10	NA	NA	8.62e-4 (4.95e-4)	47	5.60e-4 (3.89e-4)	9	4.42e-4	1	4.64e-4 (1.60e-4)	10	0.002 (0.001)	4
Other																		
Hydrogen peroxide	H_2O_2	CIT-CIMS	0.071 (0.039)	102	0.090 (0.064)	27	0.102 (0.018)	3	0.077 (0.031)	133	0.077 (0.029)	33	0.081 (0.040)	14	0.097 (0.025)	48	0.131 (0.025)	15

[1]Standard deviation is given in parentheses. [2]Where more than one instrument is listed, the EF was calculated by first taking the plume-by-plume average across the listed instruments. [3]Includes winter wheat in Table S1 of Supporting Information S2. [4]Average EF is calculated by weighting the fuel-specific average EFs by the fraction of that fuel listed in Table 1 as described in Section 3. [5]Includes shrubland in Table S1 of Supporting Information S2. [6]The two formaldehyde instruments had a slope of 1.27 (CAMS vs. ISAF) during the Western portion of FIREX-AQ likely due to differences in calibration methods (Liao et al., 2021). For the Eastern fires analyzed here, the difference was smaller (slope of 1.06). As there is no recommendation for which measurement is more accurate, we combine the measurements here. The average CAMS EF is ~10% larger than the ISAF EF. [7]PTRMS is shortened throughout from NOAA PTR-ToF-MS. [8]TOGA measurements used to speciate PTRMS measurements. [9]Methylglyoxal may have interferences from biacetyl and acetylpropionyl (Zarzana et al., 2017) therefore this EF is an upper limit. [10]Koss et al. (2018) report fractional ion contributions of 87% 2,3-butanedione and 13% 2-oxobutanal + 1,4-butanediol. [11]Koss et al. (2018) report fractional ion contributions of 44% 2,5 dimethylfuran/10% 2-ethyl furan/and 46% other C2-substituted furan isomers. [12]TOGA/WAS/iWAS measurements used to speciate PTRMS. [13]Koss et al. (2018) report fractional ion contributions of 50% 2-methylphenol and 50% anisol. [14]Koss et al. (2018) report fractional ion contributions of 50% 5-methylfurfural and 50% benzene diols. [15]Figure S1 in Supporting Information S1 shows that C9 aromatics from WAS only account for approximately 30% of PTRMS C9 aromatics. [16]Long-lived NMVOC but placed here for complete list of measured compounds. [17]Figure S2 in Supporting Information S1 shows that individual monoterpene mixing ratios (α-pinene, β-pinene, camphene, myrcene, tricyclene) only represented ~36% of total observed monoterpenes. [18]Koss et al. (2018) report fractional ion contributions of 67% acetic acid and 33% glycolaldehyde. [19]Koss et al. (2018) report fractional ion contributions of 48% hydroxyacetone/37% methyl acetate/and 14% ethyl formate with 50% uncertainty. The contribution of methyl acetate is 18% from TOGA (Figure S3 in Supporting Information S1) so we do not speciate $C_3H_6O_2$ using those contributions. Models could consider 48% hydroxyacetone, the most reactive of these ions, as a lower bound on the potential emission factor. [20]Species included in the total NMVOC emission factor are given in Table S1 of Supporting Information S2. [21]N/A is "not applicable." [22]Koss et al. (2018) report fractional ion contributions of 57% pyrrole/43% butene nitrile isomers, with 15% uncertainty. The contribution of pyrrole is 48% from TOGA (Figure S4 in Supporting Information S1) across all plumes/fin good agreement with this speciation. [23]Correlation with CO is not significant ($p < 0.05$) for pile/slash/grassland fires. [24]Included in measurement of OC and not included in PM_1 calculation. [25]NH_x EFs are given in Tomsche et al. (2023). [26]Includes HNO_3 as NO_3 measured by CIT-CIMS. [27]Calculated for plumes containing data for OC at a minimum. OA is calculated from OC emission factor as described in Section 2. [28]The geometric mean and standard deviation for the distribution are given in Section 3 for the average agricultural burning distribution.
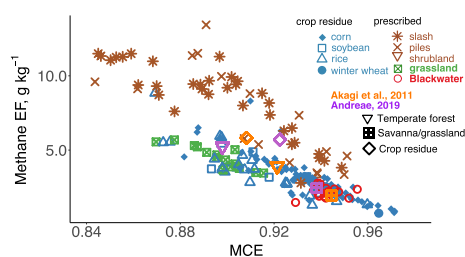
Figure 3. Methane emission factors (EFs) as a function of MCE for all 228 plumes (Table 1) organized by fuel type. The fuel types are identified by different shapes and colors (see legend). The EFs from previous global compilations (Akagi et al., 2011; Andreae, 2019) are overlaid for temperate forests, savanna and grasslands, and crop residues.

measured with greater specificity (TOGA-TOF, iWAS, WAS), and the sum of those species agreed with the NOAA PTR-ToF-MS measurement, we speciated that measurement. Where complete speciation was not available, we provided the available components for reference underneath the PTR-ToF-MS species in Table 4. For C9 aromatics and monoterpenes, <50% of the PTR-ToF-MS measurement could be speciated (Figures S1 and S2 in Supporting Information S1). Table 4 (and Figures S3 and S4 in Supporting Information S1 and Table S4 in Supporting Information S2) show where partial speciation agrees or disagrees with the fractional ion contributions from Koss et al. (2018). Table S4 in Supporting Information S2 provides the speciation of all PTR-ToF-MS species with available measurements from TOGA-TOF, WAS, and iWAS based on the average EFs across all plumes.

The most recent EF compilation available for crop residue fires (including some land-clearing activities) contains 84 NMVOCs (Andreae, 2019). Observations from FIREX-AQ analyzed in this study provide EFs for 117 NMVOCs as well as 25 nitrogen-containing species (including NO_x), 9 halogen-containing species, 11 aerosol species, and 5 sulfur-containing species.

4. Variability in Emission Factors and Modified Combustion Efficiency Across Fuel Types

The variation in fire EFs is often related to MCE which is a measure of the amount of flaming combustion (MCE near 0.99) compared to smoldering combustion (∼0.8) (e.g., Akagi et al., 2011). A histogram of observed MCE ($\equiv \Delta CO_2/(\Delta CO + \Delta CO_2)$) by burned fuel type is given in Figure 2b ranging from 0.84 to 0.97. The MCE average for cropland residue was 0.93 ± 0.02 and for prescribed fuels was 0.90 ± 0.03. For comparison, the average MCE for the FIREX-AQ wildfires was 0.90 ± 0.02 (Gkatzelis et al., 2023). The fuel-specific averages are given in Table 1. Corn residue burned at a statistically higher MCE (0.94, $p < 0.05$) than rice, soybean, grassland, slash, or pile fires. This may be due to differences in fuel moisture which impacts MCE (Chen et al., 2010; Hayashi et al., 2014). Crop residue generally dries out more quickly than woody fuels (Bradshaw et al., 1984). Corn residue also has greater biomass per acre compared to other crops and this higher fuel loading might increase MCE relative to other crops. In addition, crops like rice that are low to the ground may retain more fuel moisture even after drying before burning. Rice irrigation and variability in drying of woody fuels possibly drove the greater observed MCE variability for those fuels (Table 1). The BRSF MCE was higher than for other prescribed fires, likely due to the relatively lower moisture content of the fuels burned, consisting of understory fuels (shrubs, litter), as opposed to larger-diameter woody biomass. The sampled grassland fires occurred during the growing season when the grasses are green and moist, and thus burned at a much lower MCE (0.90) than is often observed (≥0.94) (Andreae, 2019; Hoffa et al., 1999; Urbanski, 2014; Ward et al., 1992). Similar variations in MCE (0.91–0.97) from the early to late dry season have been observed for African grassland fires (Korontzi et al., 2003).

Figure 3 shows the methane EFs for individual plumes separated by fuel type as a function of MCE. The strong relationship of MCE with methane emissions played an important role in the average EF (Table 4), which for corn residue (3.0 g kg^{-1}) was only approximately 40% of the EF for slash (8.4 g kg^{-1}). Woody fuels had the highest methane EF at any given MCE. This difference in the MCE relationship between fuels was first shown between forest and savanna fires by Hao and Ward (1993) with over >2× difference in the EF versus MCE slope. To determine MCE dependence here for the average crop residue, prescribed, and grassland EFs, we averaged the EFs into bins of approximately 0.002 MCE and calculated their slope and intercept which are provided in Table S6 of Supporting Information S2 for all species with a significant correlation (r) with MCE. We then used the MCE dependence (Table S6 in Supporting Information S2) for methane to adjust the average crop residue EF (3.2 g kg^{-1}, MCE = 0.93) and the average prescribed fuels EF (7.5 g kg^{-1}, MCE = 0.90), to an MCE of 0.92 (3.8 g kg^{-1} and 6.0 g kg^{-1}, respectively). Therefore, even at the same MCE (0.92), the crop residue EF for methane was 40% less than for prescribed fuels.

4.1. Shorter- and Longer-Lived NMVOCs

Fires may impact ozone by contributing NMVOCs to regions where ozone production is VOC-limited (Singh et al., 2012; Xu et al., 2021). Fires also transport both NO_x and radicals in reservoir species such as PAN that can
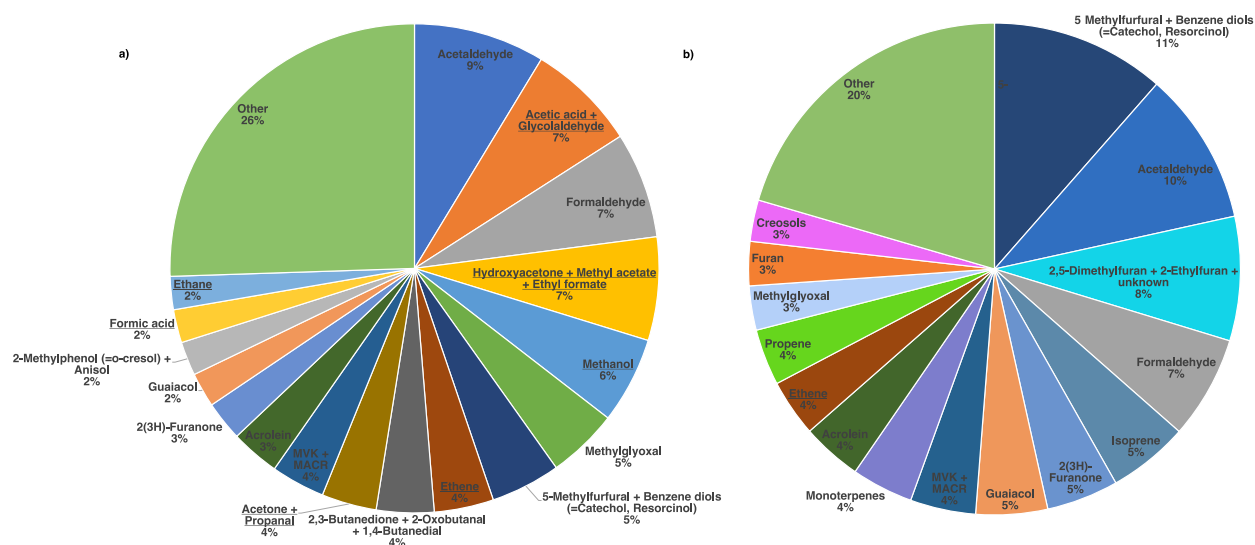
Figure 4. (a) Contribution of individual non-methane volatile organic compound (NMVOC) measurements to the total NMVOC EF across crop residues (corn, rice, soybean, wheat) and prescribed fuel types (pile, slash, grassland, shrubland, Blackwater River State Forest). Species included in Other make up less than 2% of the total on an individual basis. (b) Contribution of individual NMVOCs to reactivity (described in Section 4). Species that are underlined are long-lived VOCs (see Section 3). Species in (b) that also appear in (a) are given the same color for ease of comparison.

impact ozone chemistry downwind (M. J. Alvarado et al., 2010). Within most fire plumes, ozone production is NO_x-limited after an initial period of rapid production (Robinson et al., 2021). Fires are reported to contribute to subsequent additional ozone production when mixed with NO_x as in an urban setting (Akagi et al., 2013; Jaffe & Wigder, 2012; Jaffe et al., 2020; Rickly et al., 2023; Selimovic et al., 2020; Singh et al., 2012) although the impact of fires on ozone can be observed globally (Andreae et al., 1994; Bourgeois et al., 2021; Fishman et al., 1990). NMVOCs such as oxygenated aromatics (e.g., phenols) can also contribute to the formation of secondary organic aerosol (SOA) (Ahern et al., 2019; Akherati et al., 2020; Gilman et al., 2015; Hodshire et al., 2019).

Figure 4a shows the contribution of individual species to the overall average NMVOC EF. We did not separate this figure into different fuel categories as this will be further discussed below. Acetaldehyde was the largest contributor to the total NMVOC EF. Shorter-lived species such as formaldehyde and acetaldehyde in wildfire smoke have been shown to drive downwind ozone production (Baker et al., 2016; Ninneman & Jaffe, 2021). The extent to which these common oxidation products of NMVOC chemistry may be directly emitted from fires versus produced from secondary oxidation of longer-lived precursors is uncertain. For example, photochemical formaldehyde production varied with plume chemistry from the FIREX-AQ western wildfires but often contributed >40% of total formaldehyde (including primary emissions) after only several hours (Liao et al., 2021). Of the 17 NMVOC EFs shown in Figure 4a, 7 species or groups have a lifetime >6 hr against OH and photolysis.

To provide an additional perspective on the importance of considering both photochemical lifetime and EF magnitude, we calculated a "dummy OH reactivity" by weighting each species' EF by its molecular weight and reaction rate with OH. In this way we assess potential rapid secondary NMVOC mass in a similar manner as previous work on SOA potential (Gilman et al., 2015; Hatch et al., 2017). Figure 4b rearranges the EFs by this metric. Furans (furan, 5-methylfurfural + benzene diols, 2(3H)-furanone, benzofuran, furfural, and methylfurans + dimethylfurans) contributed ~10% to the NMVOC EF by mass (Figure 4a) but 30% when weighting by OH reactivity (Figure 4b). Aromatics (benzene, toluene, C8 and C9 aromatics, phenol, guaiacol) contributed 6% to the NMVOC EF and the same when the weighting by OH reactivity. Only one longer-lived species (and formaldehyde precursor) had sufficient mass combined with reactivity to contribute above 2% to the weighted NMVOC EF (Figure 4b, ethene). Acetic acid + glycolaldehyde was the next most important longer-lived EF when weighting by OH reactivity (1.5%). These species could be important to include in models considering transport of fire-related NMVOCs downwind.

Figure 5 shows the comparison of the total NMVOC EF in Figure 4a against MCE and split into shorter-lived (lifetime <6 hr) and longer-lived (lifetime >6 hr) species. Shorter-lived NMVOCs contributed ~60% by
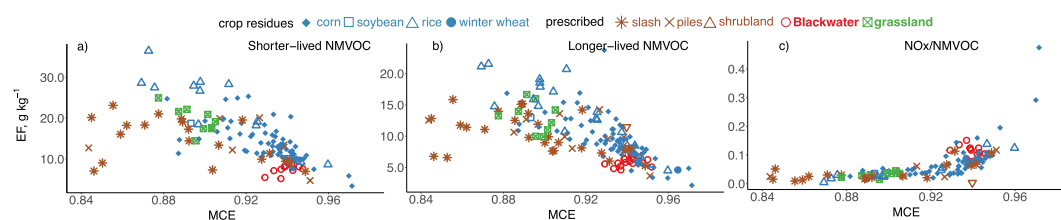
Figure 5. EFs for the sum of (a) shorter- and (b) longer-lived non-methane volatile organic compound (NMVOC) EFs (see Section 4) as a function of MCE for all 228 plumes (Table 1) organized by fuel type. Panel (c) provides the ratio of NO_x (as NO) to the total NMVOC EF. The fuel types are identified by different shapes and colors (see legend).

mass (Table 4). The largest shorter-lived NMVOCs EFs were acetaldehyde, formaldehyde, methylglyoxal, 5-methylfurfural + benzene diols, and 2,3-butanedione + 2-oxobutanal + 1,4-butanedial (Figure 4a). 2,3-Butanedione was the only species with a lifetime against photolysis (∼1 hr) shorter than OH oxidation (∼3 days). The impact of this species on near-field chemistry is thus missed only considering OH reactivity (Carter et al., 2022; Permar et al., 2023) but a model including photolysis showed it is an important radical and PAN precursor from fires in the Southeast US (Liu et al., 2016). The largest longer-lived NMVOC EFs were acetic acid + glycolaldehyde, hydroxyacetone + methyl acetate + ethyl formate, methanol, and ethene (Figure 4a). As in previous studies, NMVOCs were highly correlated with MCE (e.g., Liu et al., 2016; Permar et al., 2021; Yokelson et al., 2011). The sum of shorter- and longer-lived NMVOCs exhibited a strong relationship with MCE for crop residue ($r = -0.87$ and -0.92 respectively, Table S6 in Supporting Information S2). The relationship for prescribed fires was weaker ($r = -0.63$ and -0.68, respectively), due to the departure from a linear relationship for low MCE (<0.88). Similar behavior was observed in Yokelson et al. (2013) which could be due to the larger complexity of fuels burned in prescribed fires compared to crop residue.

Figure 6 shows the same comparison as Figure 5 for a selection of individual shorter- and longer-lived NMVOCs that illustrate both MCE-dependent and fuel-specific differences. As described above, at low MCE, prescribed fuels emitted NMVOCs with lower EFs than other fuel types (Figures 5a and 5b) and this was driven by OVOCs such as formaldehyde and acetaldehyde (Figures 6a and 6b). Stockwell et al. (2014) found that some crop residue fires had higher emissions of some OVOCs compared to other fuels and they speculated that high glycolaldehyde emissions could be due to the sugar content in pre-harvest sugar cane. Hatch et al. (2015) found that rice straw had higher emissions of OVOCs compared to non-agricultural fuels which they hypothesized was due to the greater ash content that contains metals which catalyze cellulose degradation (Patwardhan et al., 2010). Not all OVOCs exhibited this pattern (e.g., Figure 6d). We discuss additional differences below.

Crop residue and prescribed fuels are generally made up of ∼25%–40% cellulose, ∼23%–50% hemicellulose, and ∼7%–30% lignin (Saini et al., 2015). As these components are heated, multiple processes take place starting with distillation, pyrolysis, gasification, and finally flaming combustion if conditions are right for ignition. The non-flaming processes (e.g., gasification) are often collectively referred to as smoldering (Sekimoto et al., 2018; Yokelson et al., 1996). The initial distillation of the fuels emits monoterpenes from stored plant resins. This would be expected to be greatest from coniferous forest biomass (Hatch et al., 2019). Figure 6c shows the elevated monoterpenes from slash and pile fires which released 10× more monoterpenes than crop residue fires (Table 4: 0.08 vs. 0.77 g kg^{-1}).

Pyrolysis of cellulose, hemicellulose, and lignin emits different NMVOCs (Sekimoto et al., 2018). Woody biomass (slash/piles) has a higher lignin and cellulose content than crop fuels, while grasslands fall in between (Acquah et al., 2018; Saini et al., 2015; Santiago-De La Rosa et al., 2018). Thermal degradation of lignin produces guaiacols, phenol, and syringol, while breakdown of cellulose and hemicellulose produces OVOCs such as acetaldehyde, furans, and furfurals (Kibet et al., 2012; Sekimoto et al., 2018). Aromatization, occurring at high temperatures, produces aromatic hydrocarbons and PAHs (e.g., naphthalene). Figures 6d and 6e show EFs for guaiacol and 5-methylfurfural + benzene diols, where the lowest values were observed for the BRSF prescribed fire and grassland fires, possibly indicative of lower lignin. The average crop residue and slash/piles EFs for these species had a similar dependence on MCE (Table S6 in Supporting Information S2) and within a 30% difference for each species after adjusting both to MCE = 0.92. Phenol (Figure 6f) showed a statistically different EF for crop residues that was 70% higher than the EF for prescribed fires even after adjusting to the same MCE. Metals (such as potassium) that are more abundant in crop residue fuels than prescribed fuels catalyze production of
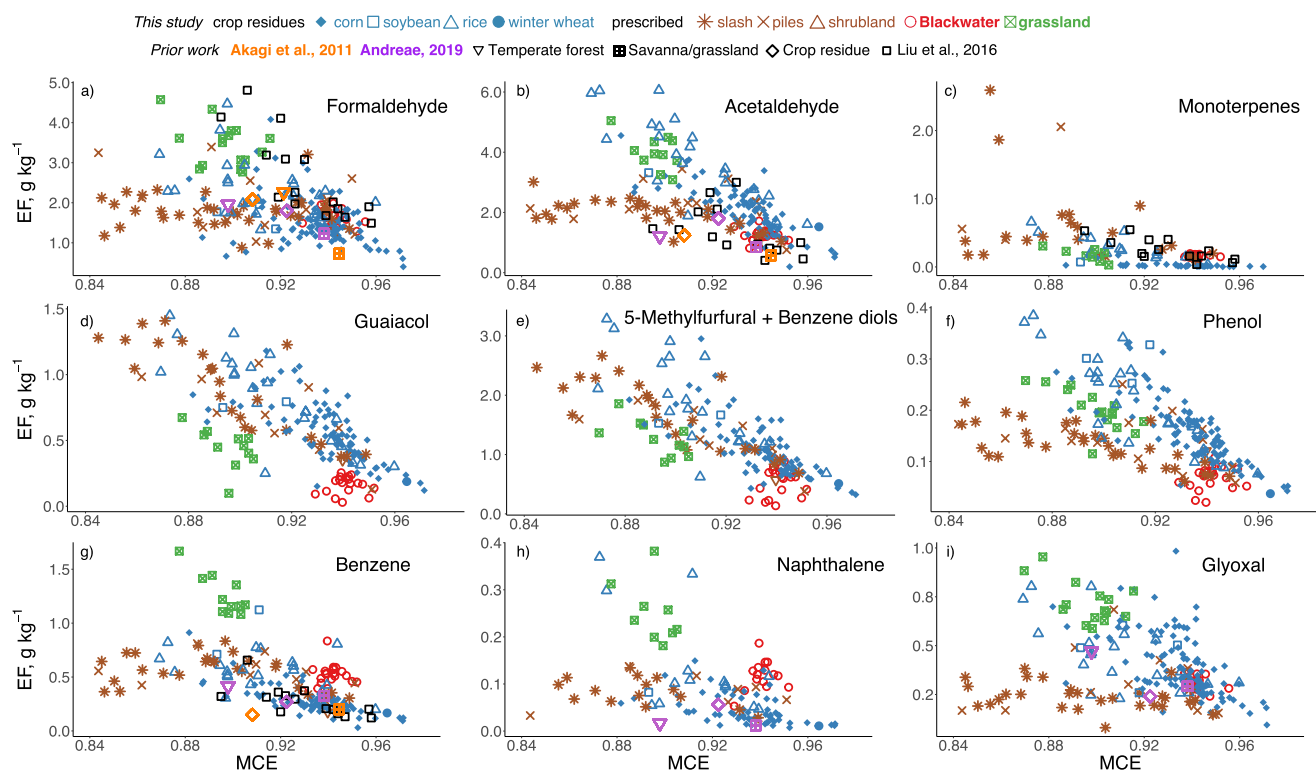
This study   crop residues ◆ corn □ soybean △ rice ● winter wheat   prescribed ✳ slash ✕ piles △ shrubland ◯ **Blackwater** ⊠ **grassland**

Prior work   **Akagi et al., 2011** **Andreae, 2019** ▽ Temperate forest ⊞ Savanna/grassland ◇ Crop residue □ Liu et al., 2016
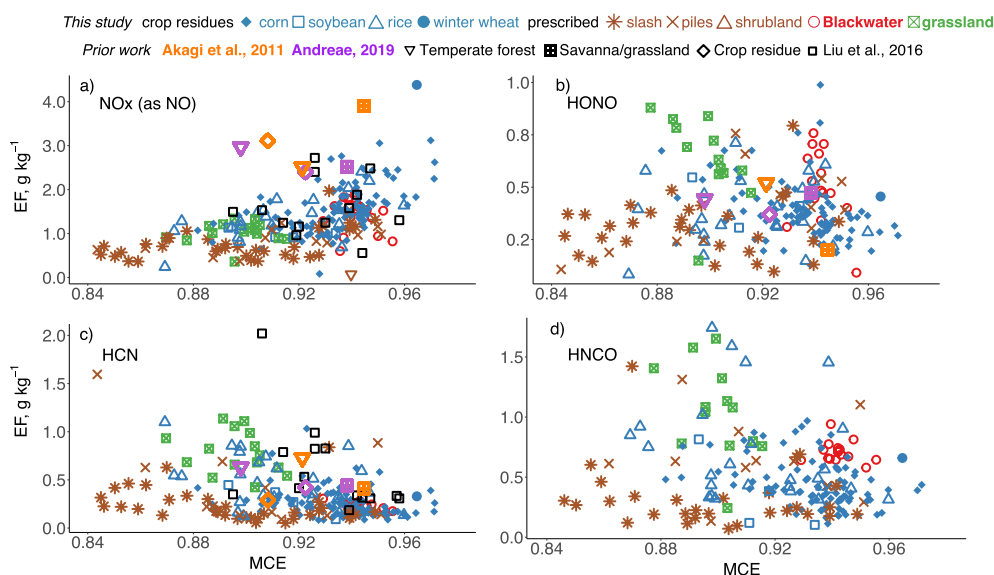

Figure 6. Individual non-methane volatile organic compound (NMVOC) EFs as a function of MCE for all 228 plumes (Table 1) organized by fuel type. The fuel types are identified by different shapes and colors (see legend) and the NMVOC names are inset. The EFs from previous global compilations (Akagi et al., 2011; Andreae, 2019) are overlaid for temperate forests, savanna and grasslands, and crop residues. The crop residue EFs from Liu et al. (2016) are also included (black squares).

OVOCs coming from cellulose and hemicellulose (Essig et al., 1989; Patwardhan et al., 2010) and this could possibly also impact phenol production although other species produced from lignin such as guaiacol (Figure 6d) or 5-methylfurfural + benzene diols (Figure 6e) did not show this effect. EFs for products of aromatization such as benzene (Figure 6g) and naphthalene (Figure 6h) were 2–4× greater for grassland fires than crop residue or other prescribed fires possibly due to the effects of higher fuel moisture (Zhang et al., 2022).

4.2. Satellite Observable Species

Several NMVOCs are observable from space, including formaldehyde (Chance et al., 2000), methanol and formic acid (Cady-Pereira et al., 2014; Razavi et al., 2011), glyoxal (Chan Miller et al., 2014), and isoprene (Wells et al., 2020). Impacts of fires on formaldehyde and glyoxal have been observed from satellites (L. M. A. Alvarado et al., 2020; Stavrakou et al., 2016). The ratio of glyoxal to formaldehyde (RGF) from satellites may be used to distinguish between source categories (anthropogenic, pyrogenic, biogenic (Vrekoussis et al., 2009)). Changes in the RGF from the emission source to downwind have been observed from satellite and used to classify different pyrogenic fuels using space-based observations of wildfires, where secondary production of formaldehyde downwind causes the RGF to decrease with age (L. M. A. Alvarado et al., 2020). Here, glyoxal EFs (Figure 6i) increased with decreasing MCE for crop residue fires ($r = -0.73$, Table S6 in Supporting Information S2) but a significant relationship was not obtained for prescribed fires. Crop residue fires emitted 60% more glyoxal than prescribed fires (Table 4). Zarzana et al. (2018) found a consistent RGF of 0.07 ± 0.02 in their FIREX lab study of mainly forest fuels. Here, the RGF (calculated using ERs, Table S2 in Supporting Information S2), was 70% higher from crop residue fires (0.12 ± 0.04) than prescribed fires (0.07 ± 0.02).

4.3. Nitrogen-Containing Species

Emissions of NO_x (Figure 7a) showed a non-linear and positive dependence on MCE for crop residue and prescribed fuels (Table S6 in Supporting Information S2), with a steep increase in EF above MCE ~ 0.92 for crop
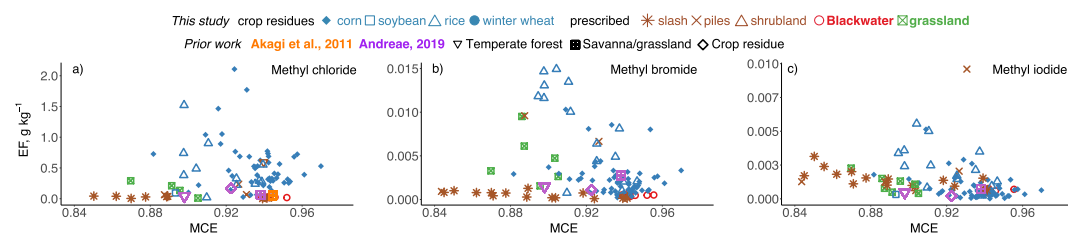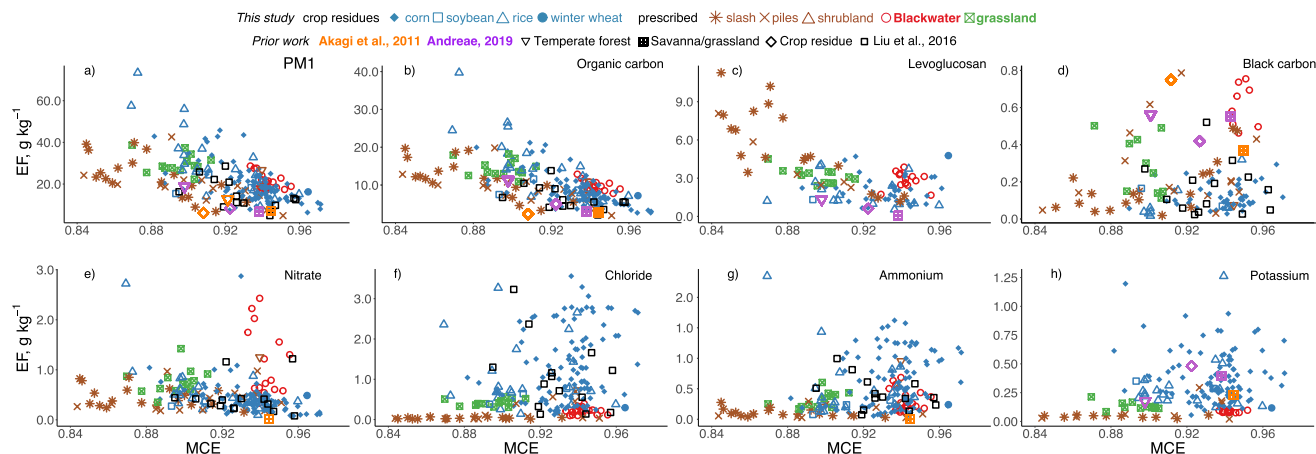
Figure 7. Individual nitrogen-containing EFs as a function of MCE for all 228 plumes (Table 1) organized by fuel type. The fuel types are identified by different shapes and colors (see legend) and the species names are inset. The EFs from previous global compilations (Akagi et al., 2011; Andreae, 2019) are overlaid for temperate forests, savanna and grasslands, and crop residues. The crop residue EFs from Liu et al. (2016) are also included (black squares).

residue. This behavior is similar to the lab-based results from Roberts et al. (2020) for the ratio of NO_x to reactive nitrogen. Herbaceous fuels (crop residue, grasslands) have higher fuel nitrogen than the woody fuels consumed in prescribed burning (Coggon et al., 2016). Crop residue fires emitted ∼2× as much NO_x as prescribed fires (Table 4). Above MCE ∼0.92, the ratio of the NO_x EF to the total NMVOC EF (Figure 5c) increased steeply from <0.10 to 0.42. For comparison, the NO_x/VOC ratio from mobile and stationary combustion sources in the US EPA inventory is much greater (0.89, US EPA, 2017).

Nitrous acid (HONO) has been observed from fires during many field (Chai et al., 2021; Peng et al., 2020; Yokelson et al., 2009) and laboratory-based studies (Chai et al., 2019; Roberts et al., 2020; Veres et al., 2010) as well as from satellites over fire hotspots (Theys et al., 2020). Laboratory studies show that HONO is produced mainly from flaming combustion (Burling et al., 2010; Roberts et al., 2010, 2020) regardless of overall MCE. Only three studies contributed to the HONO EF for crop residues in Andreae (2019). However, the Andreae value (0.37 g kg⁻¹) compares well with the average crop residue EF here (0.39 g kg⁻¹, Table 4) which could be due to the lack of dependence on MCE (Figure 7b). The average prescribed EF (0.34 g kg⁻¹) is also similar, but grassland EFs were ∼60% larger (0.64 g kg⁻¹, Table 4) possibly due to the effects of high fuel moisture also reported by Roberts et al. (2020).

Hydrogen cyanide (HCN) and isocyanic acid (HNCO) are both produced during high-temperature pyrolysis (Sekimoto et al., 2018). HCN, in addition to ammonia (NH_3), is also produced from gasification during smoldering combustion (Chai et al., 2019; Houshfar et al., 2012; Leppälahti & Koljonen, 1995). Grassland fires emitted over twice as much HCN (Figure 7c) and HNCO (Figure 7d) as crop residue or prescribed burning suggesting that gasification was the dominant contributor to this difference or that fuel moisture had a large effect. Overall, differences in organic nitrogen-containing EFs were likely primarily driven by fuel nitrogen differences with additional effects from combustion processes or the effects of fuel moisture. Ammonia measurements during FIREX-AQ required special treatment due to instrument tailing effects. These EFs are described in Tomsche et al. (2023) where no clear relationship with MCE was found and most NH_3 had partitioned into aerosol-phase ammonium at the time of sampling.

4.4. Halogenated Species

Biomass burning produces methyl halides (CH_3Cl, CH_3Br, and CH_3I) that are longer-lived ozone-depleting substances (Bahlmann et al., 2019; Blake et al., 1996; X. Hu et al., 2023; Lobert et al., 1999) and sometimes

Figure 8. Individual halogen-containing EFs as a function of MCE for all 228 plumes (Table 1) organized by fuel type. The fuel types are identified by different shapes and colors (see legend) and the species names are inset. The EFs from previous global compilations (Akagi et al., 2011; Andreae, 2019) are overlaid for temperate forests, savanna and grasslands, and crop residues.

resuspends other halogenated species likely deposited from anthropogenic activities (Eckhardt et al., 2007; Radke et al., 1991). Methyl chloride (CH_3Cl) was by far the most abundant measured halogenated species emitted from crop residue or prescribed fires during FIREX-AQ. Hydrogen chloride (HCl) may be emitted in similar amounts (Andreae, 2019) but was not measured during FIREX-AQ. Figure 8a shows the strong dependence of CH_3Cl emissions on fuel type, where the crop residue fuel EFs were 5× greater than prescribed fire fuels (Table 4) due to their higher chlorine content (Stockwell et al., 2014). Methyl bromide (CH_3Br) and methyl iodide (CH_3I) EFs were highest for rice residue (Figures 9b and 9c, Table 4). In a study of boreal fires that burned woody fuels, Simpson et al. (2011) found that dichloromethane (CH_2Cl_2) was not significantly emitted from the prescribed fires. We similarly found no relationship between CH_2Cl_2 and CO for prescribed fires ($r = 0.17$, Table S5 in Supporting Information S2) but CH_2Cl_2 did appear to be emitted by crop residue fires ($r = 0.48$, Table S5 in Supporting Information S2) which may be due to its use in agriculture chemical production (EPA, 2018).

Several halogenated species were weakly anticorrelated with CO (Table S5 in Supporting Information S2). Halon 1211 was negatively correlated with CO for both crop residue fuels ($r = -0.40$) and prescribed burns ($r = -0.41$). The brominated species bromodichloromethane ($CHBrCl_2$, $r = -0.35$), dibromochloromethane ($CHBr_2Cl$, $r = -0.32$), and bromoform ($CHBr_3$, $r = -0.25$) were negatively correlated for crop residue fuels. This negative relationship could indicate destruction of these species during flaming combustion (Simpson et al., 2011).

4.5. Aerosols

Particulate matter <1 μm (PM_1, Figure 9a) was largely emitted as OA (Figure 9b), which on average comprised 88% of crop residue and 95% of prescribed fire PM_1 (Table 4). This fraction was more variable for crop residue fires that emit larger amounts of other species (chloride, Figure 9f, ammonium, Figure 9g, potassium, Figure 9h). Nitrate exhibited a weakly negative ($r = -0.65$) relationship with MCE for crop residue (Figure 9e, Table S6 in

Figure 9. Individual aerosol EFs as a function of MCE for all 228 plumes (Table 1) organized by fuel type. The fuel types are identified by different shapes and colors (see legend) and the species names are inset. The EFs from previous global compilations (Akagi et al., 2011; Andreae, 2019) are overlaid for temperate forests, savanna and grasslands, and crop residues. The crop residue EFs from Liu et al. (2016) are also included (black squares).
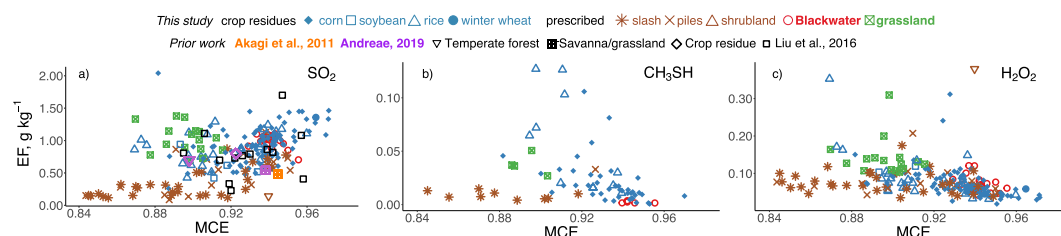
Figure 10. Individual sulfur-containing and H_2O_2 EFs as a function of MCE for all 228 plumes (Table 1) organized by fuel type. The fuel types are identified by different shapes and colors (see legend) and the species names are inset. The EFs from previous global compilations (Akagi et al., 2011; Andreae, 2019) are overlaid for temperate forests, savanna and grasslands, and crop residues. The crop residue EFs from Liu et al. (2016) are also included (black squares).

Supporting Information S2) which we suggest could be due to its production from organic nitrogen-containing species. EFs for OA are reported as OC as described in Section 3. Figures 9a and 9b show the strong negative relationship of PM_1 and OC EFs with MCE (Table S6 in Supporting Information S2). Corn residue fires emitted 50% lower OC than rice residue fires due to their higher MCE. After adjusting to MCE = 0.92, crop residue fires emitted approximately 50% more PM_1 and OC than prescribed fires. There was no statistically significant relationship of BC with MCE (Figure 9d, Table S6 in Supporting Information S2) despite BC being a product of flaming combustion (Akagi et al., 2011). This could be due to the few plumes sampled here at high MCE (>0.96 as reported by Aurell et al. (2015)), or variability due to flame turbulence (Shaddix et al., 1994). The ratio of BC to OC ERs appeared to have an exponential dependence on MCE (Figure S5 in Supporting Information S1) which may be useful for predicting aerosol optical properties (Christian, 2003; Li et al., 2019; Pokhrel et al., 2016).

Levoglucosan, a degradation product of cellulose (emitted during smoldering combustion), and potassium (emitted from flaming combustion) are both used as tracers of biomass burning (Fraser & Lakshmanan, 2000; Quinteros et al., 2023; Sullivan et al., 2014). High metal content (e.g., potassium) in fuels suppresses levoglucosan production (Essig et al., 1989; Patwardhan et al., 2010) in favor of OVOC production as described above. Fields that have been treated with agricultural chemicals may be enriched in nutrients such as potassium, sulfur, phosphorous, and nitrogen that could be released during burning (Liu et al., 2016; Lobert et al., 1999; Stockwell et al., 2014; Wortmann et al., 2012). Figures 9f–9h and Table S1 in Supporting Information S2 show that crop residue fires emitted 7× more chloride, 4× more potassium, and 3× more ammonium than prescribed fires. The elevated potassium could explain why levoglucosan (Figure 9c), was 11% of the OA EF for crop residue but 22% for prescribed fires. The relatively higher chloride emissions from crop residue fires were consistent with the 5× higher CH_3Cl EFs from crop residue fires compared to prescribed fires (see above).

Table 4 includes particle number with nominal diameters >3 nm and the average lognormal size distribution number median diameter (Dpg) and geometric standard deviation (sg). A common assumption for biomass burning particles is Dpg of 100 nm and sg of 1.8 (Pierce et al., 2007). For crop residue fires here, we calculated a Dpg of 114 nm and sg of 1.7. For prescribed burning, the distribution was difficult to characterize possibly due to the size cutoff of the Laser Aerosol Spectrometer instrument (Table 2, 0.1 mm) or fewer available samples.

4.6. Sulfur-Containing and Other Species

Most measured sulfur was emitted as SO_2. The crop residue and grassland fire EFs for SO_2 were 2× greater than prescribed fires (Figure 10a, Table 4). There was a significant positive correlation between SO_2 and MCE for crop residue and prescribed fires (Table S6 in Supporting Information S2, $r = 0.46$ to 0.72). The higher sulfur content of crop residue and grassland fuels (Hatch et al., 2015; Stockwell et al., 2014), combined with sulfur deposition and the use of sulfur-containing fertilizers (Rickly et al., 2022), are likely causes of the differences in SO_2 EF. Other sulfur-containing compounds, such as methanethiol (CH_3SH, Figure 10b), were similarly emitted in greater amounts from crop residue and grassland fires than from prescribed fuels.

Direct emissions of hydrogen peroxide (H_2O_2) have been observed from fires in addition to secondary production from plume aging (M. Lee et al., 1997; Yokelson et al., 2009) that can have impacts even on the remote atmosphere (Allen et al., 2022). H_2O_2 has a lifetime of about 1 day but is also produced from secondary chemistry, allowing for impacts on downwind oxidation capacity if lost to reaction with OH or photolysis. The H_2O_2 EF had

a negative relationship with MCE for crop residue fires (Figure 10c; from Table S6 in Supporting Information S2, $r = -0.68$). This could be due to greater prompt production from reactive NMVOCs at lower MCE (Figures 5 and 6) and lower NO_x (Figure 7a). The plumes sampled during FIREX-AQ were minimally aged and no relationship of the H_2O_2 ER was observed with the ratio of maleic anhydride to furan (as an indicator of photochemical processing, Figure S6 in Supporting Information S1). The average H_2O_2 ER for agriculture and prescribed fires (0.87 and 0.82 ppt H_2O_2 ppb CO^{-1}, respectively) was within 40% of the ER calculated by Yokelson et al. (2009) for fresh smoke in Mexico (1.5 ppt H_2O_2 ppb CO^{-1}).

4.7. Summary of Observed Relationships With MCE and Fuel Type

Figure 11 summarizes the species with a significant ($p < 0.05$) positive or negative correlation with MCE for crop residue fires. Only strongly negatively correlated species ($r^2 > 0.5$) are plotted while the remainder (and correlations for prescribed fire fuels and grassland fires) are given in Table S6 of Supporting Information S2. The strongest relationships were observed for shorter-lived OVOCs, but strong relationships were also obtained for shorter- and longer-lived NMVOCs, organic nitrogen-containing species, and OC. Weaker relationships were found for positively correlated inorganic species (NO, NO_2, SO_2). Species with no significant correlation with MCE for any fuel type (Table S6 in Supporting Information S2) included aerosol species (potassium, chloride, BC), ethanol, and other VOCs where obtaining significant correlations was difficult (low concentrations, low time resolution instruments) although an MCE dependence might be expected (e.g., furfural). Overall, we found significant relationships with MCE for 81% (35%) of sampled species for crop residue (prescribed) fires. As an example of the impact of this dependence, the methane EF calculated at 0.84 MCE would be ~11× greater than at 0.97 MCE, the range observed during FIREX-AQ (Figure 3).

Liu et al. (2016) sampled 15 agricultural fires in the Southeast US and found positive but not significant relationships with MCE for SO_2, NO_x and nitrate. Here, we obtained positive and significant correlations for SO_2 and NO_x (Figure 7a) and a negative relationship for nitrate. For the species reported by Liu et al. (2016) with negative but insignificant correlations with MCE that were also measured during FIREX-AQ (HCN, acetaldehyde, OA, sulfate, isoprene, acetonitrile, methanol, and acetone), we found significant and negative correlations with MCE for all species (Table S6 in Supporting Information S2).

To explore differences in EFs between fuels that are not solely attributable to MCE, we adjusted the EFs with a significant dependence on MCE ($p < 0.05$, $r^2 > 0.5$) for both crop residue and prescribed fires to an MCE of 0.92 (average for agricultural residue from Andreae (2019)) using the slope and intercept provided in Table S6 of Supporting Information S2. Figure 12 shows the 23 adjusted EFs for which the crop residue and prescribed values had a significant difference (using a t-test, $p < 0.05$) of at least 50%. Large enhancements in crop residue fire adjusted EFs occurred for two chlorine-containing species: aerosol chloride (7×) and methyl chloride (5×) and two other aerosol species: potassium (4×) and ammonium (3×). Eight nitrogen-containing adjusted EFs were enhanced for crop residue fires including pyrrole + butenenitrile (3×), NO (3×), and NO_2 (2×). Sulfur dioxide and seven NMVOCs had adjusted EFs approximately 2× greater from crop residue fires than prescribed fires. The monoterpene crop residue adjusted EF was only 10% of the prescribed EF. This is expected because of the emission of stored terpenes from coniferous fuels as the vegetation is heated (Simpson et al., 2011).

5. Comparison With Prior Global Compilations and Regional Studies

The comparison of average crop residue, prescribed fuels, and grassland EFs derived here to the compilation from Andreae (2019) is provided in Table S7 of Supporting Information S2. Some differences are likely due to the difference in MCE in the Andreae (2019) global compilation (0.92) compared to the average here (0.93) that is weighted toward corn fires. For example, Figure 4 shows that using the Andreae (2019) estimated "global average" methane EF for crop residue (5.7 g kg^{-1}) would result in an 80% overestimate of methane EF from FIREX-AQ (3.2 g kg^{-1}). The methane EF from grassland fires sampled during FIREX-AQ (4.5 g kg^{-1}) was a factor of two higher than the EF (2.5 g kg^{-1}) from Andreae (2019) again likely due to differences in MCE (0.90 vs. 0.94) as the sampled grassland fires here occurred during an unusually wet summer.

FIREX-AQ EFs showed large disagreement with Andreae (2019) and Akagi et al. (2011) for OC and PM_1. $PM_{2.5}$ is the metric generally reported for global compilations but is expected to be similar to PM_1. The $PM_{2.5}$ EFs for crop residue from Andreae (2019) and Akagi et al. (2011) were 8 g kg^{-1} and 6 g kg^{-1}, respectively, 60%–70% lower
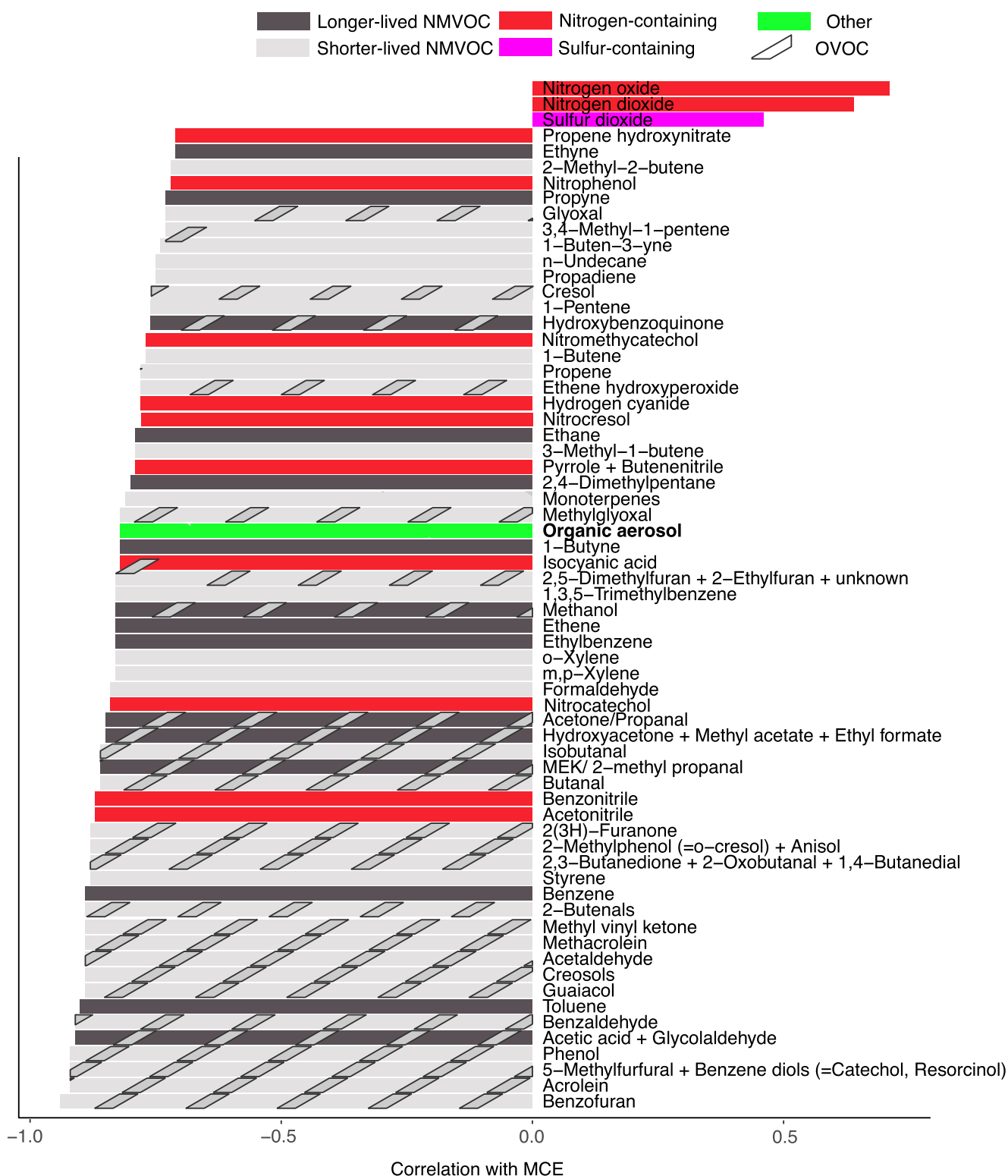
Figure 11. Species with a significant anticorrelation ($r^2 > 0.5$, $p < 0.05$) or significant positive correlation ($p < 0.05$) with MCE for agricultural residue fires, colored by their chemical classification.
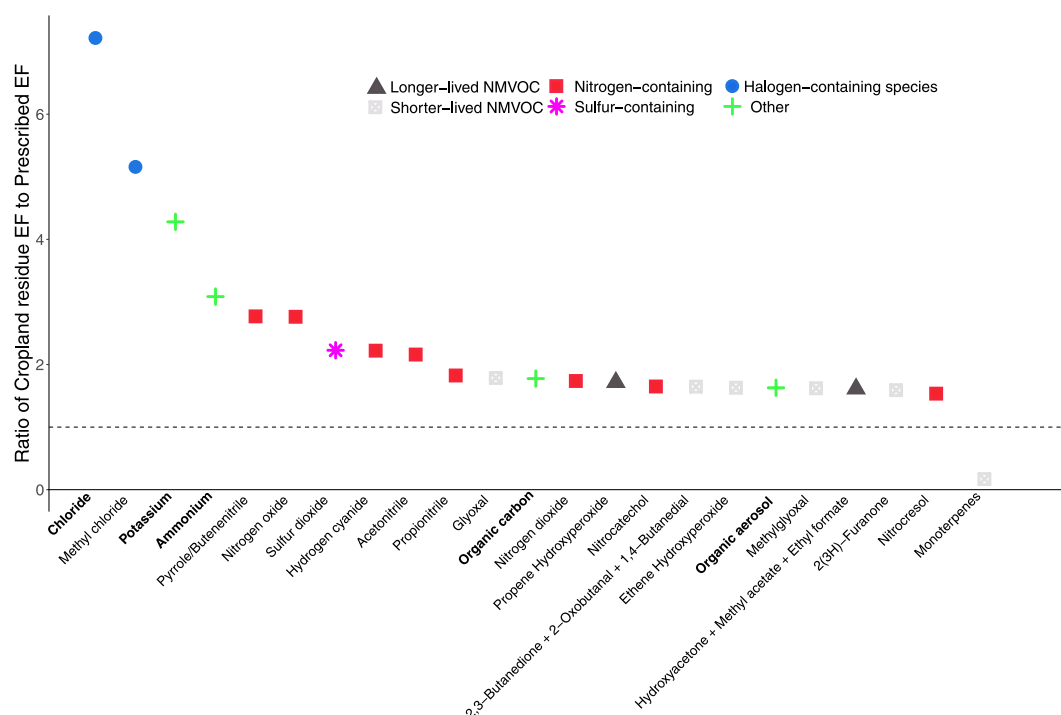
Figure 12. Statistically significant ratios between the crop residue EF and prescribed EF as described in Section 4. Colors designate species category and species that are italicized are in the aerosol phase.

than obtained here for PM_1 (21 g kg^{-1}). Those global compilations had limited data for crop residue and included some measurements based on older techniques. The FIREX-AQ crop residue average PM_1 EF agreed within approximately 50% compared to the Liu et al. (2016) average EF (15 g kg^{-1}) with overlap over the range of MCE studied (Figure 9a). Liu et al. (2016) and this study both measured speciated PM_1 using an AMS (Table 2). The FIREX-AQ BC EF (0.12 g kg^{-1}) was 70%–80% less than the values in Andreae (2019) (0.42 g kg^{-1}) and Akagi et al. (2011) (0.75 g kg^{-1}) but agreed within 20% of the Liu et al. (2016) EF (0.16 g kg^{-1}). Therefore, global EFs may significantly underestimate OA and PM_1 but overestimate BC emissions in the Eastern US from crop residue fires (i.e., Carter et al., 2020). Measurements of BC can however differ widely (30%–80%) across instrument techniques (Li et al., 2019) and this should be taken into consideration when creating average compilations of EFs across studies.

A goal of FIREX-AQ was to expand EF availability and statistics for crop residue and prescribed fires (Warneke et al., 2023). This need was emphasized by Akagi et al. (2011) and demonstrated by differences in crop residue fire EFs between the 15 crop residue fires sampled in the Southeast US by Liu et al. (2016) and the earlier global compilation of Akagi et al. (2011) that is commonly used in models and fire emission inventories. These differences motivated the need for further sampling to better determine the distribution of crop residue fire EFs. Figures 13a and 13b (and Table S8 in Supporting Information S2) show the average crop residue fire EFs from this work (Table 4) compared to Liu et al. (2016). Also overlaid are the average crop residue fire EFs from Akagi et al. (2011) and Andreae (2019). The FIREX-AQ study sampled the most crop residue fires and measured the most species to date so this data will likely have a large impact on future global averages for many EFs.

Study-average EFs between Liu et al. (2016) and FIREX-AQ for US crop residue fires agreed within 50% for 16 out of 21 comparable species (Figure 13, Table S8 in Supporting Information S2). The biggest discrepancy was for monoterpenes, where EFs from FIREX-AQ were 70% lower than in Liu et al. (2016). The rice-specific mono-terpene EF from FIREX-AQ agreed better with Liu et al. (2016) (0.28 g kg^{-1} vs. 0.26 g kg^{-1}, respectively) and therefore we attributed this difference largely to the dominance of corn residue fire EFs in the FIREX-AQ crop residue average compared to the majority rice residue fires in Liu et al. (2016). FIREX-AQ EFs were 60%–90% larger for acetaldehyde, toluene, and acetonitrile and 50% less for HCN, but still within one standard deviation of the EF from Liu et al. (2016).
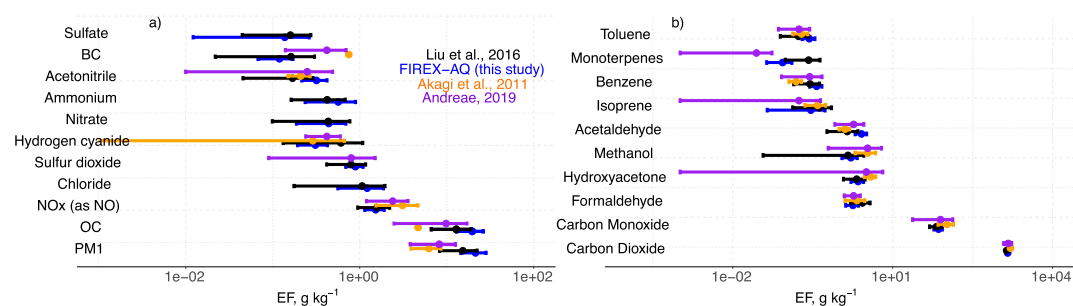
Figure 13. Average EFs from crop residue from FIREX-AQ, Akagi et al. (2011), Liu et al. (2016), and Andreae (2019) for (a) aerosol and inorganic species, and (b) CO, CO_2, and selected VOCs and OVOCs. x-axes are plotted on a logarithmic scale.

The range in MCE observed during FIREX-AQ (0.84–0.97) was larger than in Liu et al. (2016) (0.90–0.96). As shown in Figures 6, 7, 9, and 10, this led to a larger range in EFs observed from FIREX-AQ crop residue fires than in Liu et al. (2016). While fire-integrated MCE likely varies less than plume MCE, to improve accuracy in modeling crop residue (and prescribed) fire emissions, future work should focus on developing inventories that better account for fuel composition, seasonal moisture availability, and MCE variability. As a first step, the better comparison between Liu et al. (2016) and this study compared to global compilations (Akagi et al., 2011; Andreae, 2019) highlights the importance of EFs that are regionally- and seasonally-specific even if crop-specific information or the ability to vary EFs with MCE or fuel moisture cannot yet be implemented.

6. Conclusions

Crop residue and prescribed fires are widely used to remove unwanted biomass, but chemical characterization of the emissions from these fires has been limited. We calculated EFs and ERs for crop residue and prescribed fires during the Eastern US component of the 2019 NOAA/NASA FIREX-AQ campaign. These types of observations provide the basis for EFs that are used in models to predict the air quality impacts of fires. Currently-used EF compilations present global averages covering a large range of fuel types and burning conditions and are often based on a limited amount of sampling. FIREX-AQ sampled four types of crop residue burning (corn, soybean, rice, winter wheat), and four types of prescribed burning (slash, piles, shrubland, grassland), in addition to a prescribed understory fire at BRSF in Florida that was coordinated with FIREX-AQ sampling. We obtained EFs and ERs for 53 crop residue fires and 22 prescribed fires for 117 VOCs, 25 nitrogen-containing species, 9 halogenated species, 11 aerosol species, and 5 sulfur-containing species significantly expanding the number of these fire types sampled globally and making these the most chemically-detailed field measurements of these sources to date. This information can be incorporated into future compilations of crop residue or prescribed burning activities to improve overall averages for these fuel types.

During FIREX-AQ, 70% of the crop residue fires burned corn residue and this fuel type significantly influenced the crop residue average EFs in this study. Corn residue fires burned at a higher modified combustion efficiency (MCE = 0.94 ± 0.02) than other fuel types, likely due to higher fuel loadings for this crop type and drier fuels compared to other crop types. The strong negative relationship of most NMVOCs with MCE resulted in lower average EFs for corn residue burning than for other fuel types and literature averages. Grassland fires during the campaign burned at a much lower MCE (0.90 ± 0.01) than typically observed (≥0.94), because the fuels were green, moist, growing-season grasslands. Prescribed fires burned at an MCE of 0.90 which is expected for this fuel type. Misattributing any of these fuel types clearly could cause large errors in emissions just due to MCE alone.

We calculated a large difference in the importance of NMVOCs between contributions to the total by mass only or after weighting by reactivity. This can inform which species may be most important to include for near-field and far-field chemistry. Furans (furan, 5-methylfurfural + benzene diols, 2(3H)-furanone, benzofuran, furfural, and methylfurans + dimethylfurans) contributed ~30% to the NMVOC after weighting by OH reactivity (Figure 4b). Ethene and acetic acid + glycolaldehyde were longer-lived NMVOCs that had sufficient mass combined with reactivity to consider including in models of transport of fire-related NMVOCs downwind. 2,3-Butanedione was the only species that was longer-lived against OH oxidation (~3 days) but shorter-lived against photolysis (~1 hr)

and is missed when only considering OH reactivity but has been shown in box modeling studies to be an important radical and PAN precursor.

Emissions of NMVOCs from fires may impact surface ozone in urban regions that are VOC-limited. To provide insight into which NMVOCs may travel further downwind from a fire, we separated EFs by their lifetime against OH or photolysis into shorter-lived (<6 hr) or longer-lived (>6 hr) species. The total shorter-lived NMVOC EF by this definition was 60% of the total NMVOC EF. The largest shorter-lived NMVOC EFs were for acetaldehyde and formaldehyde, and the highest longer-lived NMVOC EFs were acetic acid + glycolaldehyde and hydroxyacetone + methyl acetate + ethyl formate. Furans, while only contributing 10% to the total NMVOC EF by mass, contributed 30% when weighting by both mass and OH reactivity. Ethene and acetic acid + glycolaldehyde were longer-lived NMVOCs that had sufficient mass combined with reactivity to consider including in models of transport of fire-related NMVOCs downwind. 2,3-Butanedione was the only species that was longer-lived against OH oxidation (~3 days) but shorter-lived against photolysis (~1 hr) and had the 9th highest EF of all NMVOCs. The impact of this species on near-field chemistry and downwind PAN formation is misrepresented when viewing biomass burning emissions only in terms of OH reactivity. Overall, these findings from FIREX-AQ highlight the need to use chemical mechanisms that treat the oxidation of both shorter- and longer-lived NMVOCs.

We observed significant differences in EFs across fuel types. Like prior work, OVOCs were emitted in greater amounts by crop residue fires than prescribed fires which could be due to the presence of alkali metals that reduce levoglucosan but increase OVOC production (e.g., glycolaldehyde) from cellulose. Species emitted from degradation of lignin (e.g., guaiacol) showed less of a difference. As a result, the RGF was 70% higher from crop residue fires than prescribed fires, which may have implications for interpreting observations of RGF from space. Due to the storage of monoterpenes, biomass burned in prescribed fires emitted over 10× more monoterpenes than crop residue fuels. Crop residue fires had a factor of two greater NO_x EFs compared to prescribed fires which have lower fuel nitrogen content. Likely due to high fuel halogen content as well as their use in agricultural chemicals, halogenated species were enhanced in crop residue fires, which emitted 7× more aerosol chloride and 5× more methyl chloride (CH_3Cl) than prescribed fires. Most of the PM_1 was emitted as OA and this fraction was greater for prescribed fires (95%) than crop residue fires (88%). In addition to chloride, crop residue fires emitted 4× more potassium and 3× more ammonium than prescribed fires. Likely due to higher sulfur content, the crop residue and grassland fire EFs for SO_2 were both 2× greater than prescribed fires. We also reported direct emissions of hydrogen peroxide which were similar for crop residue and prescribed fires.

Species with a strong relationship with MCE are more difficult for current models to accurately simulate as emissions inventories (e.g., Wiedinmyer et al., 2023) typically include dependence on fuel type but not burning conditions. The same fuel type (such as wet and dry grasslands) can have very different emissions when fuel moisture is higher, and MCE is lower. We found significant relationships with MCE for 81% of crop residue EFs and 35% of prescribed EFs. The strongest anticorrelations were observed for methane and OVOCs. Species with no significant correlation with MCE for any fuel type included inorganic aerosol species (potassium, chloride, BC) and some NMVOCs where obtaining significant correlations was difficult although an MCE dependence might be expected. A greater range in MCE and EFs was observed during FIREX-AQ than was observed during previous studies in the Eastern US. This range, for example, 11× for the methane EF, further motivates work to parameterize EFs as a function of MCE.

To investigate differences across fuel types not solely attributable to MCE, we adjusted all measured EFs with a strong dependence on MCE ($r^2 > 0.5$) to a value of 0.92. We exclude monoterpenes from this correction due to the large differences across crop types within the "crop" category. This step resulted in 23 species that differed by more than 50% between crop residue and prescribed fire EFs including aerosol chloride (7×), methyl chloride (5×), aerosol potassium (4×), and NO (3×), and NO_2 (2×). Sulfur dioxide and seven NMVOCs had adjusted EFs approximately 2× greater from crop residue fires than prescribed fires. The EFs for monoterpenes for agricultural residue was only 10% of the prescribed value. There may be additional significant differences between crop residue and prescribed fires EFs that we were not able to discern here for additional species. For some species, particularly some NMVOCs that were measured at lower temporal resolution, we did not obtain sufficient statistical certainty.

The EFs sampled here spanned a similar range as previous studies in the Southeast US, with the average standard deviation giving a variability of approximately 2× for most species with larger variability in fuel-specific species such as inorganic aerosols likely related to agricultural chemicals (e.g., chloride) and stored biogenic VOCs

(monoterpenes). In addition to fuel characteristics, variance was due to MCE or other factors such as fuel moisture or combustion temperature. Some efforts have been made to determine fire MCE operationally from space-based measurements such as TROPOMI CO and NO_2 or VIIRS visible energy fraction (van der Velde et al., 2021; Wang et al., 2020). These efforts could improve EFs for species that are anticorrelated with MCE (NMVOCs, OA, organic nitrogen-containing compounds). Additional information on fuel-specific EFs in inventories would improve simulations of inorganic species related to the use of agricultural chemicals and fuel composition such as nitrogen content. As a first step, the better comparison between other regionally-specific EFs and this study compared to global averages highlights the importance of EFs that are regionally- and seasonally-specific even if crop-specific information or the ability to vary EFs with MCE or fuel moisture is not yet available. Variation of EFs with season has been implemented for methane emissions from Australian savannas (Russell-Smith et al., 2013). Models could consider similarly implementing both regionally-specific and temporally varying EFs, for example, to address the "wet" or "dry" EFs based on knowledge of fuel conditions such as was observed during FIREX-AQ for grasslands. Preliminary work on such an implementation for the Eastern US. has begun combining cropland information from the CDL product with the EFs from this work and other local sources and including seasonally varying grassland EFs (Fite et al., 2023).

Data Availability Statement

FIREX-AQ observations are available at https://doi.org/10.5067/SUBORBITAL/FIREXAQ2019/DATA001. The specific observations used in this work have been compiled at https://doi.org/10.5281/zenodo.7884392. Analysis code is provided at https://doi.org/10.5281/zenodo.8276726.

References

Acquah, G., Via, B., Gallagher, T., Billor, N., Fasina, O., & Eckhardt, L. (2018). High throughput screening of elite loblolly pine families for chemical and bioenergy traits with near infrared spectroscopy. *Forests*, *9*(7), 418. https://doi.org/10.3390/f9070418

Adetona, O., Reinhardt, T. E., Domitrovich, J., Broyles, G., Adetona, A. M., Kleinman, M. T., et al. (2016). Review of the health effects of wildland fire smoke on wildland firefighters and the public. *Inhalation Toxicology*, *28*(3), 95–139. https://doi.org/10.3109/08958378.2016.1145771

Afrin, S., & Garcia-Menendez, F. (2020). The influence of prescribed fire on fine particulate matter pollution in the southeastern United States. *Geophysical Research Letters*, *47*(15), e2020GL088988. https://doi.org/10.1029/2020GL088988

Ahern, A. T., Robinson, E. S., Tkacik, D. S., Saleh, R., Hatch, L. E., Barsanti, K. C., et al. (2019). Production of secondary organic aerosol during aging of biomass burning smoke from fresh fuels and its relationship to VOC precursors. *Journal of Geophysical Research: Atmospheres*, *124*(6), 3583–3606. https://doi.org/10.1029/2018JD029068

Akagi, S. K., Yokelson, R. J., Burling, I. R., Meinardi, S., Simpson, I., Blake, D. R., et al. (2013). Measurements of reactive trace gases and variable O_3 formation rates in some South Carolina biomass burning plumes. *Atmospheric Chemistry and Physics*, *13*(3), 1141–1165. https://doi.org/10.5194/acp-13-1141-2013

Akagi, S. K., Yokelson, R. J., Wiedinmyer, C., Alvarado, M. J., Reid, J. S., Karl, T., et al. (2011). Emission factors for open and domestic biomass burning for use in atmospheric models. *Atmospheric Chemistry and Physics*, *11*(9), 4039–4072. https://doi.org/10.5194/acp-11-4039-2011

Akherati, A., He, Y., Coggon, M. M., Koss, A. R., Hodshire, A. L., Sekimoto, K., et al. (2020). Oxygenated aromatic compounds are important precursors of secondary organic aerosol in biomass-burning emissions. *Environmental Science & Technology*, *54*(14), 8568–8579. https://doi.org/10.1021/acs.est.0c01345

Allen, H. M., Crounse, J. D., Kim, M. J., Teng, A. P., Ray, E. A., McKain, K., et al. (2022). H_2O_2 and CH_3OOH (MHP) in the remote atmosphere: 1. Global distribution and regional influences. *Journal of Geophysical Research: Atmospheres*, *127*(6), e2021JD035701. https://doi.org/10.1029/2021JD035701

Alvarado, L. M. A., Richter, A., Vrekoussis, M., Hilboll, A., Kalisz Hedegaard, A. B., Schneising, O., & Burrows, J. P. (2020). Unexpected long-range transport of glyoxal and formaldehyde observed from the Copernicus Sentinel-5 Precursor satellite during the 2018 Canadian wildfires. *Atmospheric Chemistry and Physics*, *20*(4), 2057–2072. https://doi.org/10.5194/acp-20-2057-2020

Alvarado, M. J., Logan, J. A., Mao, J., Apel, E., Riemer, D., Blake, D., et al. (2010). Nitrogen oxides and PAN in plumes from boreal fires during ARCTAS-B and their impact on ozone: An integrated analysis of aircraft and satellite observations. *Atmospheric Chemistry and Physics*, *10*(20), 9739–9760. https://doi.org/10.5194/acp-10-9739-2010

Anderson, B. E., Gregory, G. L., Collins, J. E., Jr., Sachse, G. W., Conway, T. J., & Whiting, G. P. (1996). Airborne observations of the spatial and temporal variability of tropospheric carbon dioxide. *Journal of Geophysical Research*, *101*(D1), 1985–1997. https://doi.org/10.1029/95JD00413

Andreae, M. O. (2019). Emission of trace gases and aerosols from biomass burning – An updated assessment. *Atmospheric Chemistry and Physics*, *19*(13), 8523–8546. https://doi.org/10.5194/acp-19-8523-2019

Andreae, M. O., Anderson, B. E., Blake, D. R., Bradshaw, J. D., Collins, J. E., Gregory, G. L., et al. (1994). Influence of plumes from biomass burning on atmospheric chemistry over the equatorial and tropical South Atlantic during CITE 3. *Journal of Geophysical Research*, *99*(D6), 12793. https://doi.org/10.1029/94JD00263

Apel, E. C., Hornbrook, R. S., Hills, A. J., Blake, N. J., Barth, M. C., Weinheimer, A., et al. (2015). Upper tropospheric ozone production from lightning NO_x-impacted convection: Smoke ingestion case study from the DC3 campaign. *Journal of Geophysical Research: Atmospheres*, *120*(6), 2505–2523. https://doi.org/10.1002/2014JD022121

Aurell, J., Gullett, B. K., & Tabor, D. (2015). Emissions from southeastern U.S. Grasslands and pine savannas: Comparison of aerial and ground field measurements with laboratory burns. *Atmospheric Environment*, *111*, 170–178. https://doi.org/10.1016/j.atmosenv.2015.03.001

Bahlmann, E., Keppler, F., Wittmer, J., Greule, M., Schöler, H. F., Seifert, R., & Zetzsch, C. (2019). Evidence for a major missing source in the global chloromethane budget from stable carbon isotopes. *Atmospheric Chemistry and Physics*, *19*(3), 1703–1719. https://doi.org/10.5194/acp-19-1703-2019

Baker, K. R., Woody, M. C., Tonnesen, G. S., Hutzell, W., Pye, H. O. T., Beaver, M. R., et al. (2016). Contribution of regional-scale fire events to ozone and PM$_{2.5}$ air quality estimated by photochemical modeling approaches. *Atmospheric Environment*, *140*, 539–554. https://doi.org/10.1016/j.atmosenv.2016.06.032

Bell, M. L., Ebisu, K., Peng, R. D., Samet, J. M., & Dominici, F. (2009). Hospital admissions and chemical composition of fine particle air pollution. *American Journal of Respiratory and Critical Care Medicine*, *179*(12), 1115–1120. https://doi.org/10.1164/rccm.200808-1240OC

Blake, N. J., Blake, D. R., Sive, B. C., Chen, T.-Y., Rowland, F. S., Collins, J. E., et al. (1996). Biomass burning emissions and vertical distribution of atmospheric methyl halides and other reduced carbon gases in the South Atlantic region. *Journal of Geophysical Research*, *101*(D19), 24151–24164. https://doi.org/10.1029/96JD00561

Boryan, C., Yang, Z., Mueller, R., & Craig, M. (2011). Monitoring US agriculture: The US Department of Agriculture, National Agricultural Statistics Service, Cropland Data Layer Program. *Geocarto International*, *26*(5), 341–358. https://doi.org/10.1080/10106049.2011.562309

Bourgeois, I., Peischl, J., Neuman, J. A., Brown, S. S., Allen, H. M., Campuzano-Jost, P., et al. (2022). Comparison of airborne measurements of NO, NO$_2$, HONO, NO$_y$, and CO during FIREX-AQ. *Atmospheric Measurement Techniques*, *15*(16), 4901–4930. https://doi.org/10.5194/amt-15-4901-2022

Bourgeois, I., Peischl, J., Neuman, J. A., Brown, S. S., Thompson, C. R., Aikin, K. C., et al. (2021). Large contribution of biomass burning emissions to ozone throughout the global remote troposphere. *Proceedings of the National Academy of Sciences*, *118*(52), e2109628118. https://doi.org/10.1073/pnas.2109628118

Bradshaw, L. S., Deeming, J. E., Burgan, R. E., & Cohen, J. D. (1984). *The 1978 National Fire-Danger Rating System: Technical documentation (No. INT-GTR-169)* (p. INT-GTR-169). U.S. Department of Agriculture, Forest Service, Intermountain Forest and Range Experiment Station. https://doi.org/10.2737/INT-GTR-169

Burling, I. R., Yokelson, R. J., Akagi, S. K., Urbanski, S. P., Wold, C. E., Griffith, D. W. T., et al. (2011). Airborne and ground-based measurements of the trace gases and particles emitted by prescribed fires in the United States. *Atmospheric Chemistry and Physics*, *11*(23), 12197–12216. https://doi.org/10.5194/acp-11-12197-2011

Burling, I. R., Yokelson, R. J., Griffith, D. W. T., Johnson, T. J., Veres, P., Roberts, J. M., et al. (2010). Laboratory measurements of trace gas emissions from biomass burning of fuel types from the southeastern and southwestern United States. *Atmospheric Chemistry and Physics*, *10*(22), 11115–11130. https://doi.org/10.5194/acp-10-11115-2010

Cady-Pereira, K. E., Chaliyakunnel, S., Shephard, M. W., Millet, D. B., Luo, M., & Wells, K. C. (2014). HCOOH measurements from space: TES retrieval algorithm and observed global distribution. *Atmos. Meas. Tech.*, *7*(7), 2297–2311. https://doi.org/10.5194/amt-7-2297-2014

Capehart, T., & Proper, S. (2019). *Corn is America's Largest Crop in 2019*. USDA Economic Research Service. Retrieved from https://www.usda.gov/media/blog/2019/07/29/corn-americas-largest-crop-2019

Carter, T. S., Heald, C. L., Jimenez, J. L., Campuzano-Jost, P., Kondo, Y., Moteki, N., et al. (2020). How emissions uncertainty influences the distribution and radiative impacts of smoke from fires in North America. *Atmospheric Chemistry and Physics*, *20*(4), 2073–2097. https://doi.org/10.5194/acp-20-2073-2020

Carter, T. S., Heald, C. L., Kroll, J. H., Apel, E. C., Blake, D., Coggon, M., et al. (2022). An improved representation of fire non-methane organic gases (NMOGs) in models: Emissions to reactivity. *Atmospheric Chemistry and Physics*, *22*(18), 12093–12111. https://doi.org/10.5194/acp-22-12093-2022

Cazorla, M., Wolfe, G. M., Bailey, S. A., Swanson, A. K., Arkinson, H. L., & Hanisco, T. F. (2015). A new airborne laser-induced fluorescence instrument for in situ detection of formaldehyde throughout the troposphere and lower stratosphere. *Atmospheric Measurement Techniques*, *8*(2), 541–552. https://doi.org/10.5194/amt-8-541-2015

Chai, J., Dibb, J. E., Anderson, B. E., Bekker, C., Blum, D. E., Heim, E., et al. (2021). Isotopic evidence for dominant secondary production of HONO in near-ground wildfire plumes. *Atmospheric Chemistry and Physics*, *21*(17), 13077–13098. https://doi.org/10.5194/acp-21-13077-2021

Chai, J., Miller, D. J., Scheuer, E., Dibb, J., Selimovic, V., Yokelson, R., et al. (2019). Isotopic characterization of nitrogen oxides (NO$_x$), nitrous acid (HONO), and nitrate (NO$_3^-$) from laboratory biomass burning during FIREX. *Atmospheric Measurement Techniques*, *12*(12), 6303–6317. https://doi.org/10.5194/amt-12-6303-2019

Chance, K., Palmer, P. I., Spurr, R. J. D., Martin, R. V., Kurosu, T. P., & Jacob, D. J. (2000). Satellite observations of formaldehyde over North America from GOME. *Geophysical Research Letters*, *27*(21), 3461–3464. https://doi.org/10.1029/2000GL011857

Chan Miller, C., Gonzalez Abad, G., Wang, H., Liu, X., Kurosu, T., Jacob, D. J., & Chance, K. (2014). Glyoxal retrieval from the ozone monitoring instrument. *Atmospheric Measurement Techniques*, *7*(11), 3891–3907. https://doi.org/10.5194/amt-7-3891-2014

Chen, L.-W. A., Verburg, P., Shackelford, A., Zhu, D., Susfalk, R., Chow, J. C., & Watson, J. G. (2010). Moisture effects on carbon and nitrogen emission from burning of wildland biomass. *Atmospheric Chemistry and Physics*, *10*(14), 6617–6625. https://doi.org/10.5194/acp-10-6617-2010

Christian, T. J. (2003). Comprehensive laboratory measurements of biomass-burning emissions: 1. Emissions from Indonesian, African, and other fuels. *Journal of Geophysical Research*, *108*(D23), 4719. https://doi.org/10.1029/2003JD003704

Coggon, M. M., Veres, P. R., Yuan, B., Koss, A., Warneke, C., Gilman, J. B., et al. (2016). Emissions of nitrogen-containing organic compounds from the burning of herbaceous and arboraceous biomass: Fuel composition dependence and the variability of commonly used nitrile tracers. *Geophysical Research Letters*, *43*(18), 9903–9912. https://doi.org/10.1002/2016GL070562

Crounse, J. D., McKinney, K. A., Kwan, A. J., & Wennburg, P. O. (2006). Measurement of gas-phase hydroperoxides by chemical ionization mass spectrometry. *Analytical Chemistry*, *78*(19), 6726–6732. https://doi.org/10.1021/ac0604235

Decker, Z. C. J., Zarzana, K. J., Coggon, M., Min, K.-E., Pollack, I., Ryerson, T. B., et al. (2019). Nighttime chemical transformation in biomass burning plumes: A box model analysis initialized with aircraft observations. *Environmental Science & Technology*, *53*(5), 2529–2538. https://doi.org/10.1021/acs.est.8b05359

Dickinson, G. N., Miller, D. D., Bajracharya, A., Bruchard, W., Durbin, T. A., McGarry, J. K. P., et al. (2022). Health risk implications of volatile organic compounds in wildfire smoke during the 2019 FIREX-AQ campaign and beyond. *GeoHealth*, *6*(8), e2021GH000546. https://doi.org/10.1029/2021GH000546

Doubleday, A., Schulte, J., Sheppard, L., Kadlec, M., Dhammapala, R., Fox, J., & Busch Isaksen, T. (2020). Mortality associated with wildfire smoke exposure in Washington state, 2006–2017: A case-crossover study. *Environmental Health*, *19*(1), 1–10. https://doi.org/10.1186/s12940-020-0559-2

Eckhardt, S., Breivik, K., Manø, S., & Stohl, A. (2007). Record high peaks in PCB concentrations in the Arctic atmosphere due to long-range transport of biomass burning emissions. *Atmospheric Chemistry and Physics*, *7*(17), 4527–4536. https://doi.org/10.5194/acp-7-4527-2007

EPA. (2018). *Problem Formulation of the Risk Evaluation for Methylene Chloride (Dichloromethane, DCM) (No. EPA 740-R1-7016)*. Office of Chemical Safety and Pollution Prevention. Retrieved from https://www.epa.gov/sites/default/files/2018-06/documents/mecl_problem_formulation_05-31-18.pdf

Essig, M., Richards, G. N., & Schenck, E. (1989). Mechanisms of formation of the major volatile products from the pyrolysis of cellulose. In *Proceedings of the 10th Cellulose Conference*. John Wiley & Sons.

Fishman, J., Watson, C. E., Larsen, J. C., & Logan, J. A. (1990). Distribution of tropospheric ozone determined from satellite data. *Journal of Geophysical Research*, *95*(D4), 3599. https://doi.org/10.1029/JD095iD04p03599

Fite, C., Holmes, C., Kumar, A., Pierce, R. B., Ahmadov, R., Schmidt, C., et al. (2023). Impact of large emissions from prescribed fires on air quality in the eastern U.S. In *Paper presented at 103rd AMS Annual Meeting*. AMS.

Fraser, M. P., & Lakshmanan, K. (2000). Using levoglucosan as a molecular marker for the long-range transport of biomass combustion aerosols. *Environmental Science & Technology*, *34*(21), 4560–4564. https://doi.org/10.1021/es991229l

Gilman, J. B., Lerner, B. M., Kuster, W. C., Goldan, P. D., Warneke, C., Veres, P. R., et al. (2015). Biomass burning emissions and potential air quality impacts of volatile organic compounds and other trace gases from fuels common in the US. *Atmospheric Chemistry and Physics*, *15*(24), 13915–13938. https://doi.org/10.5194/acp-15-13915-2015

Gkatzelis, G. I., Coggon, M. M., Stockwell, C. E., Hornbrook, R. S., Allen, H., Apel, E. C., et al. (2023). Parameterizations of US wildfire and prescribed fire emission ratios and emission factors based on FIREX-AQ aircraft measurements. *EGUsphere*. https://doi.org/10.5194/egusphere-2023-1439

Guo, H. (2020). *Submicron Particle Composition and Acidity in Fire Plumes during FIREX-AQ aircraft study*. AGU. Retrieved from https://agu.confex.com/agu/fm20/meetingapp.cgi/Paper/686968

Guo, H., Campuzano-Jost, P., Nault, B. A., Day, D. A., Schroder, J. C., Kim, D., et al. (2021). The importance of size ranges in aerosol instrument intercomparisons: A case study for the atmospheric tomography mission. *Atmospheric Measurement Techniques*, *14*(5), 3631–3655. https://doi.org/10.5194/amt-14-3631-2021

Hall, S. R., Ullmann, K., Prather, M. J., Flynn, C. M., Murray, L. T., Fiore, A. M., et al. (2018). Cloud impacts on photochemistry: Building a climatology of photolysis rates from the atmospheric tomography mission. *Atmospheric Chemistry and Physics*, *18*(22), 16809–16828. https://doi.org/10.5194/acp-18-16809-2018

Hao, W. M., & Ward, D. E. (1993). Methane production from global biomass burning. *Journal of Geophysical Research*, *98*(D11), 20657. https://doi.org/10.1029/93JD01908

Hatch, L. E., Jen, C. N., Kreisberg, N. M., Selimovic, V., Yokelson, R. J., Stamatis, C., et al. (2019). Highly speciated measurements of terpenoids emitted from laboratory and mixed-conifer forest prescribed fires. *Environmental Science & Technology*, *53*(16), 9418–9428. https://doi.org/10.1021/acs.est.9b02612

Hatch, L. E., Luo, W., Pankow, J. F., Yokelson, R. J., Stockwell, C. E., & Barsanti, K. C. (2015). Identification and quantification of gaseous organic compounds emitted from biomass burning using two-dimensional gas chromatography–time-of-flight mass spectrometry. *Atmospheric Chemistry and Physics*, *15*(4), 1865–1899. https://doi.org/10.5194/acp-15-1865-2015

Hatch, L. E., Yokelson, R. J., Stockwell, C. E., Veres, P. R., Simpson, I. J., Blake, D. R., et al. (2017). Multi-instrument comparison and compilation of non-methane organic gas emissions from biomass burning and implications for smoke-derived secondary organic aerosol precursors. *Atmospheric Chemistry and Physics*, *17*(2), 1471–1489. https://doi.org/10.5194/acp-17-1471-2017

Hayashi, K., Ono, K., Kajiura, M., Sudo, S., Yonemura, S., Fushimi, A., et al. (2014). Trace gas and particle emissions from open burning of three cereal crop residues: Increase in residue moistness enhances emissions of carbon monoxide, methane, and particulate organic carbon. *Atmospheric Environment*, *95*, 36–44. https://doi.org/10.1016/j.atmosenv.2014.06.023

Hays, M. D., Fine, P. M., Geron, C. D., Kleeman, M. J., & Gullett, B. K. (2005). Open burning of agricultural biomass: Physical and chemical properties of particle-phase emissions. *Atmospheric Environment*, *39*(36), 6747–6764. https://doi.org/10.1016/j.atmosenv.2005.07.072

Hodshire, A. L., Akherati, A., Alvarado, M. J., Brown-Steiner, B., Jathar, S. H., Jimenez, J. L., et al. (2019). Aging effects on biomass burning aerosol mass and composition: A critical review of field and laboratory studies. *Environmental Science & Technology*, *53*(17), 10007–10022. https://doi.org/10.1021/acs.est.9b02588

Hoffa, E. A., Ward, D. E., Hao, W. M., Susott, R. A., & Wakimoto, R. H. (1999). Seasonality of carbon emissions from biomass burning in a Zambian savanna. *Journal of Geophysical Research*, *104*(D11), 13841–13853. https://doi.org/10.1029/1999JD900091

Houshfar, E., Skreiberg, Ø., Glarborg, P., & Løvås, T. (2012). Reduced chemical kinetic mechanisms for NO_x emission prediction in biomass combustion. *International Journal of Chemical Kinetics*, *44*(4), 219–231. https://doi.org/10.1002/kin.20716

Hu, X., Chen, D., Hu, L., Li, B., Li, X., & Fang, X. (2023). Global methyl halide emissions from biomass burning during 2003–2021. *Environmental Science and Ecotechnology*, *14*, 100228. https://doi.org/10.1016/j.ese.2022.100228

Hu, Y., Odman, M. T., Chang, M. E., Jackson, W., Lee, S., Edgerton, E. S., et al. (2008). Simulation of air quality impacts from prescribed fires on an urban area. *Environmental Science & Technology*, *42*(10), 3676–3682. https://doi.org/10.1021/es071703k

Jaffe, D. A., O'Neill, S. M., Larkin, N. K., Holder, A. L., Peterson, D. L., Halofsky, J. E., & Rappold, A. G. (2020). Wildfire and prescribed burning impacts on air quality in the United States. *Journal of the Air & Waste Management Association*, *70*(6), 583–615. https://doi.org/10.1080/10962247.2020.1749731

Jaffe, D. A., & Wigder, N. L. (2012). Ozone production from wildfires: A critical review. *Atmospheric Environment*, *51*, 1–10. https://doi.org/10.1016/j.atmosenv.2011.11.063

Janhall, S., Andreae, M. O., & Poschl, U. (2010). Biomass burning aerosol emissions from vegetation fires: Particle number and mass emission factors and size distributions. *Atmospheric Chemistry and Physics*, *10*(3), 1427–1439. https://doi.org/10.5194/acp-10-1427-2010

Johnson, A. S., & Hale, P. E. (2002). The historical foundations of prescribed burning for wildlife: A southeastern perspective (Vol. *13*).

Johnson, D. M., & Mueller, R. (2010). The 2009 cropland data layer. *Photogrammetric Engineering and Remote Sensing*, *76*(11), 1201–1205.

Kaulfus, A. S., Nair, U., Jaffe, D., Christopher, S. A., & Goodrick, S. (2017). Biomass burning smoke climatology of the United States: Implications for particulate matter air quality. *Environmental Science & Technology*, *51*(20), 11731–11741. https://doi.org/10.1021/acs.est.7b03292

Kelly, J. T., Koplitz, S. N., Baker, K. R., Holder, A. L., Pye, H. O. T., Murphy, B. N., et al. (2019). Assessing $PM_{2.5}$ model performance for the conterminous U.S. with comparison to model performance statistics from 2007–2015. *Atmospheric Environment*, *214*, 116872. https://doi.org/10.1016/j.atmosenv.2019.116872

Kibet, J., Khachatryan, L., & Dellinger, B. (2012). Molecular products and radicals from pyrolysis of lignin. *Environmental Science & Technology*, *46*(23), 12994–13001. https://doi.org/10.1021/es302942c

Koplitz, S. N., Nolte, C. G., Pouliot, G. A., Vukovich, J. M., & Beidler, J. (2018). Influence of uncertainties in burned area estimates on modeled wildland fire $PM_{2.5}$ and ozone pollution in the contiguous U.S. *Atmospheric Environment*, *191*, 328–339. https://doi.org/10.1016/j.atmosenv.2018.08.020

Korontzi, S., McCarty, J., & Justice, C. (2008). Monitoring agricultural burning in the Mississippi River Valley region from the moderate resolution imaging spectroradiometer (MODIS). *Journal of the Air & Waste Management Association*, *58*(9), 1235–1239. https://doi.org/10.3155/1047-3289.58.9.1235

Korontzi, S., Ward, D. E., Susott, R. A., Yokelson, R. J., Justice, C. O., Hobbs, P. V., et al. (2003). Seasonal variation and ecosystem dependence of emission factors for selected trace gases and $PM_{2.5}$ for southern African savanna fires: Seasonality of savanna fire emissions. *Journal of Geophysical Research*, *108*(D24), 4758. https://doi.org/10.1029/2003JD003730

Koss, A. R., Sekimoto, K., Gilman, J. B., Selimovic, V., Coggon, M. M., Zarzana, K. J., et al. (2018). Non-methane organic gas emissions from biomass burning: Identification, quantification, and emission factors from PTR-ToF during the FIREX 2016 laboratory experiment. *Atmospheric Chemistry and Physics*, *18*(5), 3299–3319. https://doi.org/10.5194/acp-18-3299-2018

Larkin, N. K., Raffuse, S. M., Huang, S., Pavlovic, N., Lahm, P., & Rao, V. (2020). The comprehensive fire information reconciled emissions (CFIRE) inventory: Wildland fire emissions developed for the 2011 and 2014 U.S. National Emissions Inventory. *Journal of the Air & Waste Management Association*, *70*(11), 1165–1185. https://doi.org/10.1080/10962247.2020.1802365

Lee, M., Heikes, B. G., Jacob, D. J., Sachse, G., & Anderson, B. (1997). Hydrogen peroxide, organic hydroperoxide, and formaldehyde as primary pollutants from biomass burning. *Journal of Geophysical Research*, *102*(D1), 1301–1309. https://doi.org/10.1029/96JD01709

Lee, S., Kim, H. K., Yan, B., Cobb, C. E., Hennigan, C., Nichols, L., et al. (2008). Diagnosis of aged prescribed burning plumes impacting an urban area. *Environmental Science & Technology*, *42*(5), 1438–1444. https://doi.org/10.1021/es7023059

Leppälahti, J., & Koljonen, T. (1995). Nitrogen evolution from coal, peat and wood during gasification: Literature review. *Fuel Processing Technology*, *43*(1), 1–45. https://doi.org/10.1016/0378-3820(94)00123-B

Lerner, B. M., Gilman, J. B., Aikin, K. C., Atlas, E. L., Goldan, P. D., Graus, M., et al. (2017). An improved, automated whole air sampler and gas chromatography mass spectrometry analysis system for volatile organic compounds in the atmosphere. *Atmospheric Measurement Techniques*, *10*(1), 291–313. https://doi.org/10.5194/amt-10-291-2017

Li, H., Lamb, K. D., Schwarz, J. P., Selimovic, V., Yokelson, R. J., McMeeking, G. R., & May, A. A. (2019). Inter-comparison of black carbon measurement methods for simulated open biomass burning emissions. *Atmospheric Environment*, *206*, 156–169. https://doi.org/10.1016/j.atmosenv.2019.03.010

Liao, J., Wolfe, G. M., Hannun, R. A., St. Clair, J. M., Hanisco, T. F., Gilman, J. B., et al. (2021). Formaldehyde evolution in US wildfire plumes during the Fire Influence on Regional to Global Environments and Air Quality experiment (FIREX-AQ). *Atmospheric Chemistry and Physics*, *21*(24), 18319–18331. https://doi.org/10.5194/acp-21-18319-2021

Lin, H., McCarty, J. L., Wang, D., Rogers, B. M., Morton, D. C., Collatz, G. J., et al. (2014). Management and climate contributions to satellite-derived active fire trends in the contiguous United States. *Journal of Geophysical Research: Biogeosciences*, *119*(4), 645–660. https://doi.org/10.1002/2013JG002382

Liu, X., Zhang, Y., Huey, L. G., Yokelson, R. J., Wang, Y., Jimenez, J. L., et al. (2016). Agricultural fires in the southeastern U.S. during SEAC⁴RS: Emissions of trace gases and particles and evolution of ozone, reactive nitrogen, and organic aerosol. *Journal of Geophysical Research: Atmospheres*, *121*(12), 7383–7414. https://doi.org/10.1002/2016JD025040

Lobert, J. M., Keene, W. C., Logan, J. A., & Yevich, R. (1999). Global chlorine emissions from biomass burning: Reactive chlorine emissions inventory. *Journal of Geophysical Research*, *104*(D7), 8373–8389. https://doi.org/10.1029/1998JD100077

Lopez-Hilfiker, F. D., Pospisilova, V., Huang, W., Kalberer, M., Mohr, C., Stefenelli, G., et al. (2019). An extractive electrospray ionization time-of-flight mass spectrometer (EESI-TOF) for online measurement of atmospheric aerosol particles. *Atmospheric Measurement Techniques*, *12*(9), 4867–4886. https://doi.org/10.5194/amt-12-4867-2019

Loveland, T. R., Zhu, Z., Ohlen, D. O., Brown, J. F., Reed, B. C., & Yang, L. (1999). An analysis of IGBP global land-cover characterization process. *Photogrammetric Engineering and Remote Sensing*, *65*(9), 1021–1032.

May, A. A., Lee, T., McMeeking, G. R., Akagi, S., Sullivan, A. P., Urbanski, S., et al. (2015). Observations and analysis of organic aerosol evolution in some prescribed fire smoke plumes. *Atmospheric Chemistry and Physics*, *15*(11), 6323–6335. https://doi.org/10.5194/acp-15-6323-2015

May, A. A., McMeeking, G. R., Lee, T., Taylor, J. W., Craven, J. S., Burling, I., et al. (2014). Aerosol emissions from prescribed fires in the United States: A synthesis of laboratory and aircraft measurements: Aerosols from US prescribed fires. *Journal of Geophysical Research: Atmospheres*, *119*(20), 11826–11849. https://doi.org/10.1002/2014JD021848

McCarty, J. L. (2011). Remote sensing-based estimates of annual and seasonal emissions from crop residue burning in the contiguous United States. *Journal of the Air & Waste Management Association*, *61*(1), 22–34. https://doi.org/10.3155/1047-3289.61.1.22

McCarty, J. L., Korontzi, S., Justice, C. O., & Loboda, T. (2009). The spatial and temporal distribution of crop residue burning in the contiguous United States. *Science of The Total Environment*, *407*(21), 5701–5712. https://doi.org/10.1016/j.scitotenv.2009.07.009

Melvin, M. A. (2018). *2018 National Prescribed Fire Use Survey Report (No. Technical Report 03-18)*. Coalition of Prescribed Fire Councils, Inc. Retrieved from https://www.prescribedfire.net

Min, K.-E., Washenfelder, R. A., Dubé, W. P., Langford, A. O., Edwards, P. M., Zarzana, K. J., et al. (2016). A broadband cavity enhanced absorption spectrometer for aircraft measurements of glyoxal, methylglyoxal, nitrous acid, nitrogen dioxide, and water vapor. *Atmospheric Measurement Techniques*, *9*(2), 423–440. https://doi.org/10.5194/amt-9-423-2016

Moore, R. H., Wiggins, E. B., Ahern, A. T., Zimmerman, S., Montgomery, L., Campuzano Jost, P., et al. (2021). Sizing response of the ultra-high sensitivity aerosol spectrometer (UHSAS) and laser aerosol spectrometer (LAS) to changes in submicron aerosol composition and refractive index. *Atmospheric Measurement Techniques*, *14*(6), 4517–4542. https://doi.org/10.5194/amt-14-4517-2021

Müller, M., Anderson, B. E., Beyersdorf, A. J., Crawford, J. H., Diskin, G. S., Eichler, P., et al. (2016). In situ measurements and modeling of reactive trace gases in a small biomass burning plume. *Atmospheric Chemistry and Physics*, *16*(6), 3813–3824. https://doi.org/10.5194/acp-16-3813-2016

Naeher, L. P., Brauer, M., Lipsett, M., Zelikoff, J. T., Simpson, C. D., Koenig, J. Q., & Smith, K. R. (2007). Woodsmoke health effects: A review. *Inhalation Toxicology*, *19*(1), 67–106. https://doi.org/10.1080/08958370600985875

Nault, B. A., Campuzano-Jost, P., Day, D. A., Jo, D. S., Schroder, J. C., Allen, H. M., et al. (2021). Chemical transport models often underestimate inorganic aerosol acidity in remote regions of the atmosphere. *Communications Earth & Environment*, *2*(1), 93. https://doi.org/10.1038/s43247-021-00164-0

Nault, B. A., Campuzano-Jost, P., Day, D. A., Schroder, J. C., Anderson, B., Beyersdorf, A. J., et al. (2018). Secondary organic aerosol production from local emissions dominates the organic aerosol budget over Seoul, South Korea, during KORUS-AQ. *Atmospheric Chemistry and Physics*, *18*(24), 17769–17800. https://doi.org/10.5194/acp-18-17769-2018

NIFC. (2022). Total wildland fires and acres (1983–2022) [Dataset]. National Interagency Coordination Center. Retrieved from https://www.nifc.gov/fire-information/statistics/wildfires

Ninneman, M., & Jaffe, D. A. (2021). The impact of wildfire smoke on ozone production in an urban area: Insights from field observations and photochemical box modeling. *Atmospheric Environment*, *267*, 118764. https://doi.org/10.1016/j.atmosenv.2021.118764

Nowell, H. K., Holmes, C. D., Robertson, K., Teske, C., & Hiers, J. K. (2018). A new picture of fire extent, variability, and drought interaction in prescribed fire landscapes: Insights from Florida government records. *Geophysical Research Letters*, *45*(15), 7874–7884. https://doi.org/10.1029/2018GL078679

O'Dell, K., Hornbrook, R. S., Permar, W., Levin, E. J. T., Garofalo, L. A., Apel, E. C., et al. (2020). Hazardous air pollutants in fresh and aged western US wildfire smoke and implications for long-term exposure. *Environmental Science & Technology*, *54*(19), 11838–11847. https://doi.org/10.1021/acs.est.0c04497

Ortega, A. M., Day, D. A., Cubison, M. J., Brune, W. H., Bon, D., de Gouw, J. A., & Jimenez, J. L. (2013). Secondary organic aerosol formation and primary organic aerosol oxidation from biomass-burning smoke in a flow reactor during FLAME-3. *Atmospheric Chemistry and Physics*, *13*(22), 11551–11571. https://doi.org/10.5194/acp-13-11551-2013

Ottmar, R. D., Sandberg, D. V., Riccardi, C. L., & Prichard, S. J. (2007). An overview of the fuel characteristic classification system—Quantifying, classifying, and creating fuelbeds for resource planning. *Canadian Journal of Forest Research*, *37*(12), 2383–2393. https://doi.org/10.1139/X07-077

Pagonis, D., Campuzano-Jost, P., Guo, H., Day, D. A., Schueneman, M. K., Brown, W. L., et al. (2021). Airborne extractive electrospray mass spectrometry measurements of the chemical composition of organic aerosol. *Atmospheric Measurement Techniques*, *14*(2), 1545–1559. https://doi.org/10.5194/amt-14-1545-2021

Patwardhan, P. R., Satrio, J. A., Brown, R. C., & Shanks, B. H. (2010). Influence of inorganic salts on the primary pyrolysis products of cellulose. *Bioresource Technology*, *101*(12), 4646–4655. https://doi.org/10.1016/j.biortech.2010.01.112

Peng, Q., Palm, B. B., Melander, K. E., Lee, B. H., Hall, S. R., Ullmann, K., et al. (2020). HONO emissions from western U.S. Wildfires provide dominant radical source in fresh wildfire smoke. *Environmental Science & Technology*, *54*(10), 5954–5963. https://doi.org/10.1021/acs.est.0c00126

Permar, W., Jin, L., Peng, Q., O'Dell, K., Lill, E., Selimovic, V., et al. (2023). Atmospheric OH reactivity in the western United States determined from comprehensive gas-phase measurements during WE-CAN. *Environmental Science: Atmospheres*, *3*(1), 97–114. https://doi.org/10.1039/D2EA00063F

Permar, W., Wang, Q., Selimovic, V., Wielgasz, C., Yokelson, R. J., Hornbrook, R. S., et al. (2021). Emissions of trace organic gases from western U.S. Wildfires based on WE-CAN aircraft measurements. *Journal of Geophysical Research: Atmospheres*, *126*(11), e2020JD033838. https://doi.org/10.1029/2020JD033838

Pierce, J. R., Chen, K., & Adams, P. J. (2007). Contribution of primary carbonaceous aerosol to cloud condensation nuclei: Processes and uncertainties evaluated with a global aerosol microphysics model. *Atmospheric Chemistry and Physics*, *7*(20), 5447–5466. https://doi.org/10.5194/acp-7-5447-2007

Pokhrel, R. P., Wagner, N. L., Langridge, J. M., Lack, D. A., Jayarathne, T., Stone, E. A., et al. (2016). Parameterization of single-scattering albedo (SSA) and absorption Ångströmexponent (AAE) with EC/OC for aerosol emissions from biomass burning. *Atmospheric Chemistry and Physics*, *16*(15), 9549–9561. https://doi.org/10.5194/acp-16-9549-2016

Pouliot, G., Rao, V., McCarty, J. L., & Soja, A. (2017). Development of the crop residue and rangeland burning in the 2014 National Emissions Inventory using information from multiple sources. *Journal of the Air & Waste Management Association*, *67*(5), 613–622. https://doi.org/10.1080/10962247.2016.1268982

Prichard, S. J., Sandberg, D. V., Ottmar, R. D., Eberhardt, E., Andreu, A., Eagle, P., & Swedin, K. (2013). *Fuel Characteristic Classification System version 3.0: Technical documentation (No. PNW-GTR-887)* (p. PNW-GTR-887). U.S. Department of Agriculture, Forest Service, Pacific Northwest Research Station. https://doi.org/10.2737/PNW-GTR-887

Quinteros, M. E., Blanco, E., Sanabria, J., Rosas-Diaz, F., Blazquez, C. A., Ayala, S., et al. (2023). Spatio-temporal distribution of particulate matter and wood-smoke tracers in Temuco, Chile: A city heavily impacted by residential wood-burning. *Atmospheric Environment*, *294*, 119529. https://doi.org/10.1016/j.atmosenv.2022.119529

Rabin, S. S., Ward, D. S., Malyshev, S. L., Magi, B. I., Shevliakova, E., & Pacala, S. W. (2018). A fire model with distinct crop, pasture, and non-agricultural burning: Use of new data and a model-fitting algorithm for FINAL.1. *Geoscientific Model Development*, *11*(2), 815–842. https://doi.org/10.5194/gmd-11-815-2018

Radke, L. F., Hegg, D. A., Hobbs, P. V., Nance, J. D., Lyons, J. H., Laursen, K. K., et al. (1991). Particulate and trace gas emissions from large biomass fires in North America. *Global Biomass Burning: Atmospheric, Climatic, and Biospheric Implications*, *5*, 219–220.

Randerson, J. T., Chen, Y., van der Werf, G. R., Rogers, B. M., & Morton, D. C. (2012). Global burned area and biomass burning emissions from small fires. *Journal of Geophysical Research*, *117*(G4), G04012. https://doi.org/10.1029/2012JG002128

Razavi, A., Karagulian, F., Clarisse, L., Hurtmans, D., Coheur, P. F., Clerbaux, C., et al. (2011). Global distributions of methanol and formic acid retrieved for the first time from the IASI/MetOp thermal infrared sounder. *Atmospheric Chemistry and Physics*, *11*(2), 857–872. https://doi.org/10.5194/acp-11-857-2011

Reid, C. E., Brauer, M., Johnston, F. H., Jerrett, M., Balmes, J. R., & Elliott, C. T. (2016). Critical review of health impacts of wildfire smoke exposure. *Environmental Health Perspectives*, *124*(9), 1334–1343. https://doi.org/10.1289/ehp.1409277

Richter, D., Weibring, P., Walega, J. G., Fried, A., Spuler, S. M., & Taubman, M. S. (2015). Compact highly sensitive multi-species airborne mid-IR spectrometer. *Applied Physics B*, *119*(1), 119–131. https://doi.org/10.1007/s00340-015-6038-8

Rickly, P., Guo, H., Campuzano-Jost, P., Jimenez, J. L., Wolfe, G. M., Bennett, R., et al. (2022). Emission factors and evolution of SO_2 measured from biomass burning in wild and agricultural fires (preprint). *Gases/field measurements/troposphere/chemistry (chemical composition and reactions)*. https://doi.org/10.5194/acp-2022-309

Rickly, P. S., Coggon, M. M., Aikin, K. C., Alvarez, R. J., Baidar, S., Gilman, J. B., et al. (2023). Influence of wildfire on urban ozone: An observationally constrained box modeling study at a site in the Colorado front range. *Environmental Science & Technology*, *57*(3), 1257–1267. https://doi.org/10.1021/acs.est.2c06157

Roberts, J. M., Stockwell, C. E., Yokelson, R. J., de Gouw, J., Liu, Y., Selimovic, V., et al. (2020). The nitrogen budget of laboratory-simulated western US wildfires during the FIREX 2016 Fire Lab study. *Atmospheric Chemistry and Physics*, *20*(14), 8807–8826. https://doi.org/10.5194/acp-20-8807-2020

Roberts, J. M., Veres, P., Warneke, C., Neuman, J. A., Washenfelder, R. A., Brown, S. S., et al. (2010). Measurement of HONO, HNCO, and other inorganic acids by negative-ion proton-transfer chemical-ionization mass spectrometry (NI-PT-CIMS): Application to biomass burning emissions. *Atmospheric Measurement Techniques*, *3*(4), 981–990. https://doi.org/10.5194/amt-3-981-2010

Robinson, M. A., Decker, Z. C. J., Barsanti, K. C., Coggon, M. M., Flocke, F. M., Franchin, A., et al. (2021). Variability and time of day dependence of ozone photochemistry in western wildfire plumes. *Environmental Science & Technology*, *55*(15), 10280–10290. https://doi.org/10.1021/acs.est.1c01963

Rollins, A. W., Rickly, P. S., Gao, R.-S., Ryerson, T. B., Brown, S. S., Peischl, J., & Bourgeois, I. (2020). Single-photon laser-induced fluorescence detection of nitric oxide at sub-parts-per-trillion mixing ratios. *Atmospheric Measurement Techniques*, *13*(5), 2425–2439. https://doi.org/10.5194/amt-13-2425-2020

Russell-Smith, J., Cook, G. D., Cooke, P. M., Edwards, A. C., Lendrum, M., Meyer, C. P., & Whitehead, P. J. (2013). Managing fire regimes in north Australian savannas: Applying aboriginal approaches to contemporary global problems. *Frontiers in Ecology and the Environment*, *11*(s1), e55–e63. https://doi.org/10.1890/120251

Sachse, G. W., Collins, J. E., Jr., Hill, G. F., Wade, L. O., Burney, L. G., & Ritter, J. A. (1991). Airborne tunable diode laser sensor for high-precision concentration and flux measurements of carbon monoxide and methane, *Optics, Electro-Optics, and Laser Applications in Science and Engineering* (Vol. *157*). https://doi.org/10.1117/12.46162

Sachse, G. W., Hill, G. F., Wade, L. O., & Perry, M. G. (1987). Fast-response, high-precision carbon monoxide sensor using a tunable diode laser absorption technique. *Journal of Geophysical Research*, *92*(D2), 2071–2081. https://doi.org/10.1029/JD092iD02p02071

Saini, J. K., Saini, R., & Tewari, L. (2015). Lignocellulosic agriculture wastes as biomass feedstocks for second-generation bioethanol production: Concepts and recent developments. *3 Biotech*, *5*(4), 337–353. https://doi.org/10.1007/s13205-014-0246-5

Samburova, V., Connolly, J., Gyawali, M., Yatavelli, R. L. N., Watts, A. C., Chakrabarty, R. K., et al. (2016). Polycyclic aromatic hydrocarbons in biomass-burning emissions and their contribution to light absorption and aerosol toxicity. *Science of the Total Environment*, *568*, 391–401. https://doi.org/10.1016/j.scitotenv.2016.06.026

Santiago-De La Rosa, N., González-Cardoso, G., Figueroa-Lara, J. D. J., Gutiérrez-Arzaluz, M., Octaviano-Villasana, C., Ramírez-Hernández, I. F., & Mugica-Álvarez, V. (2018). Emission factors of atmospheric and climatic pollutants from crop residues burning. *Journal of the Air & Waste Management Association*, *68*(8), 849–865. https://doi.org/10.1080/10962247.2018.1459326

Schwarz, J. P., & Fuel2Fire Team. (2023). FIREXAQ-FIREFLAG-TABULARDATA_Analysis_20190724_R12_thru20190905.xlsx [Dataset]. NASA. Retrieved from https://www-air.larc.nasa.gov/cgi-bin/ArcView/firexaq?ANALYSIS=1#SCHWARZ.JOSHUA/

Schwarz, J. P., Spackman, J. R., Fahey, D. W., Gao, R. S., Lohmann, U., Stier, P., et al. (2008). Coatings and their enhancement of black carbon light absorption in the tropical atmosphere. *Journal of Geophysical Research*, *113*(D3), D03203. https://doi.org/10.1029/2007JD009042

Sekimoto, K., Koss, A. R., Gilman, J. B., Selimovic, V., Coggon, M. M., Zarzana, K. J., et al. (2018). High- and low-temperature pyrolysis profiles describe volatile organic compound emissions from western US wildfire fuels. *Atmospheric Chemistry and Physics*, *18*(13), 9263–9281. https://doi.org/10.5194/acp-18-9263-2018

Selimovic, V., Yokelson, R. J., McMeeking, G. R., & Coefield, S. (2020). Aerosol mass and optical properties, smoke influence on O_3, and high NO_3 production rates in a western U.S. City impacted by wildfires. *Journal of Geophysical Research: Atmospheres*, *125*(16), e2020JD032791. https://doi.org/10.1029/2020JD032791

Selimovic, V., Yokelson, R. J., Warneke, C., Roberts, J. M., de Gouw, J., Reardon, J., & Griffith, D. W. T. (2018). Aerosol optical properties and trace gas emissions by PAX and OP-FTIR for laboratory-simulated western US wildfires during FIREX. *Atmospheric Chemistry and Physics*, *18*(4), 2929–2948. https://doi.org/10.5194/acp-18-2929-2018

Shaddix, C. R., Harrington, J. E., & Smyth, K. C. (1994). Quantitative measurements of enhanced soot production in a flickering methane/air diffusion flame. *Combustion and Flame*, *99*(3–4), 723–732. https://doi.org/10.1016/0010-2180(94)90067-1

Simpson, I. J., Akagi, S. K., Barletta, B., Blake, N. J., Choi, Y., Diskin, G. S., et al. (2011). Boreal forest fire emissions in fresh Canadian smoke plumes: C_1–C_{10} volatile organic compounds (VOCs), CO_2, CO, NO_2, NO, HCN and CH_3CN. *Atmospheric Chemistry and Physics*, *11*(13), 6445–6463. https://doi.org/10.5194/acp-11-6445-2011

Simpson, I. J., Blake, D. R., Blake, N. J., Meinardi, S., Barletta, B., Hughes, S. C., et al. (2020). Characterization, sources and reactivity of volatile organic compounds (VOCs) in Seoul and surrounding regions during KORUS-AQ. *Elementa: Science of the Anthropocene*, *8*, 37. https://doi.org/10.1525/elementa.434

Singh, H. B., Cai, C., Kaduwela, A., Weinheimer, A., & Wisthaler, A. (2012). Interactions of fire emissions and urban pollution over California: Ozone formation and air quality simulations. *Atmospheric Environment*, *56*, 45–51. https://doi.org/10.1016/j.atmosenv.2012.03.046

Soja, A. J., Al-Saadi, J. A., Giglio, L., Randall, D., Kittaka, C., Pouliot, G., et al. (2009). Assessing satellite-based fire data for use in the national emissions inventory. *Journal of Applied Remote Sensing*, *3*(1), 031504. https://doi.org/10.1117/1.3148859

Stavrakou, T., Müller, J.-F., Bauwens, M., De Smedt, I., Lerot, C., Van Roozendael, M., et al. (2016). Substantial underestimation of post-harvest burning emissions in the North China Plain revealed by multi-species space observations. *Scientific Reports*, *6*(1), 32307. https://doi.org/10.1038/srep32307

St. Clair, J. M., McCabe, D. C., Crounse, J. D., Steiner, U., & Wennberg, P. O. (2010). Chemical ionization tandem mass spectrometer for the in situ measurement of methyl hydrogen peroxide. *Review of Scientific Instruments*, *81*, 094102. https://doi.org/10.1063/1.3480552

Stockwell, C. E., Veres, P. R., Williams, J., & Yokelson, R. J. (2015). Characterization of biomass burning emissions from cooking fires, peat, crop residue, and other fuels with high-resolution proton-transfer-reaction time-of-flight mass spectrometry. *Atmospheric Chemistry and Physics*, *15*(2), 845–865. https://doi.org/10.5194/acp-15-845-2015

Stockwell, C. E., Yokelson, R. J., Kreidenweis, S. M., Robinson, A. L., DeMott, P. J., Sullivan, R. C., et al. (2014). Trace gas emissions from combustion of peat, crop residue, domestic biofuels, grasses, and other fuels: Configuration and fourier transform infrared (FTIR) component of the fourth fire lab at missoula experiment (FLAME-4). *Atmospheric Chemistry and Physics*, *14*(18), 9727–9754. https://doi.org/10.5194/acp-14-9727-2014

Sullivan, A. P., May, A. A., Lee, T., McMeeking, G. R., Kreidenweis, S. M., Akagi, S. K., et al. (2014). Airborne characterization of smoke marker ratios from prescribed burning. *Atmospheric Chemistry and Physics*, *14*(19), 10535–10545. https://doi.org/10.5194/acp-14-10535-2014

Theys, N., Volkamer, R., Müller, J.-F., Zarzana, K. J., Kille, N., Clarisse, L., et al. (2020). Global nitrous acid emissions and levels of regional oxidants enhanced by wildfires. *Nature Geoscience*, *13*(10), 681–686. https://doi.org/10.1038/s41561-020-0637-7

Tian, D., Hu, Y., Wang, Y., Boylan, J. W., Zheng, M., & Russell, A. G. (2009). Assessment of biomass burning emissions and their impacts on urban and regional $PM_{2.5}$: A Georgia case study. *Environmental Science & Technology*, *43*(2), 299–305. https://doi.org/10.1021/es801827s

Tomsche, L., Piel, F., Mikoviny, T., Nielsen, C. J., Guo, H., Campuzano-Jost, P., et al. (2023). Measurement report: Emission factors of NH_3 and NH_x for wildfires and agricultural fires in the United States. *Atmospheric Chemistry and Physics*, *23*(4), 2331–2343. https://doi.org/10.5194/acp-23-2331-2023

Tulbure, M. G., Wimberly, M. C., Roy, D. P., & Henebry, G. M. (2011). Spatial and temporal heterogeneity of agricultural fires in the central United States in relation to land cover and land use. *Landscape Ecology*, *26*(2), 211–224. https://doi.org/10.1007/s10980-010-9548-0

Urbanski, S. (2014). Wildland fire emissions, carbon, and climate: Emission factors. *Forest Ecology and Management*, *317*, 51–60. https://doi.org/10.1016/j.foreco.2013.05.045

US EPA. (2017). *National Emissions Inventory Report*. EPA. Retrieved from https://gispub.epa.gov/neireport/2017/

van der Velde, I. R., van der Werf, G. R., Houweling, S., Eskes, H. J., Veefkind, J. P., Borsdorff, T., & Aben, I. (2021). Biomass burning combustion efficiency observed from space using measurements of CO and NO_2 by the TROPOspheric Monitoring Instrument (TROPOMI). *Atmospheric Chemistry and Physics*, *21*(2), 597–616. https://doi.org/10.5194/acp-21-597-2021

Veres, P., Roberts, J. M., Burling, I. R., Warneke, C., de Gouw, J., & Yokelson, R. J. (2010). Measurements of gas-phase inorganic and organic acids from biomass fires by negative-ion proton-transfer chemical-ionization mass spectrometry. *Journal of Geophysical Research*, *115*(D23), D23302. https://doi.org/10.1029/2010JD014033

Veres, P. R., Neuman, J. A., Bertram, T. H., Assaf, E., Wolfe, G. M., Williamson, C. J., et al. (2020). Global airborne sampling reveals a previously unobserved dimethyl sulfide oxidation mechanism in the marine atmosphere. *Proceedings of the National Academy of Sciences*, *117*(9), 4505–4510. https://doi.org/10.1073/pnas.1919344117

Vrekoussis, M., Wittrock, F., Richter, A., & Burrows, J. P. (2009). Temporal and spatial variability of glyoxal as observed from space. *Atmospheric Chemistry and Physics*, *9*(13), 4485–4504. https://doi.org/10.5194/acp-9-4485-2009

Wang, J., Roudini, S., Hyer, E. J., Xu, X., Zhou, M., Garcia, L. C., et al. (2020). Detecting nighttime fire combustion phase by hybrid application of visible and infrared radiation from Suomi NPP VIIRS. *Remote Sensing of Environment*, *237*, 111466. https://doi.org/10.1016/j.rse.2019.111466

Ward, D. E., Susott, R. A., Kauffman, J. B., Babbitt, R. E., Cummings, D. L., Dias, B., et al. (1992). Smoke and fire characteristics for cerrado and deforestation burns in Brazil: BASE-B experiment. *Journal of Geophysical Research*, *97*(D13), 14601. https://doi.org/10.1029/92JD01218

Warneke, C., Schwarz, J. P., Dibb, J., Kalashnikova, O., Frost, G., Al-Saad, J., et al. (2023). Fire influence on regional to global environments and air quality (FIREX-AQ). *Journal of Geophysical Research: Atmospheres*, *128*(2), e2022JD037758. https://doi.org/10.1029/2022JD037758

Wells, K. C., Millet, D. B., Payne, V. H., Deventer, M. J., Bates, K. H., de Gouw, J. A., et al. (2020). Satellite isoprene retrievals constrain emissions and atmospheric oxidation. *Nature*, *585*(7824), 225–233. https://doi.org/10.1038/s41586-020-2664-3

Wentworth, G. R., Aklilu, Y., Landis, M. S., & Hsu, Y.-M. (2018). Impacts of a large boreal wildfire on ground level atmospheric concentrations of PAHs, VOCs and ozone. *Atmospheric Environment*, *178*, 19–30. https://doi.org/10.1016/j.atmosenv.2018.01.013

Wiedinmyer, C., Kimura, Y., McDonald-Buller, E. C., Emmons, L. K., Buchholz, R. R., Tang, W., et al. (2023). The fire inventory from NCAR version 2.5: An updated global fire emissions model for climate and chemistry applications (preprint). *Atmospheric Sciences*. https://doi.org/10.5194/egusphere-2023-124

Wortmann, C. S., Klein, R. N., & Shapiro, C. A. (2012). *Harvesting Crop Residues (NebGuide No. G1846)*. University of Nebraska Lincoln.

Xu, L., Crounse, J. D., Vasquez, K. T., Allen, H., Wennberg, P. O., Bourgeois, I., et al. (2021). Ozone chemistry in western U.S. wildfire plumes. *Science Advances*, *7*(50), eabl3648. https://doi.org/10.1126/sciadv.abl3648

Yevich, R., & Logan, J. A. (2003). An assessment of biofuel use and burning of agricultural waste in the developing world. *Global Biogeochemical Cycles*, *17*(4), 1095. https://doi.org/10.1029/2002GB001952

Yokelson, R. J., Burling, I. R., Gilman, J. B., Warneke, C., Stockwell, C. E., de Gouw, J., et al. (2013). Coupling field and laboratory measurements to estimate the emission factors of identified and unidentified trace gases for prescribed fires. *Atmospheric Chemistry and Physics*, *13*(1), 89–116. https://doi.org/10.5194/acp-13-89-2013

Yokelson, R. J., Burling, I. R., Urbanski, S. P., Atlas, E. L., Adachi, K., Buseck, P. R., et al. (2011). Trace gas and particle emissions from open biomass burning in Mexico. *Atmospheric Chemistry and Physics*, *11*(14), 6787–6808. https://doi.org/10.5194/acp-11-6787-2011

Yokelson, R. J., Crounse, J. D., DeCarlo, P. F., Karl, T., Urbanski, S., Atlas, E., et al. (2009). Emissions from biomass burning in the Yucatan. *Atmospheric Chemistry and Physics*, *9*(15), 5785–5812. https://doi.org/10.5194/acp-9-5785-2009

Yokelson, R. J., Goode, J. G., Ward, D. E., Susott, R. A., Babbitt, R. E., Wade, D. D., et al. (1999). Emissions of formaldehyde, acetic acid, methanol, and other trace gases from biomass fires in North Carolina measured by airborne Fourier transform infrared spectroscopy. *Journal of Geophysical Research*, *104*(D23), 30109–30125. https://doi.org/10.1029/1999JD900817

Yokelson, R. J., Griffith, D. W. T., & Ward, D. E. (1996). Open-path Fourier transform infrared studies of large-scale laboratory biomass fires. *Journal of Geophysical Research*, *101*(D15), 21067–21080. https://doi.org/10.1029/96JD01800

Yuan, B., Koss, A. R., Warneke, C., Coggon, M., Sekimoto, K., & De Gouw, J. A. (2017). Proton-Transfer-reaction mass spectrometry: Applications in atmospheric sciences. *Chemical Reviews*, *117*(21), 13187–13229. https://doi.org/10.1021/acs.chemrev.7b00325

Zanobetti, A., Franklin, M., Koutrakis, P., & Schwartz, J. (2009). Fine particulate air pollution and its components in association with cause-specific emergency admissions. *Environmental Health*, *8*(1), 58. https://doi.org/10.1186/1476-069X-8-58

Zarzana, K. J., Min, K.-E., Washenfelder, R. A., Kaiser, J., Krawiec-Thayer, M., Peischl, J., et al. (2017). Emissions of glyoxal and other carbonyl compounds from agricultural biomass burning plumes sampled by aircraft. *Environmental Science & Technology*, *51*(20), 11761–11770. https://doi.org/10.1021/acs.est.7b03517

Zarzana, K. J., Selimovic, V., Koss, A. R., Sekimoto, K., Coggon, M. M., Yuan, B., et al. (2018). Primary emissions of glyoxal and methylglyoxal from laboratory measurements of open biomass burning. *Atmospheric Chemistry and Physics*, *18*(20), 15451–15470. https://doi.org/10.5194/acp-18-15451-2018

Zeng, T., Wang, Y., Yoshida, Y., Tian, D., Russell, A. G., & Barnard, W. R. (2008). Impacts of prescribed fires on air quality over the southeastern United States in spring based on modeling and ground/satellite measurements. *Environmental Science & Technology*, *42*(22), 8401–8406. https://doi.org/10.1021/es800363d

Zhang, H., Zhang, X., Wang, Y., Bai, P., Hayakawa, K., Zhang, L., & Tang, N. (2022). Characteristics and influencing factors of polycyclic aromatic hydrocarbons emitted from open burning and stove burning of biomass: A brief review. *International Journal of Environmental Research and Public Health*, *19*(7), 3944. https://doi.org/10.3390/ijerph19073944

Zhou, L., Baker, K. R., Napelenok, S. L., Pouliot, G., Elleman, R., O'Neill, S. M., et al. (2018). Modeling crop residue burning experiments to evaluate smoke emissions and plume transport. *Science of The Total Environment*, *627*, 523–533. https://doi.org/10.1016/j.scitotenv.2018.01.237

Erratum

The originally published version of this article contained a typographical error. In the twelfth sentence of the first paragraph of Section 4.7, the value "7% (35%)" should be "81% (35%)." The error has been corrected, and this may be considered the authoritative version of record.